

## Summary.

It is a well-known fact that the real dimensions of extragalactic nebulae are considerably larger than can be seen by a careful visual inspection of the photographs. This paper presents the results obtained in an investigation of the systematic errors in the visually determined diameters. It is shown that the major and minor diameters, as well as the diameter ratios, contain serious errors, depending on the elongation of the objects and on the form of the light distribution function. The corrected diameters are used as a basis for investigations of the orientation in space of the spiral nebulae.

*Chapter I* gives an account of the procedure used for the determination of the measuring errors. Artificial nebulae are produced in the laboratory by photographing rotating light sectors of different shapes. The distributions of light in these nebulae have the form  $k r^{-n}$ , the exponent  $n$  ranging from 0.5 to 7.0. The major and minor diameters of the objects, as measured visually by five different persons, are given in the *Appendix*. Table 4 contains the diameters as obtained from photometer tracings. The ratios of the visually determined diameters and the photometric diameters are given by the curves of Fig. 8. It appears that, in a visual determination, the major diameter of an elongated nebula is measured too large as compared to the minor diameter, and that the diameter ratio is systematically falsified (Fig. 9). The major diameters, and the diameter ratios, may be corrected by means of the smoothed values given in Tables 6 and 10.

*Chapter II* gives the results obtained in a comparison between Reinmuth's diameters, as determined visually for nebulae on the Heidelberg plates, and the photometric diameters. We refer to Fig. 10 (elliptical nebulae) and Fig. 11 (spirals). Reinmuth's measuring errors seem to agree well with those determined in Chapter I.

*Chapter III* presents an investigation of the inclinations of the spiral nebulae to the celestial plane. Several previous investigations have arrived at the result that there is an excess of nebulae seen edgewise. It is shown that this excess is removed if the investigation is based on a material of nebulae representing a given volume of space, and if the systematic corrections are applied to the diameter ratios. Fig. 15, 16, and 17 give the distributions of the inclination angles as obtained from the catalogues collected by Reinmuth, Reiz, and Shapley-Ames.

*Chapter IV* gives the results obtained in an investigation of the orientation in space of the spiral nebulae. A summary of the results is given in Table 25. It

appears that the spatial distribution corresponding to all the spirals included in the investigation has a slightly flattened shape, the ratio of the smallest and largest dispersions being equal to about 0.90. Consequently, there seems to be a slight tendency to parallelism between the nebular discs. The normal of the preferential plane has the coordinates  $\alpha = 35^\circ$ ,  $\delta = -2^\circ$ . However, the mean errors of the derived dispersion values are comparatively large, and a final discussion regarding a possible preferential plane must await the accumulation of further observational data.

## CHAPTER I.

**Investigation of the systematic errors in the apparent diameters of nebulae.**

**1. Introduction.** It is the purpose of this investigation to study the systematic errors in the apparent diameters of extragalactic nebulae. Most catalogues of nebulae give the major and minor diameters of the objects as determined by direct visual measurement of the photographs. It is generally not possible to get the angular dimensions of the majority of the nebulae in any other way. It will be shown in the following pages that the diameters determined visually contain serious systematic errors, depending on the form of the light distribution curve and on the elongations of the objects. The ratios of the minor and major diameters are in most cases systematically falsified. The results are derived from measurements of artificial nebulae obtained by photographing rotating light sectors of different shapes. *Chapter I* will give an account of these measurements and the results to be obtained from them. In *Chapter II*, a comparison will be made between visually determined diameters of elliptical and spiral nebulae and the diameters obtained from photometer registrograms. In *Chapters III* and *IV*, the corrected diameters will be used for investigations of the orientation in space of the extragalactic nebulae.

It is a generally acknowledged fact that the real dimensions of extragalactic nebulae are considerably larger than can be seen by careful inspection of the photographic exposures by the naked eye or by means of an eyepiece. The faint outmost parts of the objects give rather small densities on the plate and are in general not perceptible to the human eye. Accordingly, the visually determined diameters refer only to the main bodies of the nebulae.

The systematic errors in the apparent diameters are clearly displayed if the plates are measured in a self-recording microphotometer. The minimum value of plate density measurable in the photometer is considerably smaller than that perceivable by the eye. The photometric diameters may be twice as large, or even larger, than those determined visually.

The following investigation will give the result that the measuring errors are not the same for the major and the minor diameters of the nebulae. Whereas the photometer may be assumed to give the true diameter ratio, the direct visual

measurement gives a major diameter that is systematically too large as compared to the minor diameter. The nebulae appear to be more elongated than they really are. The effect apparently is to be explained by certain properties of the human eye. In an elongated nebula, the outmost parts referring to the major axis seem to stand out more clearly against the background fog of the plate than those parts which define the minor axis. Besides, the latter parts are situated close to the bright central nucleus of the object, which results in an underestimation of their surface brightness.

The systematic errors in the diameter ratios are of special importance in investigations of the orientation of the nebulae. The spirals may, as a first approximation, be compared to spheroidal discs, and their inclinations to the celestial plane are determined by the apparent diameter ratios. Several previous investigations of this problem have arrived at the result that the distribution of the inclinations is not a random one, the number of nebulae with an edgewise orientation being too large. It will be shown that this result partly depends on the errors in the diameter ratios.

**2. *The experimental arrangements.*** It has been mentioned above that the systematic errors in the diameters will be studied by measuring photographs of artificial nebulae. The nebulae are produced in the laboratory by rotating sectors of light, and they are photographed in the ordinary way by a camera of suitable focal length. This method of investigation offers two important advantages. In the first place we may, by changing the sectors, obtain any desired distribution of light, even such distributions which have not been observed in extragalactic objects. It is, of course, supposed that the distributions are symmetrical with respect to the centres of the nebulae. Secondly, the rotating sector may be photographed under different angles, and we are thus able to produce nebulae with any desired ratio of the minor and major diameters. It may also be mentioned that we, by changing the camera distance, may obtain nebulae of various dimensions.

The experimental arrangements, as used by the writer, appear from the somewhat schematic drawing given in Fig. 1. A quadrangular box, measuring about  $20 \times 20$  cm, is mounted on the axis of an electrical motor. The inside of the box, which is painted white, is illuminated by six electrical light-bulbs. The current to these light-bulbs is supplied by a large accumulator of six volts. The front side of the box is covered by an exchangeable plate of milk glass. The plate is painted dark except for the region corresponding to the sector. The electrical motor with the box is mounted on a horizontal metal plate, as is seen from the figure. The plate rests on a table and can be turned around the point  $P$ , situated exactly below the centre of the sector. The angle between the motor axis and the direction to the camera objective is, according to the figure, called  $\varphi$ . The values of  $\cos \varphi$ , which are equal to the ratios,  $b/a$ , of the minor and major diameters of the photographed nebulae, can be read off a scale mounted on the table. The sectors have generally been photographed in five different inclinations, the values

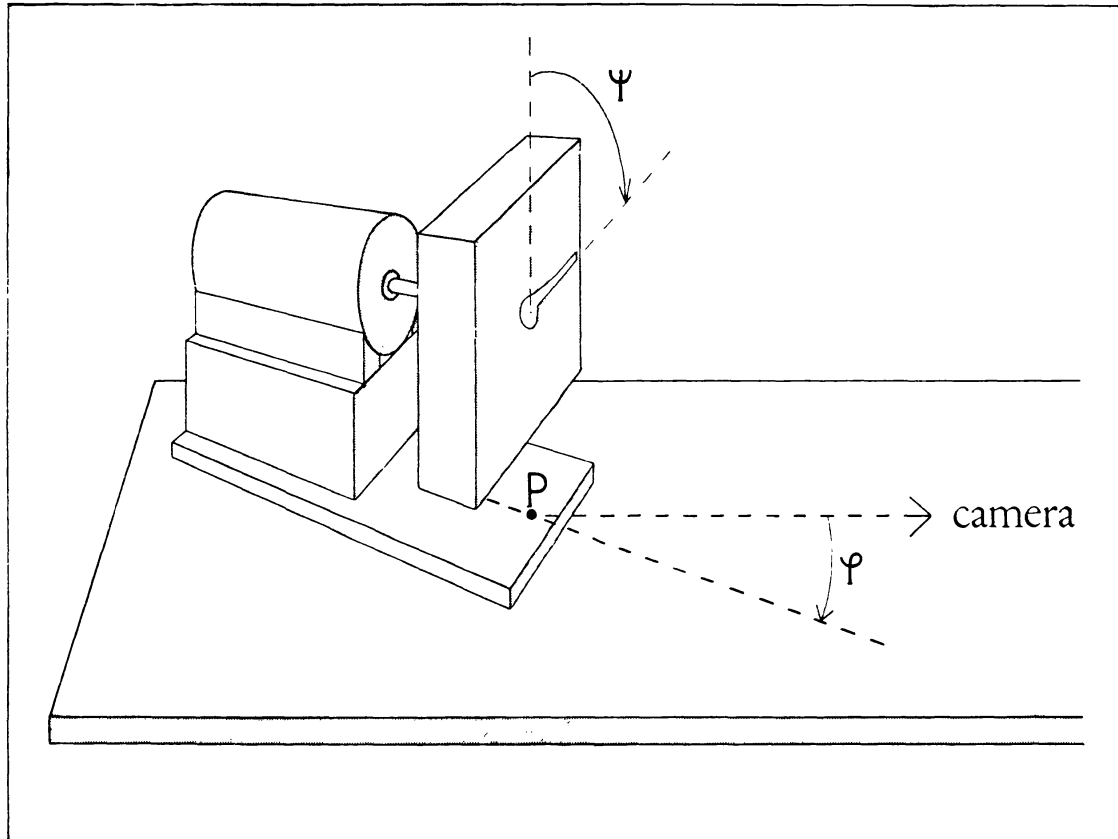


Fig. 1. The experimental arrangements. Definition of the rotation angle,  $\psi$ , and the inclination angle,  $\varphi$ , of the light sector.

of  $\cos \varphi$  being equal to 1.0, 0.8, 0.6, 0.4, and 0.2. It may be remarked that the speed of the motor has been adjusted to about seven revolutions per second.

The photographs of the rotating sector have been taken with a portrait camera movable back and forth in a photographic bench. The objective has been of the type *Zeiss Tessar*, with a focal length of 18 cm and a focal ratio of 1 : 4.5. The ratio has, however, been cut down by the diaphragm to at least 1 : 22. The photographic plates, which have been of the type *Agfa Isopan* and have measured  $9 \times 12$  cm, will be further discussed below. Generally five exposures of the sector, corresponding to the five values of  $\cos \varphi$  mentioned above, have been made on the same plate. Each sector has been photographed on at least two plates, the first plate corresponding to negative values of  $\varphi$  and the second plate to positive values. The exposures have been arranged in this symmetrical way in order to neutralize possible sources of error, as for instance the errors that are introduced in the diameter ratios if the rotation axis of the sector and the optical axis of the camera do not exactly coincide for  $\cos \varphi = 1.0$ . The exposure times have ranged from 20<sup>s</sup> to 240<sup>s</sup>, and average about 130<sup>s</sup>. It has been tried to adjust the exposure time in such a way that the plate density of the outmost parts of the



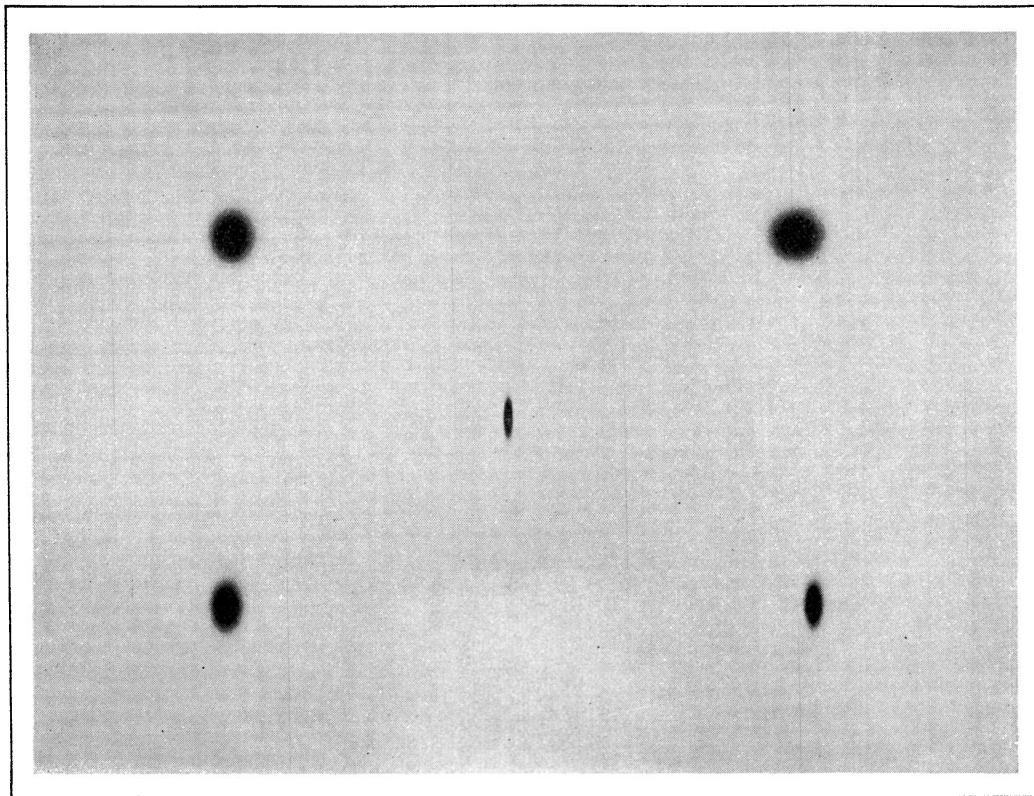


Fig. 2. Reproduction of one of the plates (natural size), showing the artificial nebulae.

nebula, corresponding to the outmost part of the sector, is barely measurable in the photometer. All the ten different sectors, which will be further described below, give a surface brightness that falls off from the centre. For a given sector the exposure times have, of course, been the same. The camera distances, which have generally amounted to 150 à 200 cm, have been adjusted so that the dimensions of the nebular images, as measured visually, have been roughly of the same size. The measured values of the major diameters of the most elongated nebulae amount, in all cases, to approximately 10 mm. During the different exposures of the same sector the camera distance is naturally kept unchanged.

The arrangement of the five nebular images on each plate is shown in Fig. 2. The most elongated nebula ( $\cos \varphi = 0.2$ ) has generally been placed at the centre of the plate. By moving the plate holder, the other four images ( $\cos \varphi = 0.4, 0.6, 0.8$ , and  $1.0$ ) are placed symmetrically around the centre. At least two plates, with in all ten nebular images, have been obtained for each sector.

It has been mentioned above that the ratio,  $b/a$ , of the minor and major diameters of a nebula is equal to  $\cos \varphi$ . This is, in fact, true only when the distance between the sector and the camera is infinitely large. The relation between the diameter ratio and  $\cos \varphi$  for a finite camera distance may be derived from Fig. 3. Here, the heavy line indicates the sector, as seen from above, whereas the horizontal

TABLE 1.  
*Relation between the diameter ratio  $b/a$  and  $\cos \varphi$ .*  
*( $l/D = 0.05$ )*

$\cos \varphi$	$b_1/a$	$b_2/a$	$b/a$
1.0000	0.5000	0.5000	1.0000
0.8000	0.3883	0.4124	0.8007
0.6000	0.2885	0.3125	0.6010
0.4000	0.1912	0.2096	0.4008
0.2000	0.0953	0.1052	0.2005

line represents the optical axis of the camera. The length of the sector is denoted by  $l$ , and the camera distance by  $D$ . If the distance from the camera objective to the photographic plate is equal to  $d$ , the following expressions are obtained for the major diameter,  $a$ , and the two minor semi-diameters,  $b_1$  and  $b_2$ :

$$\begin{aligned}
 a &= 2l \cdot d/D \\
 b_1 &= d \cdot \operatorname{tg} v_1 = a/2 \frac{\cos \varphi}{1 + l/D \sin \varphi} \\
 b_2 &= d \cdot \operatorname{tg} v_2 = a/2 \frac{\cos \varphi}{1 - l/D \sin \varphi} \\
 b &= b_1 + b_2
 \end{aligned} \tag{1}$$

In the present case the ratio  $l/D$  amounts, on an average, to 0.05. In Table 1 the numerical values are given of  $b_1/a$ ,  $b_2/a$ , and  $b/a$ , as corresponding to the five different values of  $\cos \varphi$ . It appears that the ratio  $b/a$  is generally slightly larger than the corresponding value of  $\cos \varphi$ . The table also shows that the two minor semi-diameters are slightly different, the maximum difference amounting to about ten per cent. It may be remarked that a similar asymmetry has been observed in extragalactic spiral nebulae, although it in these cases apparently is, for the most part, an absorption effect.

**3. Description of the sectors.** It has already been mentioned above that ten different sectors have been used in the investigation. All the sectors give distributions of light represented by the function  $k r^{-n}$ ,  $k$  being a constant and  $r$  the distance from the rotation axis of the sector. The values of the exponent  $n$  range from 0.5 to 7.0, the individual values being 0.5, 1.0, 1.5, 2.0, 2.5, 3.0, 4.0, 5.0, 6.0, and 7.0. Thus, the luminosity gradients vary within very wide limits.

In Fig. 4, all the sectors have been reproduced in half size. The sector in the upper left corner of the figure gives a light distribution  $k r^{-0.5}$ , whereas the sector in the lower right corner represents the function  $k r^{-7.0}$ . The rotation axes of the different sectors are denoted by the white circular spots.

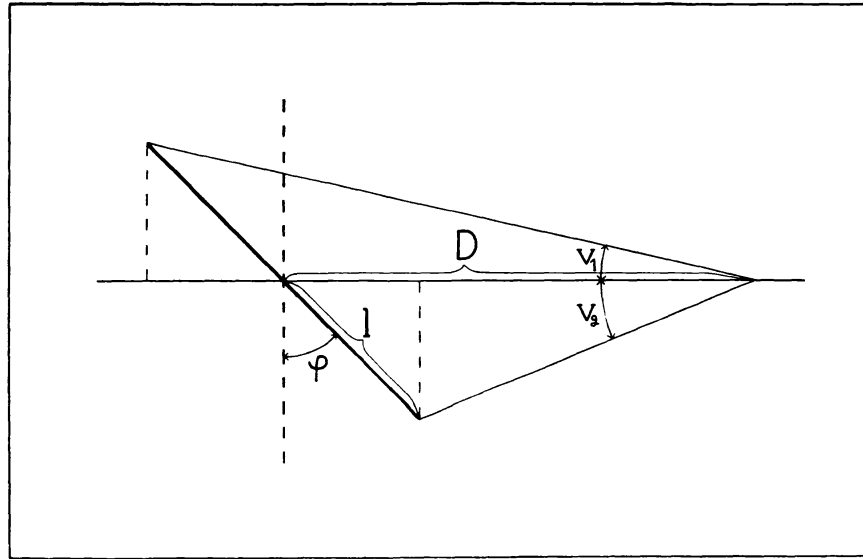


Fig. 3. The rotating sector seen from above. Definition of the angular semi-diameters  $v_1$  and  $v_2$ .

The sectors have been constructed in the following way. The contours of the sectors, which have been computed numerically, are drawn on pieces of thin paper, and the sectors are cut out. These paper strips are then pasted on the quadrangular plates of milk glass described above. The glass plates measure  $20 \times 20$  cm and have been carefully selected and tested as to homogeneity. The paper sectors are adjusted so that their centres agree with the centres of the plates. The glass plates are now sprayed with a rather thin solution of black lac-varnish. The coating should not be made thicker than is necessary to make the plates untransparent for light. When the paint has dried, the paper strips are washed off. The outlines of the transparent regions of the plates, that are obtained by this procedure, generally agree very well with the theoretically computed contours of the sectors. If minor adjustments are necessary, the boundaries may be retouched by using Indian ink.

In the ideal case, the surface brightness of the different parts of a sector should be the same and independent of the angle under which the sector is observed, *i. e.* the surface brightness should be independent of the rotation angle  $\psi$  and the inclination angle  $\varphi$ , as defined in Fig. 1. If the surface brightness changes with the distance from the rotation axis, the distribution of light, as given by the rotating sector, will deviate from the theoretical distribution function. If the surface brightness is related to the angle  $\psi$ , the result may be a diameter ratio of the artificial nebula that does not agree with the value of  $\cos \varphi$ . If, for instance, values of  $\psi$  of  $0^\circ$  and  $180^\circ$  correspond to a larger brightness than the values  $90^\circ$  and  $270^\circ$ , the ratio  $b/a$  will be smaller than  $\cos \varphi$ , and *vice versa*. A relation between the surface brightness and the inclination angle  $\varphi$  will affect the major diameter (but not the diameter ratio) of the nebula. The surface brightness of the



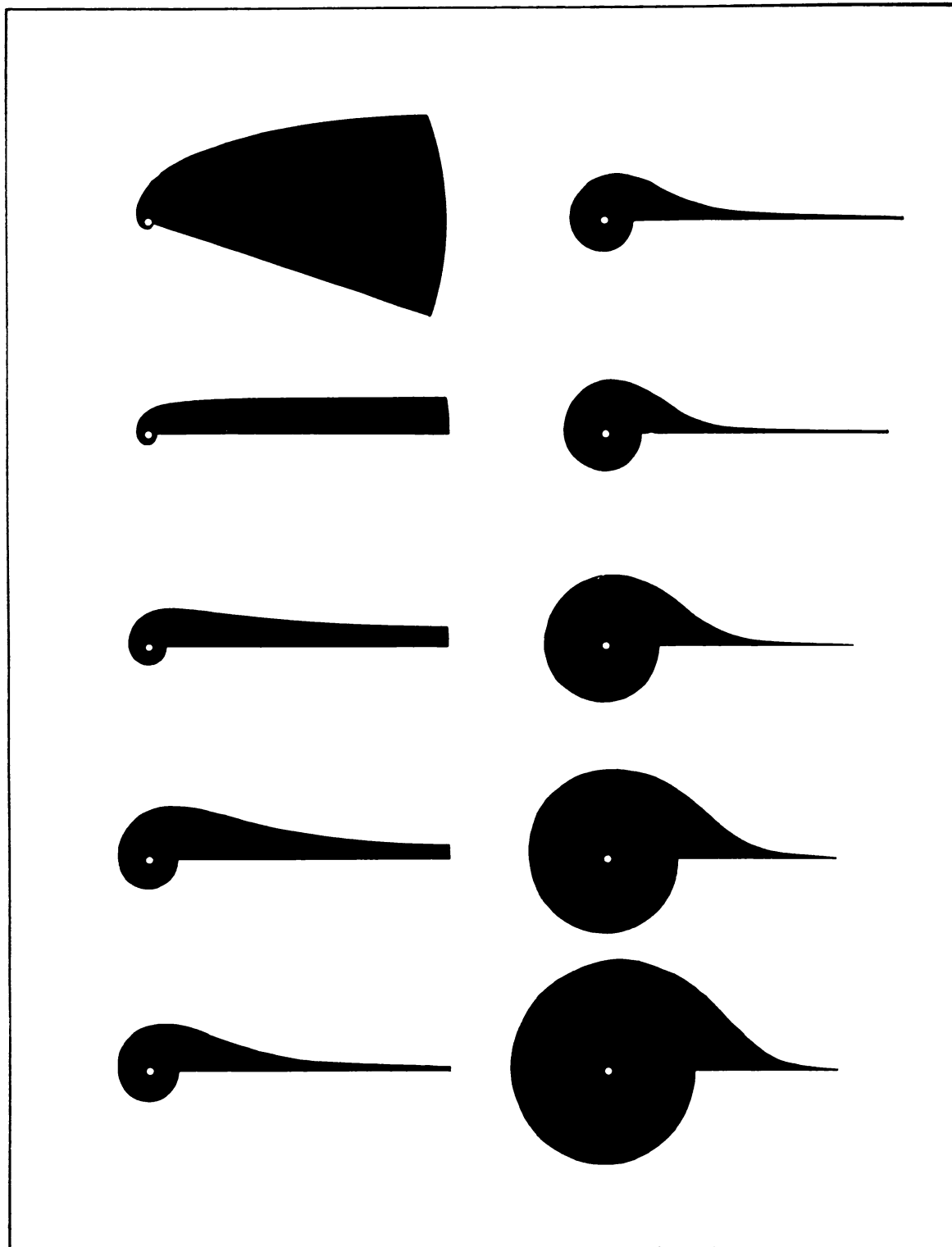


Fig. 4. Reproductions of the light sectors (half size). The sectors represent distributions of light from  $kr^{-0.5}$  to  $kr^{-7.0}$ .

milk glass plate, as seen under different angles, depends on the arrangement of the light-bulbs behind the plate and on the dispersion of light in the glass plate. Although the diameters of all the artificial nebulae will be checked by measurement in a self-recording microphotometer, it is desirable that the variations in the surface brightness of each sector are kept within reasonable limits.

The variations in the surface brightness have been investigated by using a sector representing a constant light distribution, *i. e.* a distribution of the form  $k r^0$ . The contours of the sector are formed by two straight lines intersecting each other at the rotation centre. The rotating sector has been photographed at different inclinations, and the densities of the photographic images have been measured in the microphotometer. In order to calibrate the plates, the rotating sector representing the luminosity function  $k r^{-1}$  has also been photographed on each plate. Although this procedure may not be quite satisfactory, as will be shown below, the resulting calibration curve is certainly accurate enough for the present purpose. It may be remarked that two series of plates have been taken, the first corresponding to negative values of the inclination  $\varphi$  and the second to positive values. The exposures have been made in such an order that the means of the densities corresponding to  $+\varphi$  and  $-\varphi$  are not affected by a possible decrease, or increase, in the light intensities of the light bulbs.

The intensities (in an arbitrary scale), as obtained from the photometer tracings, are given in Table 2. The table shows that the images have been measured along the major and the minor axes. It may be remarked that a positive sign refers to the upper (further) side of the rotating sector. A study of the values given in each column shows that the surface brightness of the light sector is approximately independent of the distance from the rotation axis. The differences between the

TABLE 2.

*Photometrically measured surface brightnesses obtained for a sector representing a constant light distribution ( $i = k r^0$ ).*

Distance (along the maj. axis)	$\cos \varphi =$ 1.0	0.8	0.6	0.4	0.2	Distance (along the min. axis)	$\cos \varphi =$ 1.0	0.8	0.6	0.4	0.2
−1.0 <i>a</i>	<i>i</i> =72	69	64	57	52	−1.0 <i>b</i>	<i>i</i> =72	68	64	59	53
−0.8	74	74	67	60	53	−0.8	76	71	66	61	53
−0.6	76	75	69	61	53	−0.6	77	74	68	62	54
−0.4	76	73	66	60	53	−0.4	77	73	67	61	53
−0.2	72	70	64	58	51	−0.2	73	69	64	59	52
0.0	—	—	—	—	—	0.0	—	—	—	—	—
+0.2	66	66	62	57	51	+0.2	65	68	63	58	50
+0.4	70	71	66	61	52	+0.4	68	72	66	61	51
+0.6	72	71	68	62	52	+0.6	72	74	68	63	54
+0.8	72	71	68	62	52	+0.8	71	73	68	62	52
+1.0 <i>a</i>	69	68	65	59	50	+1.0 <i>b</i>	68	70	65	60	51
means	71.9	70.8	65.9	59.7	51.9		71.9	71.2	65.9	60.6	52.3

individual values amount to only some few per cent and will be of minor importance in this connection. A comparison between the values obtained for the major and the minor axes gives the dependence of the surface brightness on the rotation angle  $\psi$ . According to the means given at the bottom of the table, there is no correlation between these two quantities. However, the brightness of the light sector apparently depends on the inclination  $\varphi$ . There is a decrease in the intensity of about 28 per cent (from 72 to 52 units) as the value of  $\cos \varphi$  changes from 1.0 to 0.2. This decrease, which is not unexpected, will produce the result that the major diameters of the artificial nebulae are to a certain degree dependent on the elongation of the objects. The variations in the diameters will be further discussed below (Cf. section 6).

In our attempts to produce certain distributions of light by means of rotating sectors we have also to take another source of error into account. It has been said above that each rotating sector represents a distribution function of the type  $k r^{-n}$ . However, this function does not define the light intensity but the *exposure time* at the distance  $r$  from the rotation axis. The total exposure time is proportional to the angular opening,  $t_r$ , of the sector at the distance  $r$  and to the number of rotations,  $m$ . The following relations are valid:

$$\begin{aligned} i_r &= E(m, t_r, i_o) \geq m t_r \cdot i_o \\ t_r &= k r^{-n} \end{aligned} \quad (2)$$

Here,  $i_o$  is the surface brightness of the sector, whereas  $i_r$  represents the *effective* light intensity<sup>1</sup> acting upon the photographic plate. In visual photometry, the intensity  $i_r$  is proportional to the product  $t_r \cdot i_o$  (Talbot's law), and the effective intensity is thus proportional to  $r^{-n}$ . In photographic photometry, however, the function  $E(m, t_r, i_o)$  may have a rather complicated form.

The above problem may be dissected into two parts, corresponding to  $m = 1$  and  $m > 1$ . In the first case, the plate is exposed only once, and the effective intensity  $i_r$  may, according to Schwarzschild's law, be put equal to  $i_o \cdot t_r^q$ . The exponent  $q$  is generally smaller than unity, which means that an increase in the exposure time does not give the same effect on the photographic plate as a corresponding increase in the intensity  $i_o$ . When  $m$  is larger than unity, an intermittence effect is added to the deviations from the reciprocity law, since  $m$  exposures of the length  $t_r$  do not give the same plate density as one exposure of the length  $m \cdot t_r$ . Several investigations have been made in order to determine the effect of intermittent exposures.<sup>2</sup> Although the results are sometimes not quite in accordance, it seems to be established that the intermittence effect and the

<sup>1</sup> The effective light intensity is defined as the intensity which, during a *continuous* exposure equal to the unit of time, produces the same density on the photographic plate as the intensity  $i_o$  during  $m$  intermittent exposures of the length  $t_r$ .

<sup>2</sup> See, for instance, Handbuch der Experimentalphysik, Vol 26 (Astrophysik), p. 647, Leipzig, 1937.

deviations from the reciprocity law will neutralize each other when the angular velocity of the rotating sector grows larger than a certain critical value, depending on the intensity. The critical velocity, which is rather small for small intensity values, increases as the intensity grows larger.

In the present case, the number of rotations of the sector has been about 400 per minute. This value is apparently larger than the above critical value, at least when small intensities are considered. Since this investigation will deal only with the systematic errors in the diameters of the nebulae, we are mainly interested in the distributions of light in the outer, faint parts of the objects. We may assume that in these outer regions the effective light intensity is, at least approximately, proportional to the product  $mt_r \cdot i_o$ , i. e. proportional to the expression  $r^{-n}$ .

**4. The plate material.** The systematic errors in the diameters obtained by direct visual measurement of the photographs of the nebulae may to a certain degree depend on the qualities of the photographic plates and on the developing procedure. According to the results obtained below, the diameter errors are intimately related to the steepness of the luminosity curve and, consequently, to the steepness of the curve representing the distribution of density on the plate. Thus the form, and steepness, of the calibration curve is of some importance in this connection. Some data concerning the plates used in our experiments will be given below.

The photographic plates have all been of the type *Agfa Isopan Feinkörnig*. The sensitivity of these plates amounts to  $27^\circ$  *Scheiner*, and extends in the red region to about 6500  $\text{\AA}$ . All the exposures have been made without filter of any kind. The developed plates have rather fine grains, the mean grain size being  $2 \text{ \AA} 3 \mu$ . The plates are backed and are completely free from any disturbing halo.

All the plates have been developed in a metol-hydroquinone developer.<sup>1</sup> The developing time has been 5 minutes at  $17^\circ \text{C}$ .

The calibration curves of a number of the plates have been determined by means of a neutral platinum filter.<sup>2</sup> The filter has an absorption of  $1^m30$ , and is placed in front of one of the light sectors. The sector, which is kept fixed in the same position, is photographed with, and without, the filter. Several pairs of exposures have been made, corresponding to different diaphragms of the camera objective. By comparing the densities of the different images we are able to construct the calibration curve by means of an integration procedure. It may be remarked that the calibration plates have, especially as regards development, been treated exactly in the same way as the other plates. The exposure time has been varied from  $20^s$  to  $120^s$ . Within this interval, the form of the calibration curve seems however to be independent of the length of the exposure.

The curve given in Fig. 5 represents the mean of all the calibration curves

<sup>1</sup> The developer contains (in 1000 ccm water) 2 gr metol, 6 gr hydroquinone, 25 gr sodium sulphite (crystals), 33 gr sodium carbonate (crystals), and 0.5 gr potassium bromide.

<sup>2</sup> The filter is composed of a very thin film of metallic platinum on a piece of glass measuring  $9 \times 12 \text{ cm}$ . The absorption of the filter, which has been carefully measured in a Schilt photometer, amounts to  $1^m30$  with local deviations of some few hundreds of a magnitude.

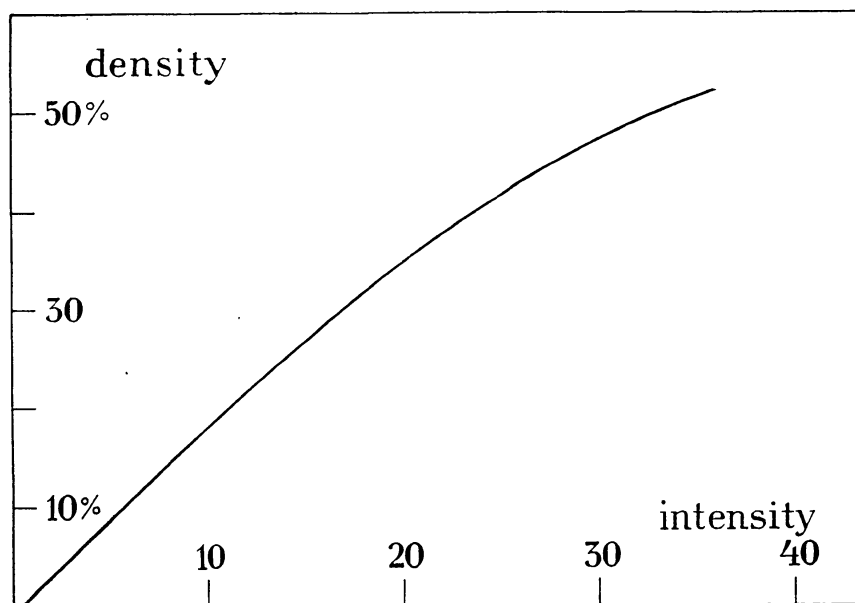


Fig. 5. Mean relation between light intensity and relative plate density as obtained for the *Agfa Isopan* plates.

obtained. The horizontal axis gives the light intensity, in an arbitrary scale. The ordinate is the relative density, *i. e.* the galvanometer deflection (clear plate *minus* image) expressed in per cent of the total deflection (clear plate *minus* zero point). In this case, we are mainly interested in the course of the curve for small densities. It appears that the curve is practically a straight line for density values smaller than 30 à 40 per cent. Accordingly, the distribution of density in the outer parts of the artificial nebulae agrees with the corresponding light distribution.

It would be of some interest to compare the above mean curve with the calibration curves derived from the photometer registrograms of the artificial nebulae. The latter curves give the relations between plate density and the theoretically computed intensity  $mt_p \cdot i_o$  (Cf. formula 2). It appears that the curves corresponding to the different light distributions agree rather well with the curve of Fig. 5, which indicates that the theoretically computed intensity is proportional to the effective intensity, as defined above.

**5. Visual measurement of the photographic images of the artificial nebulae.** Each of the rotating light sectors used in this investigation has been photographed ten times on two plates. An exception has been made for the sector representing the important luminosity function  $kr^{-2}$ , which has been photographed on four plates, in all. Each plate contains five nebular images with diameter ratios ranging from 0.2 to 1.0 ( $b/a = 0.2, 0.4, 0.6, 0.8$ , and 1.0). Thus the total number of plates is 22, whereas the number of nebular images amounts to 110.

The 110 nebulae have first been measured visually by means of scale and eye-piece and then, later on, in the photometer. In order to reduce the accidental

measuring errors it has seemed necessary to engage as many experienced persons as possible in the visual measuring work. Besides, a comparison between different measurers will enable us to study the individual systematic errors in the measured diameters. In the present case, five persons have taken part in the work, namely K. Lundmark, A. Reiz, S. Cederblad, H. Kristenson, and the writer.<sup>1</sup> The observers, who belong to the Lund Observatory, have all, except one, previous experience and training in the field of nebular work. Each of them has, independent of the others, measured the major and minor diameters of the nebulae. The term *mean observer* will be introduced to represent the mean results.

The measurements have been made by means of an ordinary Zeiss scale of glass with divisions for each half millimeter. The same eyepiece, with an enlargement of about two times, has been used for all the plates. The plates have generally been examined against the same background, consisting of a properly illuminated white surface. In order to avoid exhaustion of the eye no more than two plates have been measured in succession. The measuring difficulties increase rather rapidly when the luminosity gradient becomes smaller, *i.e.* when the exponent  $n$  in the distribution function  $k r^{-n}$  gets smaller values. Whereas the diameters are easily determined when  $n$  is larger than 4 à 5, the dimensions of the nebulae with distributions of the type  $k r^{-0.5}$ , or  $k r^{-1.0}$ , can only be approximately determined. For small values of  $n$  the observers have measured each plate twice, and the means have been taken. It may be remarked here that the observers have not been aware of the results to be derived from their diameter measures. The five series of diameter values have not been compared until after the conclusion of the work.

The results of the visual diameter determinations are given in the *Appendix*. The five different columns of each table give the major and minor diameters, in millimeters, as determined by each observer from the two plates.<sup>2</sup> The first plate corresponds to negative values of the inclination angle  $\varphi$ , as defined in Fig. 1, and the second plate to positive values. Although the exposure times of the two plates are the same, the plates may not be exactly comparable as regards the diameters, since they have not been developed simultaneously. The large letters *A—E* in the column heads represent different values of  $\cos \varphi$ , namely 1.0 (*A*), 0.8 (*B*), 0.6 (*C*), 0.4 (*D*), and 0.2 (*E*). It has been mentioned above that the true diameter ratios,  $b/a$ , are very nearly equal to the values of  $\cos \varphi$ . The definitive diameter ratios of the different nebulae will be derived later on from the photometer tracings. The last rows of the tables give the ratios of the minor and major diameters, as corresponding to the mean observer. The mean errors in these values, which have been computed from the individual diameter ratios, represent of course only first approximations, the number of observers being not more than five.

In the following pages, the true diameters, as measured in the photometer, will

<sup>1</sup> It is a pleasant duty for the writer to express his sincere thanks to his four cooperators, who very willingly and with great interest have participated in the measuring work.

<sup>2</sup> In the case of a round nebula ( $b/a = 1.0$ ), the major diameter is defined as the diameter that is parallel to the major axes of the four elongated nebulae on the same plate.



TABLE 3.

*Average values of  $\beta/a$  for the different observers.*

Observer	A	B	C	D	E
Lundmark	$0.985 \pm .010$	$0.726 \pm .015$	$0.507 \pm .012$	$0.309 \pm .008$	$0.146 \pm .005$
Reiz	$1.037 \pm .010$	$0.759 \pm .015$	$0.504 \pm .012$	$0.290 \pm .008$	$0.117 \pm .005$
Cederblad	$0.987 \pm .010$	$0.754 \pm .015$	$0.528 \pm .012$	$0.308 \pm .008$	$0.125 \pm .005$
Kristenson	$1.022 \pm .010$	$0.772 \pm .015$	$0.539 \pm .012$	$0.309 \pm .008$	$0.123 \pm .005$
Holmberg	$0.984 \pm .010$	$0.748 \pm .015$	$0.528 \pm .012$	$0.313 \pm .008$	$0.131 \pm .005$
Mean observer	$1.003 \pm .004$	$0.752 \pm .007$	$0.521 \pm .005$	$0.306 \pm .004$	$0.128 \pm .002$

always be denoted by  $a$  and  $b$ . The visually determined diameters will be denoted by  $\alpha$  and  $\beta$ .

The existence of large systematic errors in the diameters  $\alpha$  and  $\beta$  is indicated already by a superficial examination of the above tables. Whereas the true major diameter gets slightly smaller with decreasing values of the diameter ratio, as will be shown later, the diameter  $\alpha$  increases considerably when  $b/a$  changes from 1.0 to 0.2. The increase in  $\alpha$  amounts to more than 100 per cent for the distributions  $k r^{-0.5}$  and  $k r^{-1.0}$ . A corresponding systematic error is found in the ratios  $\beta/a$ . When  $b/a$  is equal to 1.0 (column *A*), the average value of  $\beta/a$  also equals unity. When the true ratio is 0.2 (column *E*), the average value of  $\beta/a$  is reduced to about 0.13, *i. e.* to 65 per cent of the real value. Accordingly, the elongation of an elongated nebula is highly overestimated. It may be remarked that the mean errors in the ratios  $\beta/a$  vary with the diameter ratio. The average mean errors are 0.015 (*A*), 0.023 (*B*), 0.017 (*C*), 0.012 (*D*), and 0.007 (*E*).

The final discussion of the results contained in the Appendix will be postponed until later on (section 7), when we have access to the true diameters and diameter ratios as determined from the photometer registrograms. The relations between the different observers may, however, be investigated here. It appears from the tables that the different diameter measures do not always agree very well. Although the differences may to a large extent represent accidental errors, a close inspection of the tables reveals that there are also differences between the individual observers of a systematic nature.

The average values of  $\beta/a$ , as computed from the 11 series, are in Table 3 given for the five observers. The mean errors, which are assumed to be the same for the different observers, have been derived from the average mean errors given above. The table shows that the final means  $\overline{\beta/a}$  (corresponding to the mean observer) range from  $0.128 \pm 0.002$  to  $1.003 \pm 0.004$ . The relations between the individual observers and the mean observer may now be investigated by means of the quotients  $\frac{\beta/a}{\overline{\beta/a}}$ .

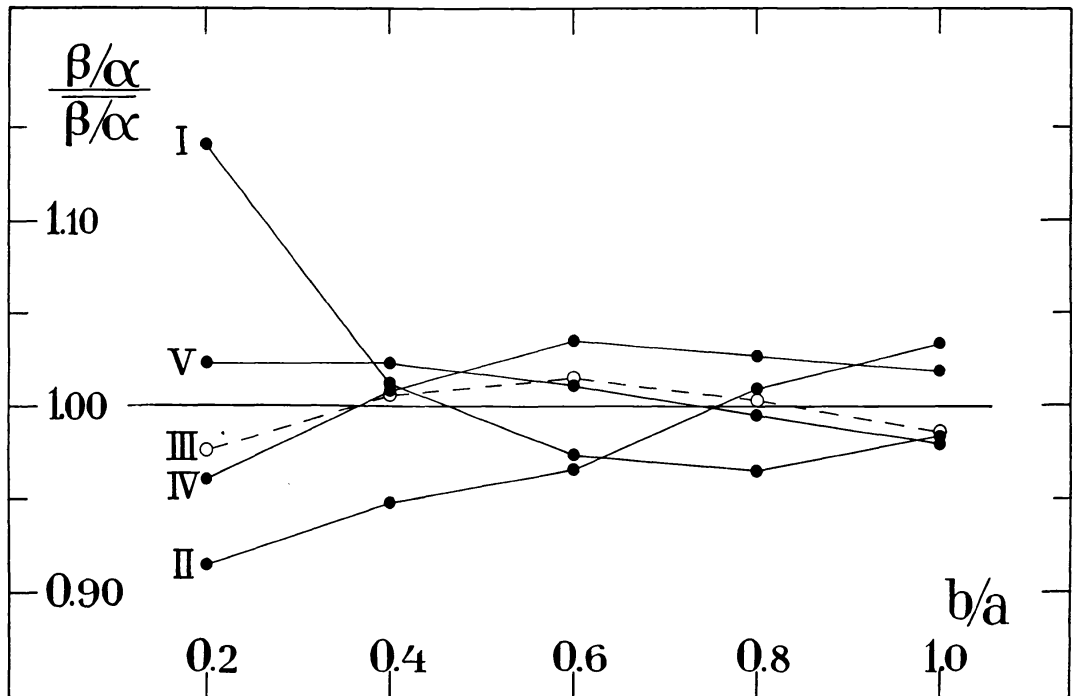


Fig. 6. Relations between the diameter ratios as measured by different observers. The curves refer to Lundmark (I), Reiz (II), Cederblad (III), Kristenson (IV), and the writer (V). The horizontal line represents the mean observer.

The systematic deviations of the diameter ratios of the five observers are shown by the curves of Fig. 6. The circles represent the quotients  $\frac{\beta/a}{\beta/a}$ , as computed from the above table. It appears that three of the observers (III, IV and V) agree very well with one another, and with the mean observer. The remaining two observers deviate from the others as regards the most elongated nebulae. These objects are measured less elongated by Lundmark, whereas Reiz's diameter values exaggerate the elongation. It is, *a priori*, to be expected that the measuring errors are not exactly the same for different observers. It will be shown in the next chapter that the diameters determined by K. Reinmuth for nebulae on the Heidelberg plates contain systematic errors which seem to agree very well with those obtained here for the mean observer.

**6. Measurement of the artificial nebulae in the photometer.** The diameters of all the 110 nebulae have been measured in a self-recording microphotometer. The photometer used in this case is of the Moll type,<sup>1</sup> and the registrograms are, as usually, obtained on photographic papers. The slit has, as projected on the emulsion of the plate, measured  $0.30 \times 0.02$  mm. The longer sides of the slit have always

<sup>1</sup> The photometer belongs to the Physical Institute of the Lund University. A description of the photometer is given by ORNSTEIN, MOLL, and BURGER in *Objektive Spektralphotometrie*, p. 60, Braunschweig, 1932.

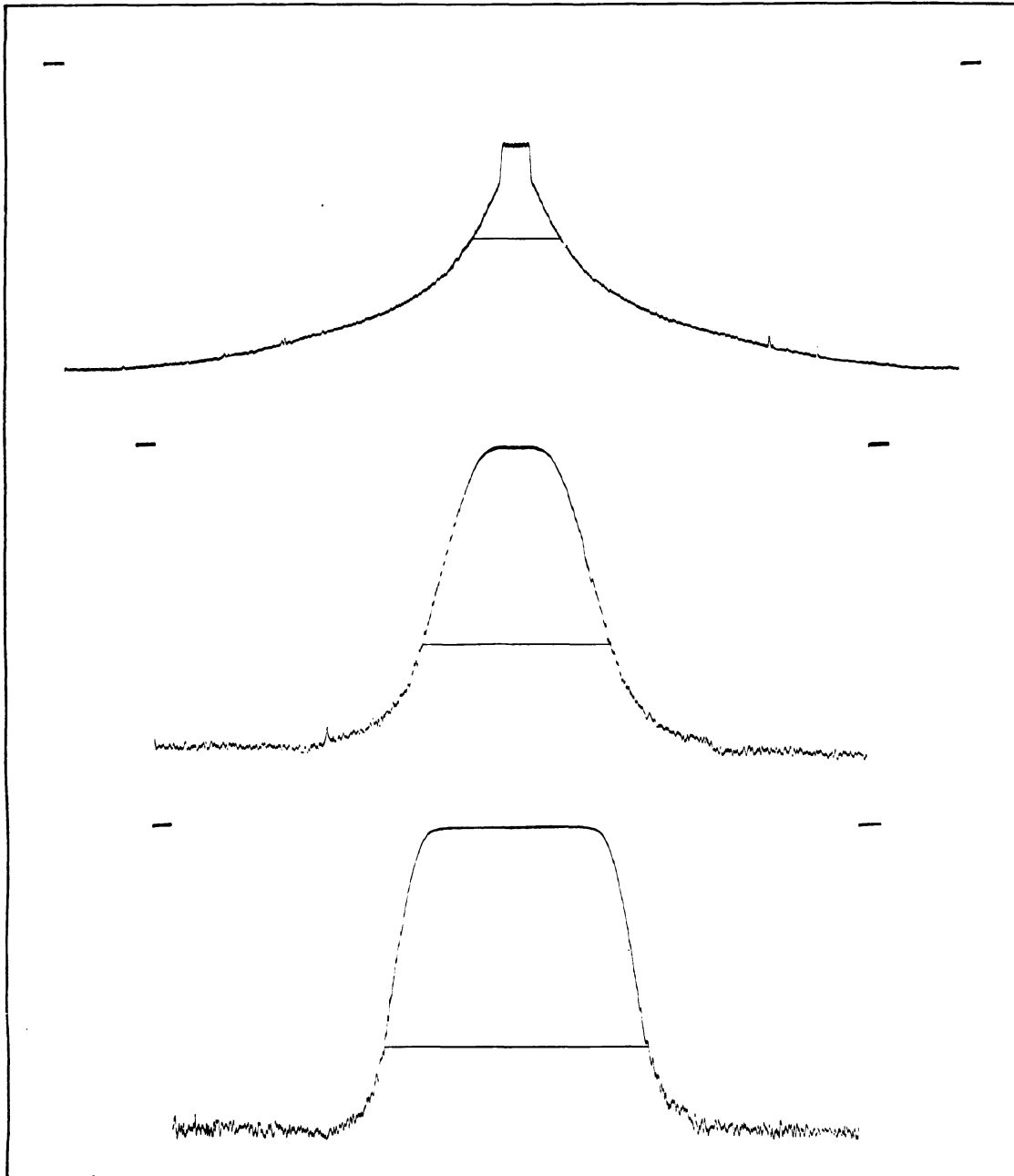


Fig. 7. Photometer tracings obtained for the major axes of three artificial nebulae. The light distributions are represented by the functions  $k r^{-1.0}$ ,  $k r^{-2.5}$ , and  $k r^{-7.0}$ .

been perpendicular to the motion of the plate holder. The linear enlargement on the registrograms has amounted to 7 times. The total galvanometer deflection, corresponding to clear plate *minus* zero point, has in most cases been adjusted to 8 cm.

All the nebulae have been measured along the major and the minor axes, and thus two tracings are obtained for each object. The registrograms corresponding

to the major axes of the distributions  $k r^{-1.0}$ ,  $k r^{-2.5}$ , and  $k r^{-7.0}$  are reproduced in Fig. 7. The curves give a good illustration of the large differences between the luminosity gradients corresponding to the different types of artificial nebulae. The straight horizontal lines indicate the minimum values of plate density perceivable in a visual inspection of the plates, *i. e.* the lengths of these lines are equal to the major diameters as given in the Appendix. The great superiority of the photometer to the human eye is clearly displayed.

The registrograms are first used for a determination of the major diameters of the nebulae. The tracings are measured by means of a millimeter scale. The derived diameters are, of course, most accurate in those cases, where the luminosity gradients are steep. For the nebulae with a light distribution of  $k r^{-0.5}$  it has not been possible to determine any reliable diameter values.

The photometric major diameters are given in Table 4. Each value represents the mean of the diameters obtained from the two plates. For the round nebulae (column *A*) the diameters range from 13.3 to 38.6 mm, whereas the most elongated nebulae (column *E*) have diameters from 10.9 to 35.0 mm. The diameters are slightly dependent on the diameter ratio. There is an average decrease in the diameters of about 10 per cent when the diameter ratio changes from 1.0 to 0.2. This apparently depends on the fact that the surface brightness of the light sectors is related to the inclination angle  $\varphi$ , as defined in Fig. 1. The surface brightness gets somewhat smaller as the inclination increases (Cf. section 3).

The above table also gives the ratios of the minor and major diameters. These diameter ratios represent the means of the ratios obtained for three different plate densities, namely 0, 25, and 50 per cent density. The major and minor diameters corresponding to these densities have been measured on the registrograms, and the ratios have been computed. Thus, each of the tabulated values represents the mean of six determinations. If all the distributions are taken together, the following average ratios are obtained: 1.001 (*A*), 0.804 (*B*), 0.605 (*C*), 0.407 (*D*), and 0.203 (*E*). We find that the average ratios agree rather well with the values of  $\cos \varphi$  (Cf. section 2). The mean errors of the tabulated ratios, as computed from the individual deviations, have on an average the following values: 0.006 (*A*), 0.005 (*B*), 0.003 (*C*), 0.003 (*D*), and 0.002 (*E*). The mean error decreases as the diameter ratio gets smaller.

**7. The results.** The photometric diameters obtained above will now be compared to the diameters determined visually. A comparison between Table 4 and the tables given in the Appendix reveals that the former diameters are considerably larger than the latter ones. The visual diameters generally refer only to the central parts of the nebulae.

In Table 5 the visually determined diameters  $a$  and  $\beta$  are expressed in per cent of the photometric diameters  $a$  and  $b$ . The ratio of the two major diameters, and of the two minor diameters, has been computed for each of the nine light distributions  $k r^{-n}$ , the exponent  $n$  ranging from 1.0 to 7.0. We find that the

TABLE 4.

*Average values of the major diameter ( $a$ ) and the diameter ratio ( $b/a$ ), as obtained from the photometer registograms.*

Light distribution	A	B	C	D	E
$k r^{-0.5}$	— 0.989	— 0.803	— 0.596	— 0.401	— 0.195
$k r^{-1.0}$	38.6 mm 1.000	37.9 mm 0.799	35.7 mm 0.636	36.8 mm 0.433	35.0 mm 0.206
$k r^{-1.5}$	27.5 1.004	27.1 0.796	26.2 0.591	25.7 0.394	23.8 0.202
$k r^{-2.0}$	22.8 0.996	23.3 0.812	22.1 0.630	21.2 0.416	20.9 0.207
$k r^{-2.0}$	22.1 0.998	21.8 0.797	21.4 0.571	21.1 0.396	20.5 0.203
$k r^{-2.5}$	20.1 1.025	20.1 0.811	20.0 0.612	18.6 0.421	18.4 0.206
$k r^{-3.0}$	17.1 1.009	16.7 0.811	16.7 0.602	14.6 0.395	14.3 0.210
$k r^{-4.0}$	13.3 0.994	12.5 0.792	11.9 0.593	11.8 0.402	10.9 0.205
$k r^{-5.0}$	15.9 1.001	15.8 0.805	15.7 0.601	15.5 0.403	15.3 0.201
$k r^{-6.0}$	19.6 0.996	18.9 0.808	18.5 0.616	18.0 0.408	17.4 0.203
$k r^{-7.0}$	19.3 1.002	18.8 0.805	18.6 0.609	18.4 0.412	18.1 0.199

minimum value of these ratios amounts to only 11 per cent, whereas the maximum value is 79 per cent.

A study of the table shows that the ratios of the diameters are smallest for  $n$  equal to 1.0, and largest when  $n$  is equal to 7.0. Thus, the not unexpected result is obtained, that *the systematic errors in the visually determined diameters are highly dependent on the steepness of the light distribution curve*. It may be assumed, that the diameter errors will grow rather small when the exponent  $n$  becomes larger than 7.0, and that they will approach zero when the exponent approaches infinity.

The table also shows, that the diameters  $\alpha$  and  $\beta$  depend on the elongation of the nebulae. When the diameter ratio  $b/a$  changes from 1.0 to 0.2, the average value of  $a/a$ , as given at the bottom of the table, increases from 43.9 to 59.3 per cent, and  $\beta/b$  decreases from 44.0 to 40.9 per cent. *Thus, the major diameter  $a$  increases as the elongation of the nebula becomes larger, whereas the minor*

TABLE 5.

*The visual diameters,  $\alpha$  and  $\beta$  (mean observer), expressed in per cent of the true (photometric) diameters,  $a$  and  $b$ .*

Light distribution	$b/a=1.0$	$b/a=0.8$	$b/a=0.6$	$b/a=0.4$	$b/a=0.2$
$k \ r-1.0$	$\alpha/a=11.1 \%$ $\beta/b=11.0$	12.6 % 12.0	15.7 % 11.8	18.3 % 11.2	26.5 % 11.0
$k \ r-1.5$	21.9 21.2	22.8 19.7	24.7 20.3	31.9 20.5	39.4 18.5
$k \ r-2.0$	37.0 37.2	39.1 34.5	43.8 37.2	47.9 32.8	56.4 31.6
$k \ r-2.0$	30.7 31.7	32.9 31.5	38.1 31.2	43.2 28.6	50.1 28.1
$k \ r-2.5$	45.3 45.0	46.8 44.3	46.9 40.8	53.2 40.7	56.8 35.6
$k \ r-3.0$	47.7 47.7	49.2 48.4	51.4 46.4	60.5 45.9	65.3 44.0
$k \ r-4.0$	55.0 55.3	58.8 58.4	63.1 60.2	65.8 58.9	75.0 57.4
$k \ r-5.0$	60.6 60.6	61.1 59.8	63.3 60.7	65.4 58.7	67.6 51.0
$k \ r-6.0$	63.1 62.8	66.0 63.9	68.9 63.3	72.9 64.6	78.9 65.4
$k \ r-7.0$	66.9 67.0	68.7 67.3	69.8 66.7	71.7 64.0	77.2 66.7
means	43.9 % 44.0	45.8 % 44.0	48.6 % 43.9	53.1 % 42.6	59.3 % 40.9

*diameter  $\beta$  grows smaller.* These diameter errors will apparently produce a rather serious systematic error in the ratio  $\beta/\alpha$ : the elongated nebulae are measured too elongated.

The systematic errors in the visual diameters are illustrated by the curves given in Fig. 8. The ratios  $\alpha/a$  (full curves) and  $\beta/b$  (broken curves) have been plotted against the diameter ratio  $b/a$ . Six pairs of curves are given, corresponding to different luminosity functions. The large systematic errors in the diameters are clearly displayed. The full curves and the broken curves, which agree very nicely for  $b/a=1.0$ , become more and more separated as the ratio  $b/a$  grows smaller.

In Chapter III of this paper an investigation will be made of the orientation of the spiral nebulae with respect to the celestial plane. The material of nebulae used for this investigation will be selected by means of the apparent major diameters of the objects, *i. e.* the diameters are used as distance indicators. It is very important, that the nebulae of different elongations are collected from the same volume of space. Consequently, the distance indicator must not be related to the ratio of the minor and major diameters. The major diameters of the nebulae,



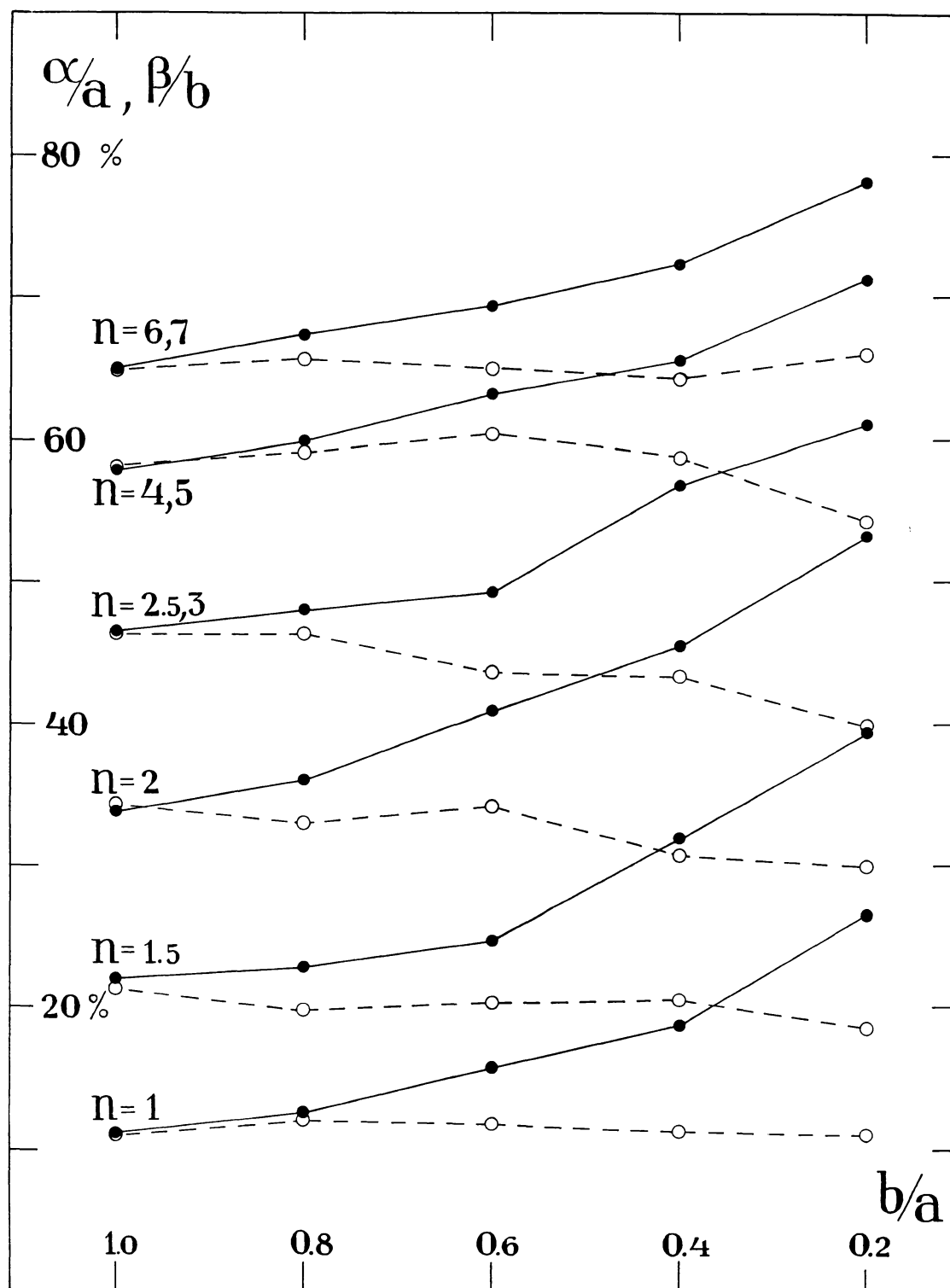


Fig. 8. The visually measured diameters  $a$  and  $\beta$  expressed in per cent of the photometric diameters  $a$  and  $b$ . The full curves refer to the major diameters, whereas the minor diameters are represented by the broken curves.

TABLE 6.

*Smoothed values of the quotient  $a'/a'_r$ . The table shows the relative increase in the visual major diameter, as the diameter ratio  $b/a$  decreases from 1.0 to 0.1.*

$b/a$	$k\ r^{-1.5}$	$k\ r^{-2.0}$	$k\ r^{-2.5}$	$k\ r^{-3.0}$	$k\ r^{-4.0}$	$k\ r^{-5.0}$
1.0	100 %	100 %	100 %	100 %	100 %	100 %
0.9	103	102	102	102	102	101
0.8	108	105	104	104	104	103
0.7	114	110	108	107	106	105
0.6	123	115	112	110	108	107
0.5	133	123	117	114	111	110
0.4	146	132	124	119	115	113
0.3	161	142	131	125	119	117
0.2	179	154	140	131	124	121
0.1	—	169:	150:	139:	131:	127:

as measured visually on the plates, must be corrected, *i. e.* they must be reduced to the values corresponding to  $b/a = 1.0$ . The reduction may be made by means of the figures given in Table 6. Here, the ratio  $a/a$  has been denoted by  $a'$ , whereas  $a'_r$  means the value of  $a/a$  corresponding to a round nebula ( $b/a = 1.0$ ). The table gives, for six different distributions of light, the quotient  $a'/a'_r$  as a function of the diameter ratio  $b/a$ . The tabulated values show the *relative* increase in the diameter  $a$ , as the ratio  $b/a$  grows smaller. If the visually determined diameters are divided by these values, they will be independent of the orientation of the nebulae. It may be remarked that the values given in the table represent *smoothed* values, as derived from Table 5, and that they refer to the mean observer.

After this discussion of the major and minor diameters we will turn our interest to the systematic errors in the diameter ratio  $\beta/a$ . We have found above, that the major diameter of a nebula is generally measured too large as compared to the minor diameter, which results in an overestimation of the elongation of the object. The systematic effect may be studied in Table 7, where the visually measured ratios  $\beta/a$  are compared to the true (photometric) ratios  $b/a$ . The quotients  $\frac{\beta/a}{b/a}$  have been computed for the ten different distributions of light. It may be remarked that the values refer, as before, to the mean observer.

The mean values given at the bottom of the table show that, for round nebulae, the ratio of the diameters  $\beta$  and  $a$  also equals unity. When the elongation of the nebulae increases, the ratio becomes systematically too small, and it amounts to only 63 per cent of the true value in the last group ( $b/a = 0.2$ ). However, the systematic error also depends on the form of the light distribution function, or rather on the steepness of the luminosity gradient. When the exponent  $n$  in the function  $k\ r^{-n}$  changes from 0.5 to 7.0, the quotient  $\frac{\beta/a}{b/a}$  increases from 43 to 86

TABLE 7.

The visual diameter ratios,  $\beta/a$  (mean observer), expressed in per cent of the true (photometric) ratios,  $b/a$ .

Light distribution	$b/a=1.0$	$b/a=0.8$	$b/a=0.6$	$b/a=0.4$	$b/a=0.2$
$k r^{-0.5}$	101.1 %	74.8 %	64.1 %	52.9 %	42.6 %
$k r^{-1.0}$	98.6	94.7	75.3	61.2	41.3
$k r^{-1.5}$	96.9	86.6	82.1	64.5	47.0
$k r^{-2.0}$	100.5	88.2	84.9	68.5	56.0
$k r^{-2.0}$	103.3	95.7	81.8	66.2	56.2
$k r^{-2.5}$	99.5	94.6	87.3	76.7	62.6
$k r^{-3.0}$	100.0	98.3	90.2	75.9	67.1
$k r^{-4.0}$	100.5	99.2	95.4	89.6	76.1
$k r^{-5.0}$	99.9	97.9	95.8	89.8	75.6
$k r^{-6.0}$	99.4	96.9	92.0	88.5	82.8
$k r^{-7.0}$	100.1	97.9	95.6	89.3	86.4
mean	100.0 %	93.2 %	85.9 %	74.8 %	63.1 %

per cent, according to the values given in the last column of the table. We may assume that, for still larger values of  $n$ , the quotient will approach unity.

The relation between the quotient  $\frac{\beta/a}{b/a}$  and the distribution function is illustrated in Fig. 9. The full circles give the values of the quotient corresponding to the five different values of  $b/a$ . The smoothed curves, which represent certain theoretical expressions to be discussed below, agree very well with the observed values. Only for the distributions  $k r^{-0.5}$  and  $k r^{-1.0}$  certain systematic deviations are indicated. It must, however, be remarked that nebulae with such small luminosity gradients are very difficult to measure. When the exponent  $n$  decreases, the different curves approach the vertical axis corresponding to  $n=0$ . On the other hand, the curves approach the horizontal axis  $\frac{\beta/a}{b/a} = 1.0$ , when the exponent grows larger. The full circles corresponding to  $b/a = 1.0$  agree very nicely with the latter axis. The deviations of the individual values from the smoothed curves may be considered as accidental errors. The dispersion in the deviations corresponds approximately to the mean errors in the ratios  $\beta/a$  and  $b/a$ , as derived above.

The systematic errors in the ratios  $\beta/a$  are explained by the fact that the parts of an elongated nebula corresponding to the extremities of the major axis are more easily perceived against the background fog of the plate than the parts corresponding to the extremities of the minor axis. Let us denote the apparent light distribution along the major axis of a nebula by  $F(2r)$ . The distribution along the minor axis may then be put equal to  $F(2r/q)$ ,  $q$  being the true diameter ratio  $b/a$ . The following relations are obtained between the minimum values of surface brightness  $F(a)$  and  $F(b/q)$ , as corresponding to the minimum values of plate density measurable in the photometer, and the visual minimum values  $F(\alpha)$  and  $F(\beta/q)$ :

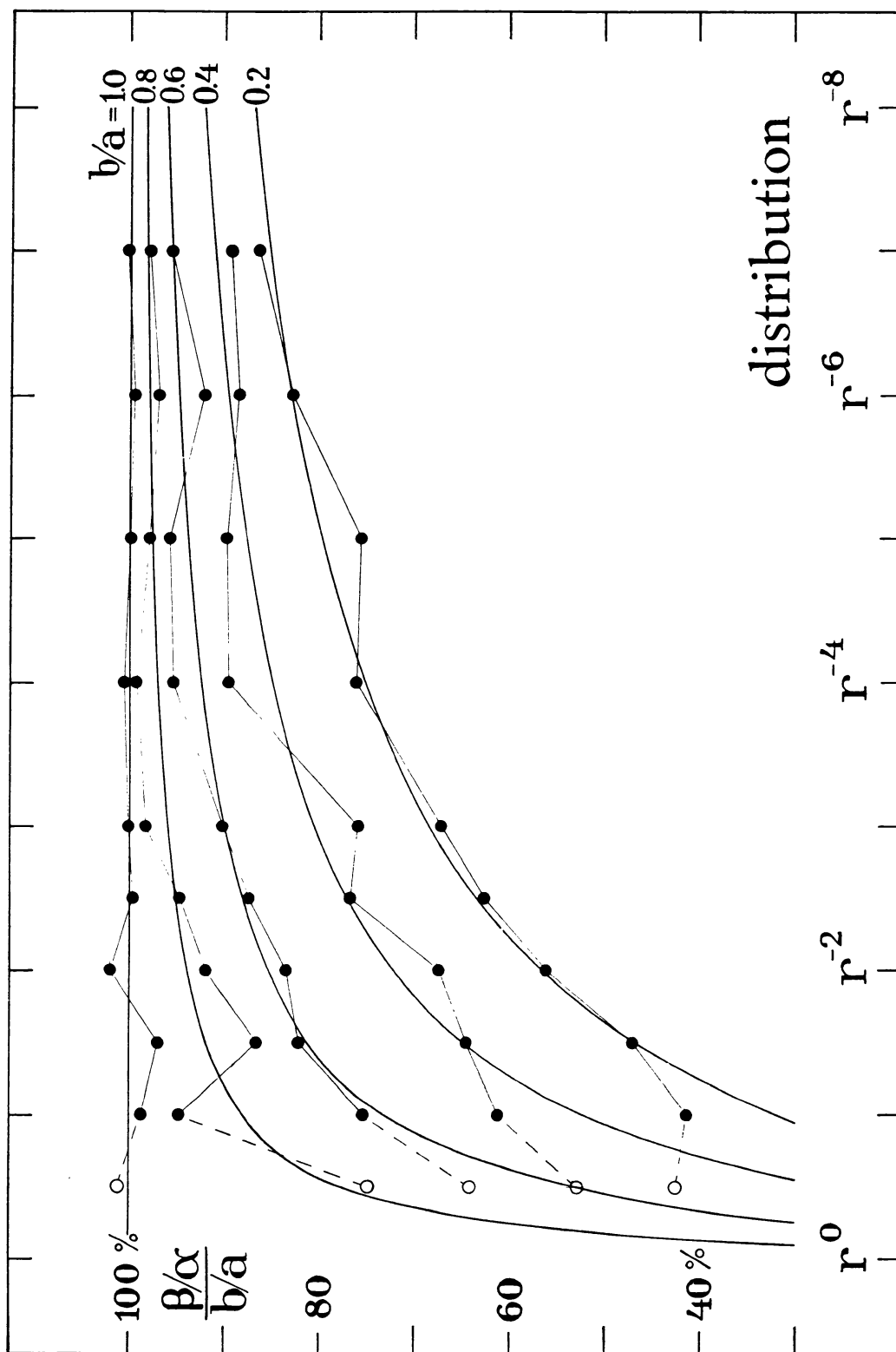


Fig. 9. Relation between the quotient  $\frac{\beta/\alpha}{b/a}$  and the light distribution function. The different curves correspond to different values of the true diameter ratio  $b/a$ .

$$\begin{aligned}
F(a) &= F(b/q) \\
F(\alpha) &= p_\alpha F(a) > F(a) \\
F(\beta/q) &= p_\beta F(b/q) > F(b/q) \\
F(\alpha) &= p_\alpha/p_\beta F(\beta/q)
\end{aligned} \tag{3}$$

If the minimum values  $F(a)$  and  $F(b/q)$  are put equal to unity, the factors  $p_\alpha$  and  $p_\beta$  represent the minimum values of surface brightness that correspond to the smallest values of plate density perceivable in a visual inspection of the plate. The above investigation has shown, that the factor  $p_\alpha$  is generally smaller than  $p_\beta$ , and that both of them are larger than unity. If the factors had the same value,  $F(\alpha)$  would be equal to  $F(\beta/q)$  and, consequently,  $\beta/\alpha$  equal to  $b/a$ .

In the present case, the distribution function  $F(2r)$  is equal to  $kr^{-n}$ . By introducing this expression into the above relations, the following equations are obtained:

$$\begin{aligned}
p_\alpha &= (a/\alpha)^n \\
p_\beta &= (b/\beta)^n \\
p_\alpha/p_\beta &= \left( \frac{\beta/\alpha}{b/a} \right)^n
\end{aligned} \tag{4}$$

Thus, the numerical values of the factors  $p_\alpha$  and  $p_\beta$  may be computed from the photometric and the visual diameters derived above. The resulting values are given in Table 8, and they clearly display the great differences in sensitivity between the photometer and the eye. The smallest  $p$ -value amounts to about 3, and it refers, of course, to the major axis of one of the most elongated nebulae. According to the means given at the bottom of the table the value of  $p_\alpha$  decreases from 10.9 to 4.3, when the diameter ratio  $b/a$  changes from 1.0 to 0.2, whereas  $p_\beta$  increases from 10.9 to 13.7. The table also shows the dependence of the factors on the form of the light distribution function. The sensitivity of the eye appears to grow larger, as the luminosity gradient gets less steep. For the function  $kr^{-1.0}$ , the values of  $p_\alpha$  and  $p_\beta$  are approximately only half as large as those corresponding to the function  $kr^{-7.0}$ . In spite of this, the systematic errors in the visually measured diameters are largest in the first case, as has been shown above.

It may be remarked, that the values given in the above table presumably depend also on the photographic plates and on the developing procedure. The steepness of the calibration curve of the plate may have a certain influence on the values of the factors  $p$ . The plates used in the present case have been described in section 4.

The quantity  $p_\alpha/p_\beta$  represents the quotient of the minimum surface brightness corresponding to the major axis and the minimum value corresponding to the minor axis. This ratio is of a certain interest, and the numerical values have been computed in Table 9. For elongated nebulae, the ratio is always smaller than unity. It appears from the table that  $p_\alpha/p_\beta$  is independent of the form of the luminosity function and that it, consequently, depends only on the diameter ratio  $b/a$ . The average values (with mean errors), which are given at the bottom of the table,

TABLE 8.

*Resulting values of the factors  $p_\alpha$  and  $p_\beta$  (mean observer).*

Light distribution	$b/a=1.0$	$b/a=0.8$	$b/a=0.6$	$b/a=0.4$	$b/a=0.2$
$k\ r^{-1.0}$	$p_\alpha=9.0$	7.9	6.4	5.5	3.8
	$p_\beta=9.1$	8.3	8.5	8.9	9.1
$k\ r^{-1.5}$	9.8	9.2	8.1	5.5	4.0
	10.2	11.4	10.9	10.8	12.6
$k\ r^{-2.0}$	7.3	6.5	5.2	4.4	3.1
	7.2	8.4	7.2	9.3	10.0
$k\ r^{-2.0}$	10.6	9.2	6.9	5.4	4.0
	10.0	10.1	10.3	12.2	12.7
$k\ r^{-2.5}$	7.2	6.7	6.6	4.8	4.1
	7.4	7.7	9.4	9.5	13.2
$k\ r^{-3.0}$	9.2	8.4	7.4	4.5	3.6
	9.2	8.8	10.0	10.3	11.7
$k\ r^{-4.0}$	10.9	8.4	6.3	5.3	3.2
	10.7	8.6	7.6	8.3	9.2
$k\ r^{-5.0}$	12.2	11.8	9.8	8.4	7.1
	12.2	13.1	12.1	14.4	29.0
$k\ r^{-6.0}$	15.9	12.1	9.3	6.7	4.1
	16.3	14.7	15.6	13.8	12.8
$k\ r^{-7.0}$	16.7	13.8	12.4	10.3	6.1
	16.5	16.0	17.0	22.7	17.0
means	10.9	9.4	7.8	6.1	4.3
	10.9	10.7	10.9	12.0	13.7

TABLE 9.

*Resulting values of the quotient  $p_\alpha/p_\beta$  (mean observer).*

Light distribution	$b/a=1.0$	$b/a=0.8$	$b/a=0.6$	$b/a=0.4$	$b/a=0.2$
$k\ r^{-0.5}$	(1.01)	(0.86)	(0.80)	(0.73)	(0.65)
$k\ r^{-1.0}$	0.99	0.95	0.75	0.61	0.41
$k\ r^{-1.5}$	0.95	0.81	0.74	0.52	0.32
$k\ r^{-2.0}$	1.01	0.78	0.72	0.47	0.31
$k\ r^{-2.0}$	1.07	0.92	0.67	0.44	0.32
$k\ r^{-2.5}$	0.99	0.87	0.71	0.52	0.31
$k\ r^{-3.0}$	1.00	0.95	0.73	0.44	0.30
$k\ r^{-4.0}$	1.02	0.97	0.83	0.64	0.34
$k\ r^{-5.0}$	1.00	0.90	0.81	0.58	0.25
$k\ r^{-6.0}$	0.96	0.83	0.61	0.48	0.32
$k\ r^{-7.0}$	1.01	0.86	0.73	0.45	0.36
mean	1.00	0.88	0.73	0.52	0.32
	$\pm .009$	$\pm .021$	$\pm .017$	$\pm .023$	$\pm .010$



TABLE 10.

*Smoothed values of the quotient  $\frac{\beta/a}{b/a}$  (mean observer).*

$b/a$	$k r-1.5$	$k r-2.0$	$k r-2.5$	$k r-3.0$	$k r-4.0$	$k r-5.0$
1.0	100.0 %	100.0 %	100.0 %	100.0 %	100.0 %	100.0 %
0.9	96.0	97.0	97.5	98.0	98.5	98.8
0.8	91.8	93.8	95.0	95.8	96.9	97.5
0.7	86.9	90.0	91.9	93.2	94.9	95.9
0.6	81.1	85.4	88.2	90.0	92.4	93.9
0.5	73.5	79.4	83.1	85.7	89.1	91.2
0.4	64.7	72.1	77.0	80.4	84.9	87.7
0.3	55.2	64.0	70.0	74.3	80.0	83.7
0.2	46.8	56.6	63.4	68.4	75.2	79.6
0.1	39.	49.	57.	62.	70.	75.

range from 1.00 for the round nebulae to 0.32 for the most elongated objects. The dispersion of the individual values in each column may be entirely explained as a result of the accidental measuring errors. However, the values corresponding to the function  $k r^{-0.5}$  have not been included in the final means. Nebulae with a light distribution of this type are extremely difficult to measure, and the derived diameter values are rather uncertain.

Since the quotient  $p_a/p_\beta$  is independent of the light distribution function, we may assume, that it is also independent of the function representing the distribution of silver grains on the plate. Consequently, the quotient is independent of the steepness of the calibration curve. This result is of a certain importance, since it implies, that the average values derived in Table 9 do not depend on the qualities of the photographic plates used, or on the developing procedure.

The smoothed curves which have been given in Fig. 9 above are based on the average values of  $p_a/p_\beta$  computed in Table 9. The relation between this quotient and  $\frac{\beta/a}{b/a}$  is given by the third equation in formula (4). As might be expected, the smoothed curves derived in this way represent the individual observations very well.

In investigations of the orientation in space of the extragalactic nebulae the ratios of the minor and major diameters of the objects must be corrected for the systematic measuring errors. The correction factors contained in Table 10 represent the smoothed values of the quotient  $\frac{\beta/a}{b/a}$  corresponding to the above average values of  $p_a/p_\beta$ . The corrected diameter ratios  $b/a$  are obtained by a division of the visual ratios by these factors. It may be recollected that the correction factors refer to the mean observer, as defined above.

## CHAPTER II.

**Investigation of the diameters given in Reinmuth's catalogue.**

**8. Reinmuth's catalogue of nebulae.** One of the most complete and homogeneous collections of nebular data has been given by K. REINMUTH<sup>1</sup> in his large catalogue *Die Herschel-Nebel*. The catalogue is based on several thousand plates taken with three different telescopes. The main instrument has been the Bruce refractor, having a focal distance of 202 cm. The catalogue comprises all *General Catalogue* objects north of declination  $-20^\circ$ , the total number of nebulae (and clusters) amounting to 4445. For these objects the positions have been corrected and the descriptions revised. The types of the nebulae are given in Wolf's classification scheme, the different types being denoted by letters from *a* to *w*.

The catalogue gives the apparent major and minor diameters, as measured by Reinmuth, for practically all of the nebulae, *i. e.* for all objects having a measurable size. The diameters, which are given in tenths of a minute of arc, have been measured by means of a small scale and an eyepiece having a magnifying power of about five times. It may be remarked that, on the Bruce plates, one minute of arc corresponds to 0.59 mm.

**9. Relation between Reinmuth and the Mean Observer.** In the following chapters, the diameters given in Reinmuth's catalogue will be used for investigations of the orientation in space of the extragalactic nebulae. The inclination of a spiral nebula to the celestial plane is indicated by the ratio of the apparent minor and major diameters. The spirals may, at least from a statistical point of view, be treated as spheroidal discs, and their inclinations are intimately connected with the apparent elongations. However, the apparent diameters, as measured by scale and eyepiece, contain serious systematic errors, as has been shown in the first chapter of this paper. The following investigation will deal with the systematic errors in Reinmuth's diameter values.

The diameter errors derived in the first chapter are referred to a certain *mean observer*, representing the mean of five individual observers. The first step in the investigation will be to try to find the relation between Reinmuth and this mean observer. For this purpose, we may use two catalogues of nebulae which are also

---

<sup>1</sup> Heidelberg Veröff 9, 1926.

based on the Heidelberg plate material. The first catalogue, which has been collected by the writer,<sup>1</sup> contains 1854 components of double and multiple systems to be found on the Bruce plates. The second catalogue has been published by A. REIZ,<sup>2</sup> and it comprises all nebulae in the north galactic cap ( $b = 50^\circ - 90^\circ$ ) appearing on the Bruce plates, in all 4666 objects. Both Reiz and the writer are included among the above five observers, and the relations between their diameter ratios and the ratios corresponding to the mean observer are obtained from Table 3 and Fig. 6.

TABLE 11.

*Investigation of Reinmuth's diameter ratios.*

A. Comparison between Reinmuth (Rh) and Holmberg (Hg).

$(\beta/\alpha)_{Hg}$	Number	$\overline{(\beta/\alpha)}_{Hg}$	$\overline{(\beta/\alpha)}_{Rh}$	Rh - Hg
$\leq 0.20$	30	0.145	0.147	+1.4 %
.21 - .30	20	0.250	0.248	-0.8
.31 - .50	24	0.417	0.404	-3.1
.51 - .80	20	0.661	0.672	+1.7

B. Comparison between Reinmuth (Rh) and Reiz (Rz).

$(\beta/\alpha)_{Rz}$	Number	$\overline{(\beta/\alpha)}_{Rz}$	$\overline{(\beta/\alpha)}_{Rh}$	Rh - Rz
$\leq 0.20$	70	0.147	0.163	+10.9 %
.21 - .30	48	0.262	0.276	+ 5.3
.31 - .50	56	0.405	0.429	+ 5.9
.51 - .80	31	0.632	0.651	+ 3.0

C. Comparison between Reinmuth and the Mean Observer.

$(\beta/\alpha)_{Rh}$	Reinmuth - Mean Observer		
	Comp. with Hg	Comp. with Rz	Mean
0.15	+3.7 %	+2.3 %	+3.0 %
0.26	+1.5	-0.6	+0.4
0.42	-1.7	+1.7	0.0
0.66	+1.7	+2.6	+2.2

In Table 11 A a comparison is made between the diameter ratios as determined by Reinmuth and by the writer. Only those nebulae, in common to both catalogues, have been included which have major diameters larger than, or equal to 2.0

<sup>1</sup> Lund Ann 6, 1937.

<sup>2</sup> Lund Ann 9, 1941.

according to both sources. Diameter values, which are denoted as uncertain, have been rejected. Furthermore, seven objects have been excluded on account of very large differences between the measured ratios.<sup>1</sup> There remain 94 nebulae which have diameter ratios smaller than, or equal to 0.80, as measured by the writer. The average values of the ratios  $\beta/\alpha$  have been computed for four different intervals of  $(\beta/\alpha)_{Hg}$ , as appears from the table. There seems to be a good agreement between the two catalogues as regards the ratios of the apparent diameters. The average differences Reinmuth *minus* Holmberg range from  $-3.1$  to  $+1.7$  per cent. The differences seem to be of a more or less accidental nature.

The result of a similar comparison between Reinmuth and Reiz is shown in Table 11 B. The material has been selected in the same way as above. In this case, 16 objects have been excluded on account of too large differences between the diameter ratios. There remain 205 nebulae with values of  $(\beta/\alpha)_{Rz}$  smaller than, or equal to 0.80. The table shows, that there is a certain systematic difference between the diameter ratios of the two catalogues. Reinmuth's ratios are, on an average, larger than those given by Reiz. The difference Reinmuth *minus* Reiz amounts to  $+10.9$  per cent for the most elongated objects.

The determination of the relation between Reinmuth and the mean observer will now be based on the above two comparisons. By means of the curves II and V in Fig. 6, the differences  $Rh - Hg$  and  $Rh - Rz$  are transformed into the corresponding differences Reinmuth *minus* mean observer. The results, as obtained for the four classes of  $\beta/\alpha$ , appear in the second and third columns of Table 11 C. The mean values given in the fourth column show that the maximum difference amounts to only about 3 per cent. Thus the diameter ratios, as computed from Reinmuth's catalogue, agree very well with the values corresponding to the mean observer. We may conclude that the systematic corrections, which have been derived in the previous chapter for the mean observer, may without any change be applied also to Reinmuth's catalogue.

It may be remarked that the above result is based on the assumption that the measuring errors, as made by Reiz and by the writer, have not changed during the past 5 à 10 years. The material contained in Reiz's catalogue has been collected during the years 1937 and 1938, whereas the writer's catalogue was completed in 1936. A comparison between the two catalogues gives a relation between the two sets of  $\beta/\alpha$ -values that is practically the same as that obtained in the previous chapter from the measurements of the artificial nebulae. It seems reasonable to assume that the measuring errors of both observers have remained unchanged.

**10. Reinmuth's diameter ratios for elliptical nebulae.** It has been shown above, that Reinmuth's measuring errors agree very well with the errors corresponding to the mean observer, as defined in the previous chapter. However, it would be of great interest if Reinmuth's diameter ratios could be compared directly to the ratios

---

<sup>1</sup> Some of these nebulae belong to the special types of spirals, as *e.g.* the Wolf type *v*, for which the major and minor axes cannot be properly defined.

that are obtained in photometric measurements of extragalactic nebulae. In a comparison of this kind it is advisable to divide the material into two groups: elliptical nebulae and spirals. It seems to be established that the light distribution in the former kind of nebulae is approximately of the form<sup>1</sup>  $k r^{-2}$ . At the edges of the spirals, as corresponding to the measured diameters, the luminosity gradient generally seems to be somewhat steeper, and may correspond to a luminosity function of the form  $k r^{-3}$ , or  $k r^{-4}$ . It has been shown in the previous chapter that the measuring errors in the diameters depend on the steepness of the light distribution curve.

All the photometric data available as regards the diameters of elliptical nebulae have been collected in Table 12. The measurements have been made by E. HUBBLE,<sup>2</sup> and by R. O. REDMAN and E. G. SHIRLEY.<sup>3</sup> Hubble's list contains 10 nebulae which have been measured along the major and minor axes. The latter authors have given data for 15 elliptical objects. The diameter ratios which are given in the fourth column of the table represent the quotients of the constants  $a$  contained in Table IV in Hubble's paper. The ratios in the fifth and sixth columns have been derived from those isophotes, as given by Redman and Shirley, the major diameters of which are equal to Reinmuth's diameters. The ellipticity of an elliptical nebula seems to depend to a certain degree on the distance from the centre of the object. Two of the nebulae in the table have diameter ratios determined by two authorities. In the case of NGC 221 the agreement between the two values is good. The values given for NGC 4649 do not agree so well; their mean may be provisionally accepted as the most probable diameter ratio.

All the 23 nebulae contained in the above table are included in Reinmuth's catalogue. The major and minor diameters, as given in the catalogue, are reproduced in the second column of the table. The diameter ratios have been computed for 18 nebulae, objects with uncertain diameter values or with major diameters smaller than 0.5 being excluded. The quotients of the visually measured diameter ratios  $\beta/a$  and the true (photometric) ratios  $b/a$  are given in the last column. The quotients range from 44 to 123 per cent, the average value being 82 per cent. They are all, except two, smaller than unity.

The eighteen values of  $\frac{\beta/a}{b/a}$  have in Fig. 10 been plotted against the true ratios  $b/a$ . The curved line represents the relation obtained by the mean observer for the artificial nebulae which have a light distribution of  $k r^{-2.0}$  (Cf. Table 10). *The majority of the elliptical nebulae agree very well with this relation.* The largest deviations are found for NGC 2672, 2768, 3379, and 4374. For the remaining 14 objects two mean values of  $\frac{\beta/a}{b/a}$  have been computed, corresponding to the groups

<sup>1</sup> According to HUBBLE's investigations of fifteen elliptical nebulae the distributions of light in these objects may be represented by the function  $k(r+a)^{-2}$ . However, the constant  $a$  may be neglected when the distance  $r$  is put equal to half the diameter of the object.

<sup>2</sup> Mt Wilson Contr 398, ApJ 71, p. 231, 1930.

<sup>3</sup> MN 96, p. 588, 1936 and MN 98, p. 613, 1938.

TABLE 12.

*Comparison between Reinmuth's diameter ratios ( $\beta/a$ ) and the diameter ratios ( $b/a$ ) obtained from photometric measurements. (Elliptical nebulae.)*

Object	$\alpha \times \beta$ (Reinmuth)	$\beta/a$	$b/a$			$\frac{\beta/a}{b/a}$
			Hubble	Redman	Redm. — Shirl.	
NGC 205	11'0" × 5'0"	0.45			0.65	69 %
221	2.9 2.0	0.69	0.81	0.79		86
410	0.4 0.4	—	0.77			—
2672	0.75 0.4	0.53		0.92		58
2693	0.4 0.3	—			0.80	—
2768	4.5 1.0	0.22		0.50		44
3115	4.0 0.7	0.18	0.28			64
3377	2.0 0.8	0.40			0.44	91
3379	2.7 1.7	0.63			0.94	67
3605	0.55 0.3	0.55		0.65		85
3607	1.45 0.9	0.62		0.82		76
3608	1.1? 0.8?	—		0.85		—
3610	1.0 0.7	0.70			0.72	97
4111	3.8 0.5	0.13			0.22	59
4278	1.5? 1.5?	—	0.67			—
4374	2.0 1.8	0.90	0.73			123
4382	4.0 2.0	0.50	0.56			89
4406	3.4? 2.5	0.74	0.75			99
4472	4.0 3.0	0.75	0.73			103
4621	2.4 1.2	0.50	0.54			93
4649	2.7 2.2	0.81	0.72		0.95	97
5557	0.7? 0.7?	—			0.80	—
7454	0.7 0.4	0.57			0.69	83

mean 82 %

$b/a \leq 0.65$  and  $b/a > 0.65$ . The means, which in the figure are represented by open circles, fall almost exactly on the mean observer's curve. The deviations of the diameter ratios of the individual nebulae depend, for the most part, on the accidental errors in Reinmuth's diameter values.

The comparisons between the ratios  $\beta/a$  and  $b/a$  for the elliptical nebulae give, as regards the systematic errors in  $\beta/a$ , strong support to the results obtained in the previous chapter from the artificial nebulae. Furthermore, they support the conclusion arrived at above concerning the agreement between Reinmuth and the mean observer.

**11. Reinmuth's diameter ratios for spiral nebulae.** A comparison will now be made between Reinmuth's diameter ratios for spiral nebulae and the corresponding ratios obtained from photometric measurements.

In Table 13 photometric data have been collected by the writer for 31 spiral nebulae. The second column gives the types of the objects according to the



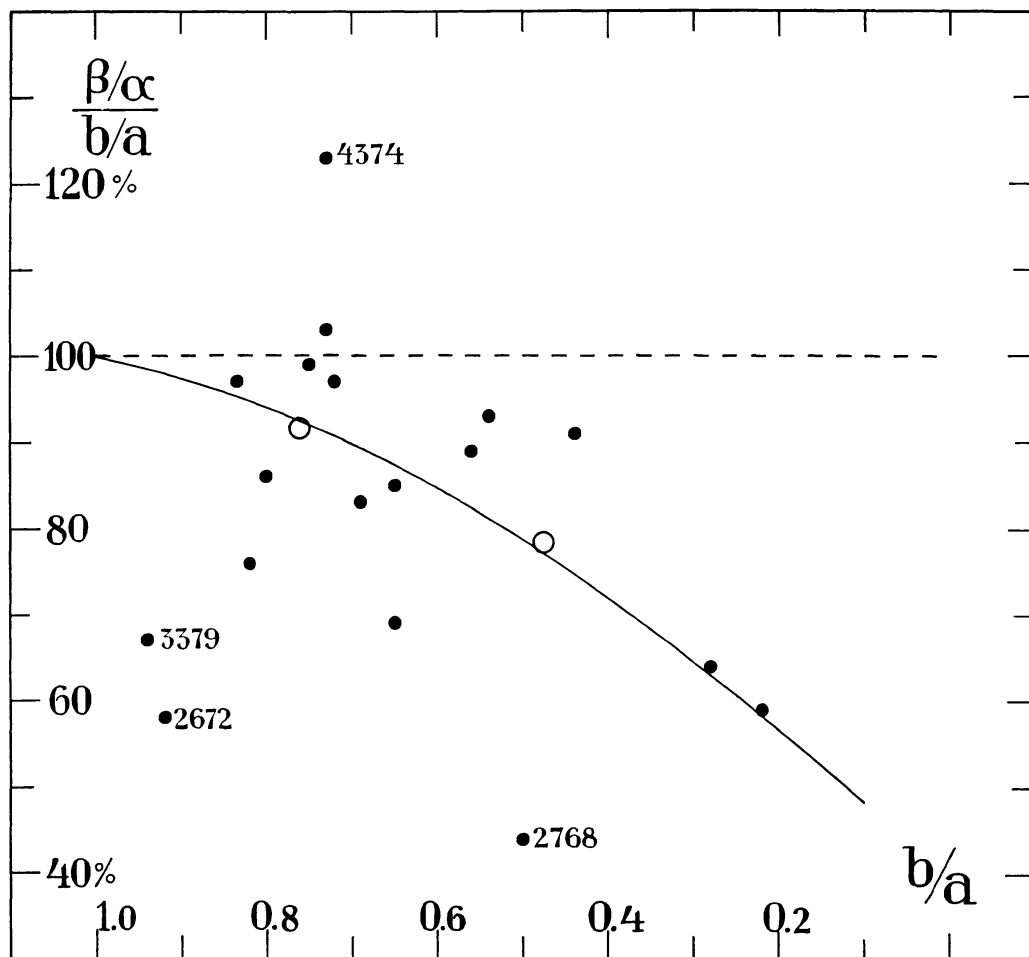


Fig. 10. Comparison between Reinmuth's diameter ratios for elliptical nebulae and the ratios obtained from photometric measurements. The curve represents the relation obtained for artificial nebulae with a light distribution of  $k r^{-2}$ .

Shapley-Ames catalogue.<sup>1</sup> All types of normal spirals are represented, from *Sa* to *Sc*. The third column contains the major and minor diameters, as given in Reinmuth's catalogue. The fifth column gives the diameters as obtained from photometer registrograms. Two of the nebulae, NGC 891 and 3623, have been previously investigated by the writer on plates taken with the 60-inch telescope of the Mount Wilson Observatory.<sup>2</sup> The remaining objects have also been measured by the writer.<sup>3</sup> However, in these cases no original plates, but only diapositives,

<sup>1</sup> Harvard Ann 88, No 2, 1932.

<sup>2</sup> Lund Medd, Ser II, No 114, 1945.

<sup>3</sup> A study of the available literature shows that there is great need of investigations of the light distribution in spiral nebulae. It may be remarked that some of the papers on this subject refer only to the central parts of the objects and do not give any diameter values. The distribution curves obtained by C. K. SEYFERT (ApJ 91, p. 528, 1940) for five spirals are given on a very small scale and will not be used in this connection.

TABLE 13.

*Comparison between Reinmuth's diameter ratios ( $\beta/a$ ) and the diameter ratios ( $b/a$ ) obtained from photometric measurements. (Spiral nebulae.)*

Object	Type	$a \times \beta$ (Reinmuth)	$\beta/a$	$a \times b$	$b/a$	$\frac{\beta/a}{b/a}$
NGC 151	S	3.5 $\times$ 1.3	0.37	2.5 $\times$ 1.4	0.56	66 %
891	S	10.0 1.3	0.13	13.6 2.5	0.18	72
1068	Sb	2.0 1.7	0.85	3.8 3.1	0.82	104
1084	Sc	1.9 1.0	0.53	2.5 1.4	0.56	95
2683	Sc	9.0 1.5	0.17	8.4 2.3	0.27	63
2841	Sb	7.5 2.5	0.33	7.0 2.9	0.41	80
2903	Sc	11.0 4.5	0.41	8.3 4.0	0.48	85
2964	Sc	2.0 1.1	0.55	3.2 1.8	0.56	98
3198	Sc	5. 2.0?	0.40	8.6 3.3	0.38	105
3521	Sc	8.0 3.5	0.44	7.5 5.1	0.68	65
3623	Sb	8.0 1.7	0.21	11.4 3.2	0.28	75
3627	Sb	8.3 3.0	0.36	8.8 3.6	0.41	88
3756	Sc	3.5 1.4	0.40	4.9 2.2	0.45	89
4088	Sc	4.8 1.7	0.35	5.0 1.9	0.38	92
4096	Sc	6.2 1.5	0.24	7.8 1.9	0.24	100
4151	Sb	2.7 1.8	0.67	3.0 2.6	0.87	77
4216	Sb	7.5 1.0	0.13	7.9 2.2	0.28	46
4244	Sb	17.0 1.1	0.065	13.7 2.3	0.17	38
4501	Sc	6.0 3.0	0.50	5.5 2.8	0.51	98
4517	Sc	10.0 0.9	0.09	12.1 1.9	0.16	56
4527	S	5.1 1.7	0.33	6.1 2.2	0.36	92
4565	Sb	15.0 1.4	0.093	15.7 2.1	0.13	72
4594	Sa	6.0 1.9	0.32	8.5 4.5	0.53	60
4736	Sb	6.0 4.5	0.75	7.6 5.8	0.76	99
4826	Sb	8.0 4.0	0.50	10.4 5.2	0.50	100
5005	Sc	4.6 2.0	0.43	5.5 2.5	0.45	96
5055	Sb	8.0 3.5	0.44	8.6 4.8	0.56	79
5746	Sb	6.5 0.8	0.12	7.5 1.3	0.17	71
5907	Sc	12.0 1.0	0.083	12.3 1.5	0.12	69
7331	Sb	10.0 2.0	0.20	11.5 4.5	0.39	51
7448	Sc	1.8 0.7	0.39	2.5 1.3	0.52	75

mean 79 %

have been at the writer's disposal. The diapositives,<sup>1</sup> which are of excellent quality, have been made from plates taken with the 60-inch telescope at Mount Wilson and with the Crossley reflector at the Lick Observatory. Although the outmost and faintest parts of the nebulae are lost in the copying procedure, we may assume that no serious errors are introduced in the ratios of the apparent diameters. The diapositives have been measured in the self-registering microphotometer of Moll type, described in the previous chapter. The measurements, which only aim at

<sup>1</sup> The writer wishes to express his thanks to Dr. Knut Lundmark who has placed the material of diapositives at his disposal.

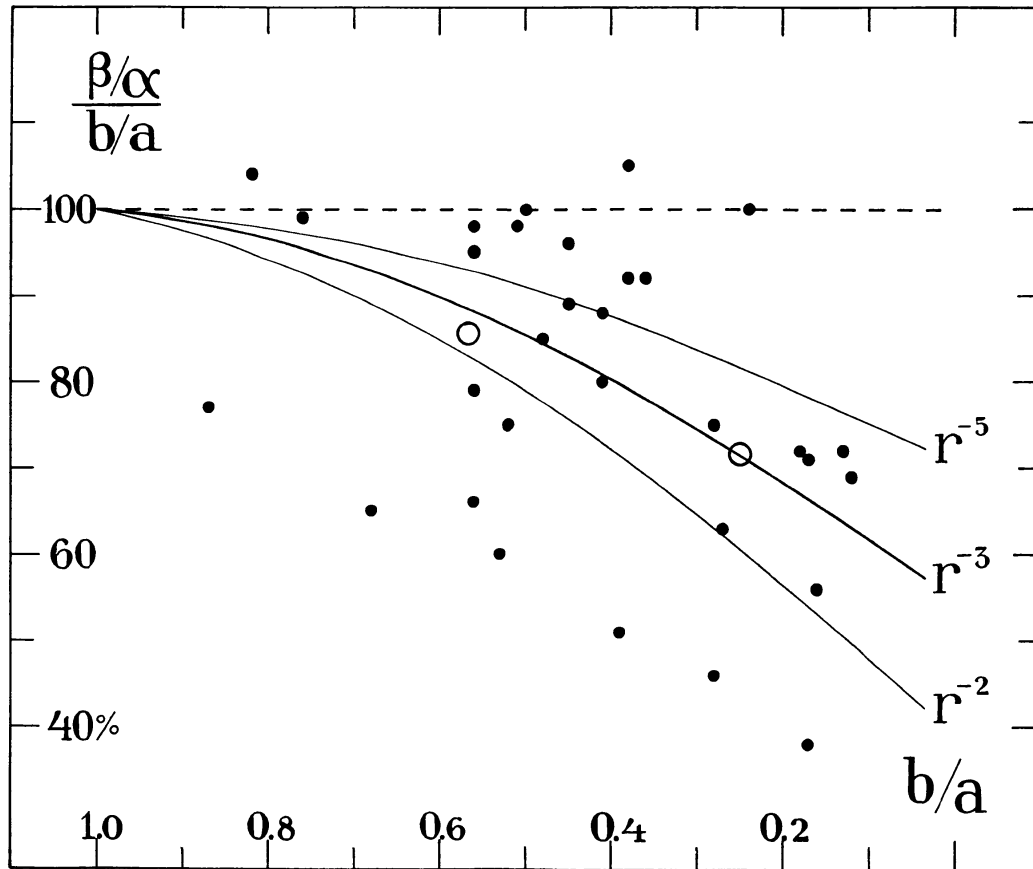


Fig. 11. Comparison between Reinmuth's diameter ratios for spiral nebulae and the ratios obtained from photometric measurements. The curves represent the relations obtained for artificial nebulae with light distributions equal to  $k r^{-2}$ ,  $k r^{-3}$ , and  $k r^{-5}$ .

the diameters, refer to the major and minor axes of the nebular ellipses. It appears from the table that the major diameters obtained in this way are, on an average, only slightly larger than those given by Reinmuth. Consequently, the diameter ratios correspond approximately to the same isophotes.

The true (photometric) ratios,  $b/a$ , of the minor and major diameters are given in the sixth column of the table, whereas the resulting values of  $\frac{\beta/a}{b/a}$  are contained in the last column. All these quotients, except two, are smaller than, or equal to unity. The individual values range from 38 to 105 per cent, and average 79 per cent.

The quotients  $\frac{\beta/a}{b/a}$  are in Fig. 11 plotted against the true ratios  $b/a$ . The open circles represent average values of the quotients computed for the two classes  $b/a \leq 0.40$  and  $b/a > 0.40$ . The numbers of objects in the two groups are 14 and 17, respectively. The three curves given in the figure represent the relations

TABLE 14.

*Comparisons between the photometric diameter ratios ( $b/a$ ) and the ratios ( $\beta/\alpha$ ) determined by Reinmuth, Holmberg, and Reiz. (Spiral nebulae.)*

$b/a$	Reinmuth		Holmberg		Reiz	
	$N$	$\overline{\left(\frac{\beta/\alpha}{b/a}\right)}$	$N$	$\overline{\left(\frac{\beta/\alpha}{b/a}\right)}$	$N$	$\overline{\left(\frac{\beta/\alpha}{b/a}\right)}$
$\leq 0.40$	14	72 % (72)	6	72 % (74)	11	67 % (66)
$0.41 - 1.00$	17	86 (88)	2	—	11	84 (85)

obtained in the previous chapter for the mean observer. They refer to artificial nebulae having distributions of light equal to  $kr^{-2}$ ,  $kr^{-3}$ , and  $kr^{-5}$ . A study of the figure shows that *the spiral nebulae agree, on an average, with the relation curve corresponding to the distribution  $kr^{-3}$* . It is true, that the dispersion in the individual values of  $\frac{\beta/\alpha}{b/a}$  is rather large. This apparently depends on the fact that

spirals of different types and forms are included in the material. The luminosity distribution presumably varies considerably from one spiral to another.

In this connection, it would be of a certain interest to study the relation between the ratios  $b/a$  for spiral nebulae and the ratios  $\beta/\alpha$  as given by other observers. It has been mentioned above, that the Heidelberg plate material has been used also by Reiz and by the writer for investigations of extragalactic nebulae. In Table 14 the average values of  $\frac{\beta/\alpha}{b/a}$ , as corresponding to the two classes of  $b/a$ ,

have been given for Reinmuth, Holmberg, and Reiz. For the first observer, the average values, which are represented by the open circles in the above figure, amount to 72 per cent and 86 per cent. The numbers within brackets give the values corresponding to the mean observer and the light distribution  $kr^{-3}$ . As regards the writer's catalogue, only eight nebulae are available for a comparison. In the class  $b/a \leq 0.40$  an average quotient of 72 per cent is obtained, as corresponding to 74 per cent for the artificial nebulae with the above light distribution. It may be remarked that the latter value does not refer to the mean observer but to the writer's measurements, as given by curve V in Fig. 6. In Reiz's catalogue 22 nebulae are available for comparisons. The average values of  $\frac{\beta/\alpha}{b/a}$  agree very well with the values obtained by him in the previous chapter

for the distribution  $kr^{-3}$ . It seems reasonable to draw the conclusion that the spiral nebulae may, as regards the systematic errors in the measured diameter ratios, be compared to the artificial nebulae with the distribution function  $kr^{-3}$ .

The results obtained above indicate that the luminosity gradients at the edges of spiral nebulae, as defined by the measured diameters, correspond on an average

to a luminosity function of the type  $k r^{-3}$ . It may be remarked here that the above investigation by the writer of the distributions of light in NGC 891 and NGC 3623 confirms this indication. At the edges of NGC 891, as defined by Reinmuth's major and minor diameters, the average value of the observed luminosity gradients along the two axes corresponds to a distribution function of  $k r^{-2.4}$ . In NGC 3623, the luminosity gradients correspond to the function  $k r^{-3.4}$ . This problem may be further investigated when additional material becomes available.

## CHAPTER III.

**On the inclinations of the spiral nebulae to the celestial plane.**

**12. Introduction.** It seems to be an established fact that the spiral nebulae are stellar systems with a more or less spheroidal shape. The orientation in space of the principal planes of these nebular spheroids represents a problem of great interest, which has been repeatedly discussed during the past 25 years. The orientation problem may, in fact, be studied from two different points of view. In the first place, an investigation may be made of the orientation of the nebular planes with respect to the celestial plane. In this case the inclinations of the nebulae to the tangential plane of the celestial sphere are determined and the distribution of the inclination angles is analysed. Secondly, we may investigate the possibility of the existence of a certain preferential plane, *i. e.* a plane in space with respect to which the nebular discs have a systematic orientation.

It may be remarked here that if the nebulae are orientated at random in space, *i. e.* if there exists no preferential plane, we may assume that the orientation with respect to the celestial plane is also of an accidental nature. On the other hand, the existence of a preferential plane will influence the orientation as regards the celestial plane, especially if small areas of the sky are treated separately. If the investigation is extended over large areas, or the whole sky, the influence of the preferential plane on the latter orientation grows smaller.

In this chapter we will deal only with the inclinations of the nebulae to the celestial plane. The main purpose of the investigation is to show that the distribution of these inclination angles is an accidental one. A random distribution seems, *a priori*, to be the most reasonable one, especially as the existence of a preferential plane in space does not seem to be definitely established. (Cf. Chapter IV.) Only spiral nebulae will be included in the investigation. The elliptical and irregular nebulae are excluded since they do not satisfy the necessary condition of being discoid.

A short summary will be given here of previous investigations on the orientation of the nebulae with respect to the celestial plane. In 1920, J. H. REYNOLDS<sup>1</sup> arrived

---

<sup>1</sup> MN 81, p. 129, 1920. See also MN 82, p. 510, 1922.



at the result that there is an excess of spirals seen edgewise. Several attempts have been made to explain this deviation from a random distribution, which has frequently been the result of earlier investigations. Thus, E. ÖRIK<sup>1</sup> has pointed out that the average surface brightness of a spiral nebula grows larger as the inclination to the celestial plane increases. This will cause an increase in the apparent major axis, as measured on the plate, and the result will be that a too large number of nebulae with an edgewise orientation are included in the material, if the objects are selected according to their major diameters.

In a previous paper,<sup>2</sup> the writer has shortly discussed the distribution of the inclination angles for nebulae of different diameter classes. However, all types of nebulae have been included in the investigation, and the results are, of course, only preliminary.

In 1937 the spatial orientation of the spiral nebulae was taken up to a renewed discussion by M. S. EIGENSON.<sup>3</sup> The material consisted of the 488 nebulae brighter than the thirteenth magnitude included in the catalogue given in Harvard Annal 88, No 4 (1934). The result was a random distribution of the inclinations to the celestial plane. It must, however, be remarked that the material used is not complete down to a certain limiting diameter, or magnitude, and that it consequently is not representative of a given volume of space.

A later investigation by F. G. BROWN<sup>4</sup> has been based on the large material collected by K. REINMUTH in his catalogue of the Herschel-nebulae.<sup>5</sup> The analysis is based on all non-galactic nebulae in this catalogue having major diameters of 2' or more. The result is a rather large excess of small inclinations to the line of sight. Brown expresses the opinion that this excess is a real phenomenon. His results have been criticized by H. KNOX-SHAW,<sup>6</sup> who has made a similar investigation of the objects included in the Shapley-Ames catalogue. The material consists of all nebulae which in this catalogue are classified as spirals. For objects with major diameters of 2', or more, a random distribution is obtained of the inclinations.

It appears that the results obtained up till now as regards the inclinations of the spiral nebulae are rather contradictory. The explanation seems to be that in the previous investigations no attention has been paid to the systematic errors in the major and minor diameters of the nebulae. It has been shown in the first chapter that these errors introduce a very serious systematic effect in the diameter ratios. Furthermore, all the above investigations have been based on materials containing more or less serious selection effects. It seems, in fact, to be a very difficult task to try to collect a representative material of nebulae corresponding to a given volume of space. The apparent major diameter and the apparent magni-

---

<sup>1</sup> Obs 46, p. 51, 1923.

<sup>2</sup> Lund Ann 6, p. 68, 1937.

<sup>3</sup> Pulkovo Circ 22—23, 1937.

<sup>4</sup> MN 98, p. 218, 1938. MN 99, p. 14, 1938. Obs 61, p. 250, 1938.

<sup>5</sup> Heidelberg Veröff 9, 1926.

<sup>6</sup> MN 98, p. 587, 1938.

tude, which represent the only distance indicators available in the present case, are both related to the apparent diameter ratio, *i. e.* related to the inclination. The radial velocity, which seems to be the only distance indicator independent of the inclination, has been determined only for a comparatively small number of extragalactic objects.

**13. The inclination and the apparent diameter ratio.** The inclination of a spiral nebula to the celestial plane is determined from the ratio of the apparent minor and major axes. The determination is based on the assumption that the spirals may, at least in a statistical sense, be treated as oblate spheroids. We have, in any case, to assume that the spiral bodies possess rotational symmetry with respect to the smallest of the absolute axes.

In individual cases, the spiral nebulae may deviate considerably from the above simple model. The deviations seem to be most conspicuous for late type spirals (type *Sc*), as well as for barred spirals (type *SB*). The earlier types of normal spirals apparently show a better agreement with the spheroidal model. In statistical investigations of the orientation of the nebulae we may consider the errors in the inclination angles introduced by deviations from the adopted symmetrical model as accidental errors.

If the thickness of the nebular disc is neglected the following simple relation is obtained between the inclination to the celestial plane,  $\varphi$ , and the apparent diameter ratio,  $b/a$ :

$$\cos \varphi = b/a \quad (5\ a)$$

If the thickness is taken into consideration a slightly different expression is obtained. For a spheroid, having a ratio of the smallest to the largest of the absolute axes equal to  $q$ , the following relation<sup>1</sup> is valid:

$$\cos^2 \varphi = \frac{(b/a)^2 - q^2}{1 - q^2} \quad (5\ b)$$

We refer to Fig. 12, where a spheroidal nebula is seen edgewise. The celestial plane is supposed to be perpendicular to the plane of the figure. The axes of the spheroid are denoted by  $a$  and  $q \cdot a$ , whereas  $b$  is the distance between the two lines of sight which are tangents to the elliptical cross-section of the nebula shown in the figure. A closer study of the figure gives the above relation between  $\cos \varphi$ ,  $b/a$ , and  $q$ .

For the application of formula (5 b) to the spiral nebulae we have to determine the value of the flattening  $q$ . When the ratio  $b/a$  has a large value a certain error in the adopted value of  $q$  is of small importance. However, for nebulae with an almost edgewise orientation the derived inclination is rather sensitive to a possible change of the constant  $q$ . The flattening of the nebular disc is apparently slightly different for different types of spirals. It will be shown in the following pages, that a study of the distribution of the apparent diameter ratios of the spirals points

---

<sup>1</sup> Cf. Mt Wilson Contr 324, ApJ 64, p. 321, 1926.

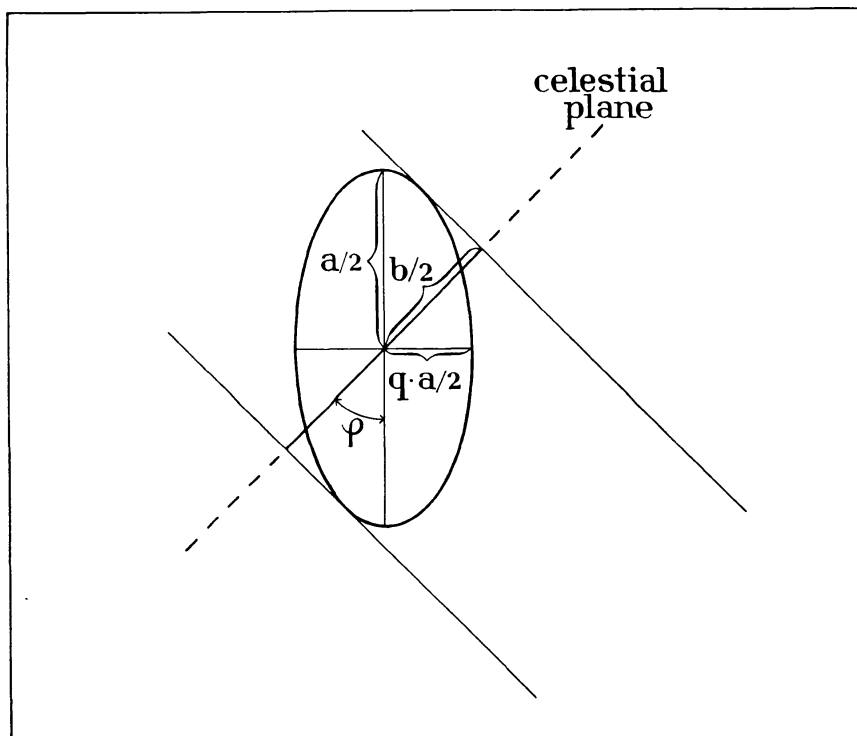


Fig. 12. A spheroidal nebula seen edgewise.

to an average value of  $q$  of about 0.20. In deriving this value we have taken the systematic errors in the diameter ratios into consideration.

In Table 15 we have computed the inclination angles corresponding to different values of the ratio  $b/a$  and the flattening  $q$ . The table is based on equation (5 b). The diameter ratios range from 0.14 to 1.00, whereas  $q$  has been given values from 0.14 to 0.26. The majority of the spiral nebulae presumably have values of  $q$  between these limits. On account of the deviations of the individual spirals from the above simplified model we cannot hope to determine the inclination with an error smaller than one, or some few degrees. The table shows that, for values of  $b/a$  larger than about 0.3, the inclination angle is approximately independent of the adopted value of  $q$ . It ought to be remarked that  $b/a$  means, as before, the apparent diameter ratio corrected for the systematic measuring errors.

**14. The distribution of the inclination angles.** The main purpose of this investigation is to show that the inclinations ( $\varphi$ ) of the spiral nebulae to the celestial plane are distributed at random. A random distribution implies that the distribution function of  $\cos \varphi$  is a constant, which means that the distribution curve is a straight line. This result is easily proved if the polar axes of the nebular ellipsoids are considered. A random distribution is obtained if these axes are accidentally distributed in space, *i. e.* if their intersection points with the celestial sphere are evenly distributed over the surface of the sphere. Thus, the number of nebulae having inclinations within a certain interval of  $\varphi$  should be proportional to the corresponding

TABLE 15.

*The inclination of a spiral nebula to the celestial plane as a function of the apparent diameter ratio ( $b/a$ ) and the ratio of the absolute axes ( $q$ ).*

$\begin{array}{c} q \\ b/a \end{array}$	0.14	0.16	0.18	0.20	0.22	0.24	0.26
0.14	90°0						
0.16	85.5	90°0					
0.18	83.4	85.2	90°0				
0.20	81.7	83.0	84.9	90°0			
0.22	80.1	81.2	82.6	84.6	90°0		
0.24	78.6	79.6	80.7	82.2	84.4	90°0	
0.26	77.2	78.0	79.0	80.2	81.8	84.1	90°0
0.30	74.5	75.1	75.9	76.8	77.9	79.3	81.1
0.35	71.1	71.6	72.2	73.0	73.8	74.8	76.0
0.40	67.8	68.2	68.7	69.3	70.0	70.8	71.6
0.45	64.4	64.8	65.2	65.7	66.3	66.9	67.6
0.50	61.0	61.3	61.7	62.1	62.6	63.1	63.7
0.55	57.5	57.8	58.1	58.5	58.9	59.3	59.9
0.60	53.9	54.1	54.4	54.7	55.1	55.5	55.9
0.65	50.1	50.3	50.6	50.9	51.2	51.5	51.9
0.70	46.2	46.3	46.6	46.8	47.1	47.4	47.7
0.75	41.9	42.1	42.3	42.5	42.7	42.9	43.2
0.80	37.3	37.4	37.6	37.8	38.0	38.2	38.4
0.85	32.1	32.3	32.4	32.5	32.7	32.9	33.1
0.90	26.1	26.2	26.3	26.4	26.5	26.7	26.8
0.95	18.4	18.4	18.5	18.6	18.7	18.8	18.9
1.00	0.0	0.0	0.0	0.0	0.0	0.0	0.0

surface of the sphere. It is easily shown, that the result will be a constant distribution function as regards  $\cos \varphi$ .

In trying to determine  $\cos \varphi$ , and the distribution of  $\cos \varphi$ , for a certain material of spiral nebulae we have to take several sources of error into consideration. They may be summarized as follows:

1. The deviations of the individual nebulae from the adopted spheroidal model.
2. Deviations of the flattening  $q$  from the adopted mean value.
3. The systematic errors in the apparent diameter ratios.
4. The systematic selection effects to be found in any material of nebulae selected according to apparent diameters, or apparent magnitudes.

As regards the deviations of the nebulae from the spheroidal model it has been mentioned above, that late type spirals and barred spirals seem to have the least symmetrical shapes. We may, for instance, refer to the plate given by Reinmuth in his above-mentioned catalogue of the Herschel-nebulae. The types of spirals denoted by  $u$ ,  $v$ , and  $w$  (Wolf's system) are probably in many cases situated in the celestial plane, although their diameter ratios deviate from unity. From a statistical point of view we may, however, consider these deviations as representing accidental errors. It is generally not possible to exclude the late type spirals in an investigation of

TABLE 16.

*Changes in the distribution of  $\cos \varphi$  corresponding to a certain error in the assumed ratio ( $q$ ) of the absolute axes. True ratio = 0.20.*

$\cos \varphi$	$q=0.16$	$q=0.18$	$q=0.20$	$q=0.22$	$q=0.24$
0.000—0.200	0.800	0.900	1.000	1.100	1.200
0.201—0.400	1.119	1.058	1.000	0.946	0.894
0.401—0.600	1.041	1.020	1.000	0.978	0.955
0.601—0.800	1.023	1.013	1.000	0.986	0.972
0.801—1.000	1.017	1.009	1.000	0.990	0.979

the orientation of the nebulae since the classifications are not accurate enough as regards small and faint objects. Besides, the material would be too small. If, in determining the distribution of  $\cos \varphi$ , the class breadth is kept sufficiently large, the effects of the above deviations are to a certain degree neutralized.

In this connection we may also mention the existence of certain decimal errors in the different catalogues of nebulae. It is generally found that a diameter ratio of 1.0 is overrepresented in the material, whereas values of 0.8 à 0.9 are underrepresented. There are also some other ratios, as for instance  $1/3$ ,  $1/2$ , and  $2/3$ , which occur too frequently. If the intervals of  $\cos \varphi$  are chosen large enough these errors will be of minor importance.

We will now turn our attention to *point 2* in the above summary. It has been mentioned previously that a certain deviation in the adopted value of  $q$  from the true value produces the largest error in  $\cos \varphi$  for nebulae with an almost edgewise orientation. As regards the errors introduced in the distribution of  $\cos \varphi$  we refer to Table 16. In this table the true value of  $q$  has been assumed to be equal to 0.20. The distributions of  $\cos \varphi$  have been computed for five different values of  $q$ , ranging from 0.16 to 0.24. For  $q = 0.20$ , the numbers of nebulae in the five different classes of  $\cos \varphi$  are the same (random distribution), and they have been put equal to unity. The distributions corresponding to the other values of  $q$  have been computed from formula (5 b) by means of a numerical procedure. It appears that a too small value of  $q$  results in a too small number of objects in the class  $\cos \varphi = 0.0—0.2$ , whereas the opposite result is obtained for values of  $q$  that are too large. However, a deficit in the first class corresponds to a considerable excess in the second class, and *vice versa*. In the other three classes the deviations only amount to one, or some few per cent.

We may conclude, that the deviations in the distribution of  $\cos \varphi$  produced by a certain error in the quantity  $q$  are comparatively small supposed that the class intervals are sufficiently large. In the following investigations we will use the same five classes of  $\cos \varphi$  as those given in the above table. If the number of objects in the two first classes equals the number in the two last classes, it seems reasonable to assume that the distribution of  $\cos \varphi$  is an accidental one even in the case that the investigation has been based on a slightly erroneous value of the constant  $q$ .

TABLE 17.  
*Determination of the distribution of  $\cos \varphi'$ .*  
*( $i = k r^{-3}$ ;  $q = 0.20$ )*

$\cos \varphi$	$b/a$	$\beta/a$	$\cos \varphi'$	$\Delta \cos \varphi'$	$\frac{\Delta \cos \varphi}{\Delta \cos \varphi'}$
0.000	0.200	0.137	0.000	0.075	1.33
.100	.223	.156	.075	.080	1.25
.200	.280	.206	.155	.088	1.14
.300	.356	.277	.243	.095	1.05
.400	.440	.362	.338	.104	0.96
.500	.529	.459	.442	.107	0.93
.600	.621	.561	.549	.113	0.88
.700	.714	.670	.662	.112	0.89
.800	.809	.779	.774	.113	0.88
.900	.904	.889	.887	0.113	0.88
1.000	1.000	1.000	1.000		

As regards the systematic errors in the diameter ratios (*point 3*) we refer to the first two chapters of this paper. In Table 10, the systematic errors have been given for artificial nebulae with different distributions of light. Fig. 11 gives the relation between Reinmuth's diameter ratios, as measured for spiral nebulae on the Heidelberg plates, and the ratios that are obtained from photometer registrograms. It appears that the systematic deviations are, on an average, the same as those obtained for artificial nebulae having a light distribution of the form  $k r^{-3}$ . In the following investigations, the systematic corrections to be applied to the diameter ratios will be based on these results.

It would be of a certain interest to investigate how the systematic errors in the diameter ratios affect the distribution of  $\cos \varphi$ . Such a computation has been made in Table 17. The first column gives values of  $\cos \varphi$ , ranging from zero to unity. The second column gives the corresponding values of  $b/a$ , computed by means of formula (5 b). The true ratio of the apparent diameters is, as before, denoted by  $b/a$ , whereas the visually measured ratio is denoted by  $\beta/a$ . The values of the latter ratio are given in the third column of the table. They are based on the average values of  $\beta/a$  contained in the fifth column of Table 10. The inclination angles which are computed from the ratios  $\beta/a$  are denoted by  $\varphi'$ . The fourth column of the table gives the resulting values of  $\cos \varphi'$ . It may be remarked here that in the computation of  $b/a$  from  $\cos \varphi$  the value of  $q$  has been put equal to 0.20, which equals the minimum value of  $b/a$ . In the computation of  $\cos \varphi'$ , the value of  $q$  must accordingly be put equal to the minimum value of  $\beta/a$ , *i. e.* equal to 0.137. The last column of the table gives the resulting ratios  $\frac{\Delta \cos \varphi}{\Delta \cos \varphi'}$ . The relation between the distribution of  $\cos \varphi'$  [ $=F'(\cos \varphi')$ ] and the distribution of  $\cos \varphi$  [ $=F(\cos \varphi)$ ] is now given by the expression

$$\frac{F'(\cos \varphi')}{F(\cos \varphi)} = \frac{d(\cos \varphi)}{d(\cos \varphi')} \simeq \frac{\Delta(\cos \varphi)}{\Delta(\cos \varphi')} \quad (6)$$



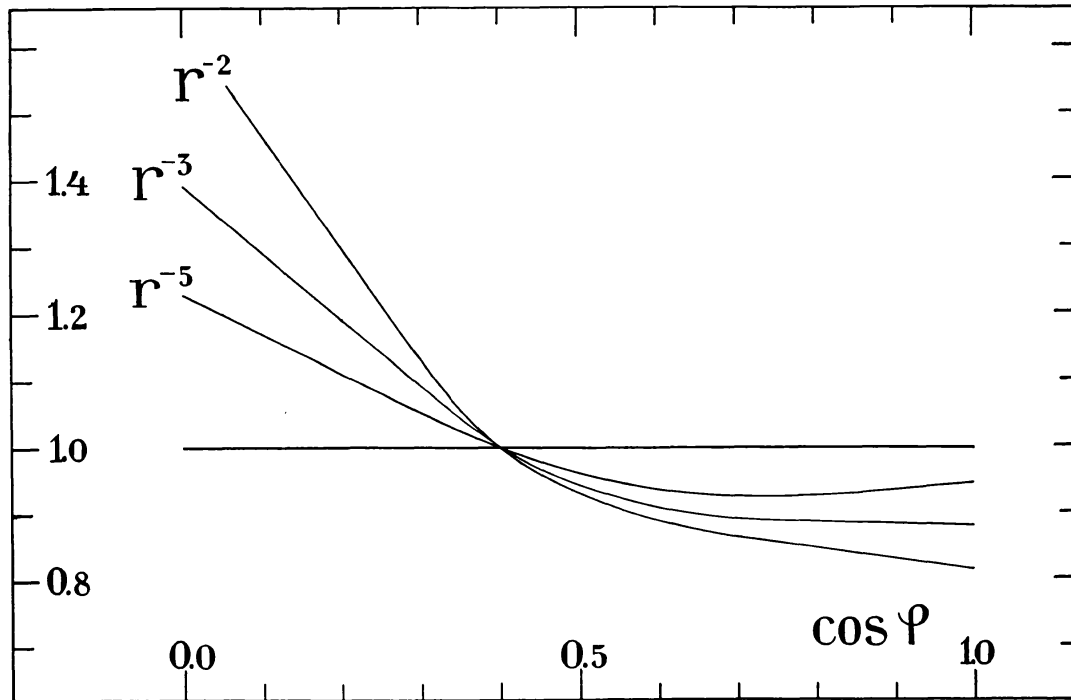


Fig. 13. The disturbances in the distribution of  $\cos \varphi$  produced by the systematic diameter errors, as obtained for artificial nebulae with different distributions of light. The horizontal line represents a random distribution.

The curves in Fig. 13 give a good illustration of the large disturbances caused by the systematic errors in the diameter ratios. The horizontal line represents the distribution of  $\cos \varphi$ , which is supposed to be an accidental one. The distribution of  $\cos \varphi'$ , as obtained from the above table, is given by the curve denoted by  $r^{-3}$ . It may be recollected that the relation between  $\beta/a$  and  $b/a$  has been based on the results obtained for artificial nebulae with a light distribution equal to  $kr^{-3}$ . The new distribution curve gives an apparent excess of nebulae having an edgewise orientation. The excess amounts to 50 à 60 per cent. If the above computation is repeated, using the values of  $\frac{\beta/a}{b/a}$  obtained for the artificial nebulae having a luminosity function  $kr^{-2}$ , or  $kr^{-5}$  (columns 3 and 7 of Table 10), the other two distribution curves given in the figure are obtained. The excess of edgewise nebulae decreases when the exponent  $n$  in the luminosity function  $kr^{-n}$  gets larger values. This is explained by the fact that the systematic errors in the ratios  $\beta/a$  grow smaller with increasing values of  $n$ .

The fourth source of error (*point 4*) is represented by the selection effects. Disturbances of this kind are to be expected in any material of nebulae which are selected according to their apparent diameters, or apparent magnitudes. Since an investigation of the orientation of the nebulae must necessarily be referred to a given volume of space, it is of great importance that no correlation exists between

the distance indicator and the diameter ratios of the nebulae. However, the apparent major diameter is related to the diameter ratio, both on account of the systematic measuring errors and on account of the increase in surface brightness with increasing inclination. The apparent magnitudes, as given in the available catalogues, must also be assumed to depend to a certain degree on the diameter ratio. The estimated magnitudes presumably contain certain systematic errors corresponding to the errors in the diameters. To this may be added, that the absolute magnitude of a spiral nebula grows fainter with increasing inclination on account of the absorption within the nebula. The selection difficulties would be partly overcome if we had access to photometrically determined diameters and magnitudes. It has been mentioned above, that the radial velocity seems to represent the only ideal distance indicator in the present case.

**15. *The orientation of nebulae as obtained from Reinmuth's catalogue.*** The large catalogue published by K. REINMUTH<sup>1</sup> comprises all *General Catalogue* nebulae north of declination  $-20^\circ$ , in all 4445 objects. The major and minor diameters have been measured for the majority of the nebulae, *i. e.* for all nebulae having a measurable size. The systematic errors in the diameters have been investigated in Chapter II.

From Reinmuth's catalogue all nebulae are selected which have major diameters larger than, or equal to 3'.0. The following objects are rejected: (a) all known clusters and galactic nebulae, (b) all nebulae which in the Shapley-Ames catalogue are classified as elliptical or irregular objects, and (c) eight additional nebulae, the types of which are by Reinmuth denoted by a question-mark.<sup>2</sup> The remaining number of objects amounts to 270.

Some explanation may be needed as regards the choice of a limiting diameter equal to 3'.0. It appears that if a smaller diameter value is chosen, we will encounter difficulties as regards the classification of the nebulae. This especially refers to nebulae having a small diameter ratio. A study of the available catalogues shows that the descriptions of small nebulae are much more incomplete for elongated objects than for round ones. To this may be added that Reinmuth's catalogue does not seem to be complete below a diameter of 3'.0. The completeness may be examined by comparisons with the catalogue by A. REIZ,<sup>3</sup> which is also based on the Heidelberg plate material and refers to the north galactic polar cap ( $b = 50^\circ$ — $90^\circ$ ). This catalogue, containing 4666 objects, comprises all nebulae which appear on the plates, and we may assume that it is complete down to a rather small limiting diameter. It appears that Reiz's catalogue contains 13 nebulae larger than, or equal to 3'.0, which have not been included by Reinmuth. If the comparison is

<sup>1</sup> Heidelberg Veröff 9, 1926.

<sup>2</sup> Five of these objects have a galactic latitude smaller than  $25^\circ$  and may be regarded as galactic nebulae. It may be remarked here that the objects NGC 224 and NGC 598 are not included in the material. Reinmuth's catalogue does not give any definitive diameter values for these two nebulae.

<sup>3</sup> Lund Ann 9, 1941.

TABLE 18.

*Distribution of the types of the nebulae included in the determination of the distribution of  $\cos \varphi$ . (Reinmuth's catalogue.)*

Solution	$S$	$SB$	$r, s, w$	$o, q$	$\begin{smallmatrix} g-s \\ h-s \\ h_0-q \end{smallmatrix}$	$h, i, k$	$h_0$
I ( $N=270$ )	195	24	21	3	8	12	7
III ( $N=136$ )	117	12	5	—	—	—	2

extended to nebulae of a smaller size, the difference grows still larger. A comparison with the writer's catalogue of double and multiple nebulae,<sup>1</sup> which comprises all double and multiple systems to be found on the Heidelberg plates, gives a similar result. This catalogue contains 6 nebulae larger than, or equal to 3'.0, which have not been included by Reinmuth.

Before proceeding further, we will give some data concerning the types of the above 270 objects. We refer to Table 18, where the first row gives the distribution of the types. It appears that 195 objects are classified as normal spirals ( $S$ ,  $Sa$ ,  $Sb$ ,  $Sc$ ) by the Shapley-Ames catalogue,<sup>2</sup> whereas 24 nebulae are given as barred spirals. For the remaining 51 objects we have to rely on the types, in Wolf's classification system, which are given by Reinmuth. It appears that 21 nebulae belong to the open spiral types  $r$ ,  $s$ , and  $w$ , whereas 30 nebulae belong to types which we may assume represent spirals with an edgewise orientation. Since most of the latter objects are small and very elongated, it is in many cases difficult to establish definitely their spiral nature. However, practically all of these nebulae will be excluded in the final solution (Solution III), since their diameters fall below the corrected limiting diameter value. Only 136 nebulae will be included in the final solution based on the diameter corrections corresponding to the luminosity function  $k r^{-3}$ . (Cf. Table 20.) The distribution of the types of the nebulae included in this reduced material is given in the second row of the table. It appears that 134 of these objects have been definitely classified as spirals by Shapley-Ames, or by Reinmuth.

The *first step* in a study of the orientation of the above nebulae is the determination of the distribution of the apparent diameter ratios. The apparent diameters, as given in Reinmuth's catalogue, are denoted by  $\alpha$  and  $\beta$ . The distribution of the ratios  $\beta/\alpha$  is given in Table 19. The numbers are given for intervals equal to 0.100 ( $\beta/\alpha > 0.3$ ) and 0.050 ( $\beta/\alpha < 0.3$ ). It appears that the numbers increase, when the diameter ratio grows smaller. The lower limit of  $\beta/\alpha$  amounts to about 0.06. According to Reinmuth's diameter values, the smallest ratio is, in fact, found for NGC 4731 where  $\beta/\alpha$  is equal to 0.05s.

<sup>1</sup> Lund Ann 6, 1937.

<sup>2</sup> Harvard Ann 88, No 2, 1932. It may be remarked that the revisions and additions given in Harvard Ann 88, No 4, 1934, have been taken into account.

TABLE 19.

*Distribution of the diameter ratios  $\beta/a$  for spiral nebulae with major diameters larger than, or equal to  $3'.0$ . (Reinmuth's catalogue.)*

$\beta/a$	Number
$\leq 0.049$	0
0.050–0.099	12
0.100–0.149	29
0.150–0.199	20
0.200–0.249	35
0.250–0.299	24
0.300–0.399	33
0.400–0.499	30
0.500–0.599	27
0.600–0.699	20
0.700–0.799	10
0.800–0.899	6
0.900–1.000	24

total 270

The distribution of  $\beta/a$  may also be studied in Fig. 14. The full circles represent the class frequencies given in the above table. However, some of the classes have been taken together two and two. On account of the accidental errors (including the decimal errors) in the diameter ratios, the class breadths should be kept as large as possible. The distribution of the ratios may, for large and intermediate values of  $\beta/a$ , be represented by the smooth curve given in the figure. The left part of the curve is an extrapolation,<sup>1</sup> and is supposed to represent the distribution that would be obtained if there were no accidental errors in the diameter ratios, and if the ratio ( $q$ ) of the absolute minor and major axes were the same for all the nebulae. A comparison between the observed distribution and the distribution given by the curve will enable us to determine, approximately, the »effective» minimum value of  $\beta/a$ . The procedure is similar to that used in determining the effective limiting magnitude of a magnitude catalogue.

In the above figure, the vertical broken line is supposed to represent the effective minimum of  $\beta/a$ , *i. e.* the observed number of  $\beta/a$ -values to the left of this line is equal to the difference between the »theoretical» number (as given by the curve) and the observed number to the right. It appears that the minimum value of  $\beta/a$  that is obtained in this way is equal to 0.13 à 0.14. The corresponding minimum of the true ratios  $b/a$  may be derived by means of the correction factors given in the fifth column of Table 10. We arrive at a minimum value of  $b/a$  equal to 0.20.

<sup>1</sup> It can be proved that a random distribution of the inclinations of the nebulae corresponds to a distribution of the diameter ratios that is of the type given by this curve. The selection effects inherent in the present material of nebulae, which will cause certain deviations from a random distribution, will mainly produce the result that the maximum of the curve is increased.

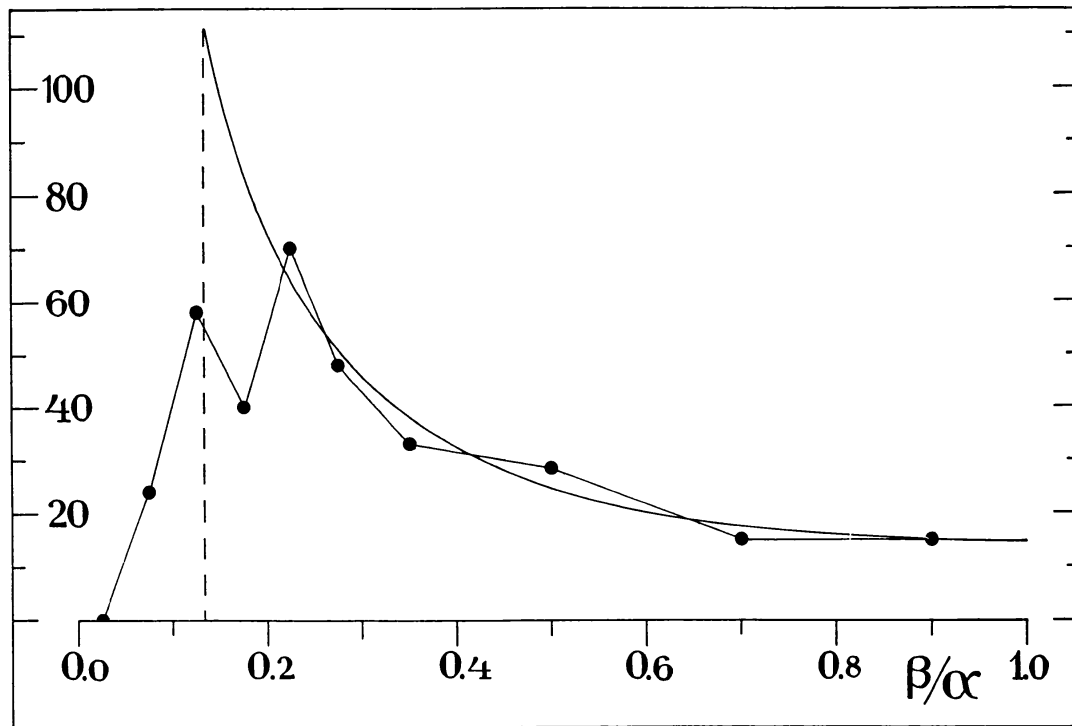


Fig. 14. The distribution of the diameter ratios  $\beta/a$  of spiral nebulae, as obtained from Reinmuth's catalogue. The broken line represents the effective minimum value of  $\beta/a$ .

This value will, in the following investigations, be adopted to represent the true average ratio ( $q$ ) of the absolute minor and major axes of the spirals. It may be remarked that a study of our own stellar system seems to result in an axis ratio of the same order of size.

After the determination of a proper value of the constant  $q$ , the *second step* will be the computation of the inclinations of the nebulae as corresponding to the observed diameter ratios  $\beta/a$ . The value of  $\cos \varphi$  is obtained from formula (5 b), if  $b/a$  is replaced by  $\beta/a$ , and  $q$  by  $f \cdot q$ . The quantity  $q$  is put equal to the value derived above, whereas  $f$  is the factor given in Table 10 for  $b/a = 0.20$ . It has been shown in Chapter II, that the spiral nebulae give, on an average, the same relation between  $\beta/a$  (as determined by Reinmuth) and  $b/a$  as is obtained for the artificial nebulae with a luminosity function  $k r^{-3}$ . For the sake of completeness, the following investigation will however be based on the values of  $f$  corresponding to three different distributions of light, namely  $k r^{-2}$ ,  $k r^{-3}$ , and  $k r^{-5}$ . This will enable us to study more closely the effects produced by the systematic diameter errors, the errors being different for different distributions of light.

The distributions of the above uncorrected values of  $\cos \varphi$  are given in Fig. 15. The full circles give the numbers of objects in five different classes of  $\cos \varphi$ , the class breadth being equal to 0.2. It may be recollected that the total number of nebulae is 270. It appears that the distributions give a considerable excess of

TABLE 20.

*Numbers of spiral nebulae, with major diameters larger than or equal to 3'.0, which are included in the solutions I, II, and III. (Reinmuth's catalogue.)*

Assumed light distribution	I (no diameter corrections)	II (major diameters corrected for measuring errors)	III (major diameters also corrected for diff. in surf. brightness)
$k r^{-2}$	270	153	111
$k r^{-3}$	270	184	136
$k r^{-5}$	270	194	156

nebulae with an edgewise orientation. The curve in the middle of the figure, corresponding to the light distribution  $k r^{-3}$ , shows that the number increases from 30 ( $\cos \varphi = 0.8-1.0$ ) to 94 ( $\cos \varphi = 0.0-0.2$ ). The other two curves give an increase of approximately the same size. The differences between the three curves depend, of course, on the differences in the quantity  $f \cdot q$ . The straight horizontal lines represent random distributions of the inclination angles.

The large excess of nebulae with an edgewise orientation that is obtained above, gives a good illustration of the large disturbances caused by the systematic errors in the apparent diameters. It will be shown below, that if due attention is paid to these errors, a random distribution is obtained of the inclination angles. It may be remarked, that the results obtained so far agree well with previous investigations.

In the *third step*, the apparent diameters are corrected for the systematic measuring errors. The ratios  $\beta/a$  are divided by the factors given in the third, fifth, and seventh columns of Table 10, whereas the major diameters  $a$  are divided by the factors given in Table 6. In this way we obtain the true ratio  $b/a$ , and a major diameter that is not dependent on the inclination of the nebula. The values of  $\cos \varphi$  are recomputed by means of formula (5 b). The constant  $q$  is, as before, put equal to 0.20. All nebulae, which have corrected major diameters smaller than 3'.0, are rejected. The remaining numbers of objects are 153 ( $k r^{-2}$ ), 184 ( $k r^{-3}$ ), and 194 ( $k r^{-5}$ ), as appears from Table 20. The majority of the excluded nebulae are very elongated, the corrections to the major diameters being rather large for these objects. For round nebulae the diameter correction is zero.

The distributions of the new values of  $\cos \varphi$  are given by the open circles in Fig. 15. It may be remarked, that the different class frequencies have been multiplied by such a factor that the total number becomes equal to the previous number of 270. Thus, the different distribution curves are directly comparable. It appears that the new distributions differ considerably from those discussed above. The large excess of edgewise nebulae is removed, or is considerably diminished. The distribution corresponding to  $k r^{-3}$  gives an increase from 30 objects ( $\cos \varphi = 0.8-1.0$ ) to 45 ( $\cos \varphi = 0.0-0.2$ ), *i. e.* the excess has been



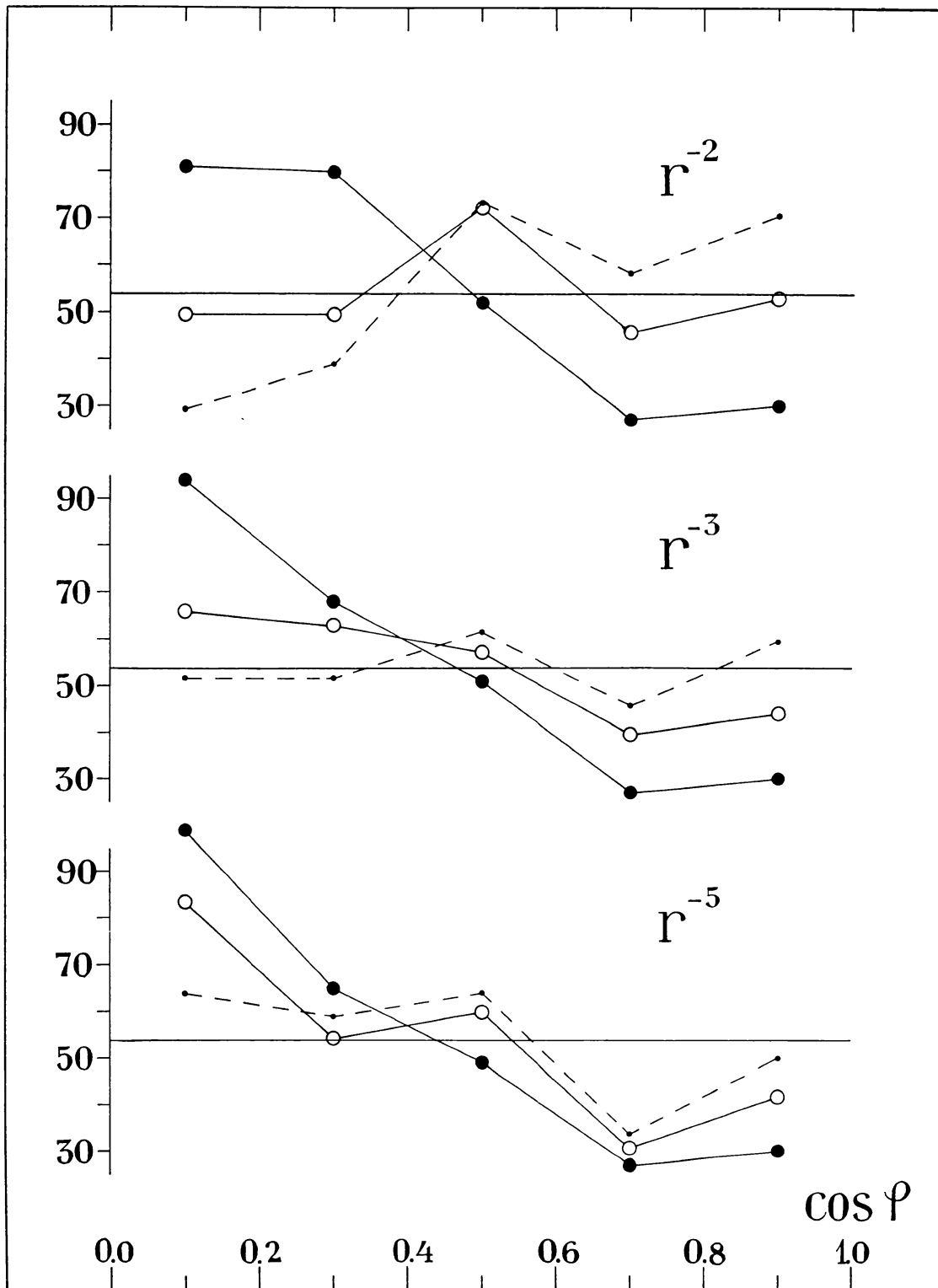


Fig. 15. The distribution of  $\cos \varphi$  as obtained for spiral nebulae in Reinmuth's catalogue. The full circles represent the distributions derived from the uncorrected diameter ratios. The broken lines give the corrected distributions.

reduced from over 200 % to 50 %. As regards the luminosity function  $k r^{-2}$ , the excess has been entirely removed, the systematic corrections to the apparent diameters being larger in this case.

It has been mentioned above, that the corrections to be applied to Reinmuth's diameter ratios for spiral nebulae are, on an average, the same as those obtained for the artificial nebulae with a luminosity function  $k r^{-3}$ . The excess of nebulae with an edgewise orientation that is obtained, even when these corrections are applied, certainly depends on the fact that the surface brightness of a nebula is related to the inclination. Objects with an edgewise orientation presumably have a larger surface brightness than nebulae situated in the celestial plane. If there were no absorption within the galaxies, the average surface brightness ought to be proportional to the inverse value of the apparent surface, *i.e.* the relative surface brightness would be equal to  $a/b$ . The occulting matter to be found in probably all of the spiral nebulae causes an absorption of light that apparently increases with the inclination. If we try to express the relative surface brightness by the simple function  $(a/b)^n$ , the average value of the exponent  $n$  ought to be smaller than unity, but presumably larger than zero. We may assume that the diameter ratio  $b/a$  is, at least approximately, independent of a certain increase, or decrease, in the surface brightness. However, both the diameters, as measured on the plate, will become larger as the surface brightness increases. Since our material of nebulae is selected according to the major diameters of the objects, the result will be a certain excess of elongated nebulae, *i.e.* the spirals with an edgewise orientation are collected from a larger volume of space.

The *fourth step* in the investigation will be to try to correct the major diameters of the nebulae for the effects produced by the differences in the surface brightness. If the distribution of light is of the form  $k r^{-3}$ , the major diameter is reduced to zero inclination by a division with the factor  $(a/b)^{n/3}$ . For the luminosity functions  $k r^{-2}$  and  $k r^{-5}$  the reduction factors are  $(a/b)^{n/2}$  and  $(a/b)^{n/5}$ , respectively.

When a large material of photometrically measured nebulae becomes available, it will be possible to determine a definitive value of the exponent  $n$ . For the present, we have to be satisfied with an approximation. If  $n$  is put equal to zero, the distribution of  $\cos \varphi$  is given by the open circles in Fig. 15. If  $n$  is given a value of unity, the distribution of  $\cos \varphi$  (for  $i = k r^{-3}$ ) is overcorrected, *i.e.* the excess of nebulae with an edgewise orientation changes into a deficit of about the same size. We have here an indication that the true value of  $n$  is situated somewhere in between these extremities.

The broken curves given in Fig. 15 show the results that are obtained if the exponent  $n$  is put equal to  $1/2$ , *i.e.* if the relative surface brightness is assumed to be equal to  $\sqrt{a/b}$ . The nebulae with corrected major diameters smaller than 3.0 have, as before, been rejected. The remaining numbers of objects are given in the fourth column of Table 20. It appears that (for  $i = k r^{-3}$ ) *a random distribution is obtained of the distribution angles*. In fact, the number of objects (52) in the first two classes ( $\cos \varphi = 0.0-0.4$ ) is almost exactly the same as the

number (53) in the two last groups ( $\cos \varphi = 0.6-1.0$ ). For  $i = k r^{-2}$ , the distribution of  $\cos \varphi$  has been overcorrected whereas, for  $i = k r^{-5}$ , there still remains a certain excess of nebulae with an edgewise orientation.

It may be recollected, that the above result is based on the systematic corrections which have been derived for Reinmuth's diameters in Chapter II of this paper. The only assumption that has been made refers to the relation between surface brightness and inclination. It may, however, be remarked that a certain deviation of the above exponent  $n$  from the adopted value  $1/2$  gives a comparatively small change in the distribution of  $\cos \varphi$ . Considering the accidental errors in the different class frequencies, we find that a more or less random distribution of the inclinations is obtained for values of  $n$  ranging from 0.4 to 0.6. A random distribution being *a priori* highly probable, we may, in fact, consider the latter values as a result of this investigation.

**16.** *The orientation of nebulae as obtained from Reiz's catalogue.* An investigation of the orientation of the spiral nebulae will now be made by using the large material collected by A. REIZ.<sup>1</sup> This catalogue, which is also based on the Heidelberg plate material, comprises 4666 nebulae situated in the north galactic cap ( $b = 50^\circ-90^\circ$ ). The catalogue contains all nebulae which appear on the plates, and may be assumed to be as homogeneous as Reinmuth's catalogue. The major and minor diameters have been given for all the objects.

From Reiz's catalogue all nebulae are selected which have major diameters larger than, or equal to 3'.0. Although the catalogue is certainly complete down to a smaller diameter value, the objects smaller than 3.0 will not be included on account of the classification difficulties. The following objects are rejected: (a) all nebulae which in the Shapley-Ames catalogue<sup>2</sup> are classified as elliptical or irregular objects, (b) two nebulae which by Reiz are classified as belonging to the types  $g$  and  $g-h_0$  (Wolf's system), and which are probably elliptical objects. The remaining number of nebulae amounts to 156.

The distribution of the types of the 156 nebulae is similar to that obtained for Reinmuth (Table 18). In the Harvard catalogue, 122 of the objects have been classified as normal, or barred spirals. The remaining objects belong, according

---

<sup>1</sup> Lund Ann 9, 1941. It may be remarked here that the writer's catalogue (Lund Ann 6, 1937), containing 1854 components of double and multiple systems, is also based on the Heidelberg plate material. However, this material is not suitable for an investigation of the orientation of the nebulae, since it may be assumed to contain certain selection effects. A double nebula has been included in the catalogue only if the distance between the two components is smaller than, or equal to, twice the sum of the two major diameters. Since the major diameter of an elongated nebula is measured too large as compared to that of a round object, the limiting distance between the components of a double system is larger when the objects have an edgewise orientation than when the objects are situated in the celestial plane. The result is apparently that a too large number of elongated nebulae are included in the catalogue.

<sup>2</sup> The additions and revisions given in Harvard Ann 88, No 4, 1934, have been taken into account.

TABLE 21.

*Distribution of the diameter ratios  $\beta/a$  for spiral nebulae with major diameters larger than, or equal to 3'.0. (Reiz's catalogue.)*

$\beta/a$	Number
$\leq 0.049$	0
0.050–0.099	10
0.100–0.149	29
0.150–0.199	11
0.200–0.249	20
0.250–0.299	14
0.300–0.399	16
0.400–0.499	13
0.500–0.599	13
0.600–0.699	16
0.700–0.799	2
0.800–0.899	4
0.900–1.000	8

total 156

to Reiz, to the Wolf types given in the column heads of Table 18. However, all the latter objects will be excluded when the corrections to the apparent diameters are applied. Of the 67 objects which are included in the final solution, all are spirals according to the Harvard catalogue.

The distribution of the ratios  $\beta/a$ , corresponding to Reiz's diameter values, appears from Table 21. There seems to be a considerable excess of elongated objects. The diameter ratios are, on an average, somewhat smaller than those given by Reinmuth. The smallest ratio is, according to Reiz, found for NGC 4244, which has a ratio  $\beta/a$  equal to 0.050.

The values of  $\cos \varphi$ , as corresponding to the ratios  $\beta/a$ , are now computed for the above 156 nebulae. In formula (5 b)  $b/a$  is exchanged for  $\beta/a$ , and  $q$  for  $f \cdot q$ . The constant  $q$  (ratio of absolute minor and major axes) is, as before, put equal to 0.20. In determining the value of the factor  $f$  we have to take into account that Reiz differs from the mean observer as regards the measuring errors. We refer to Fig. 6, where the relations are given between the individual observers on the one hand and the mean observer on the other. The factor  $f$  is obtained if the ratio of Reiz to the mean observer, as obtained from this figure (curve II), is multiplied by the factors (corresponding to  $b/a = 0.20$ ) given in Table 10. The result is a value of  $f \cdot q$  equal to 0.125, if the light distribution is of the type  $kr^{-3}$ . An analysis of the distribution of  $\beta/a$ , as given in Table 21, also results in an effective minimum value of  $\beta/a$  of this order of size.

The resulting distribution of  $\cos \varphi$  is given by the full circles in Fig. 16. In this case only one computation, corresponding to the light function  $kr^{-3}$ , has been made. It appears that there is a considerable excess of nebulae with an edgewise orientation. The number of objects (69) in the class  $\cos \varphi = 0.0-0.2$

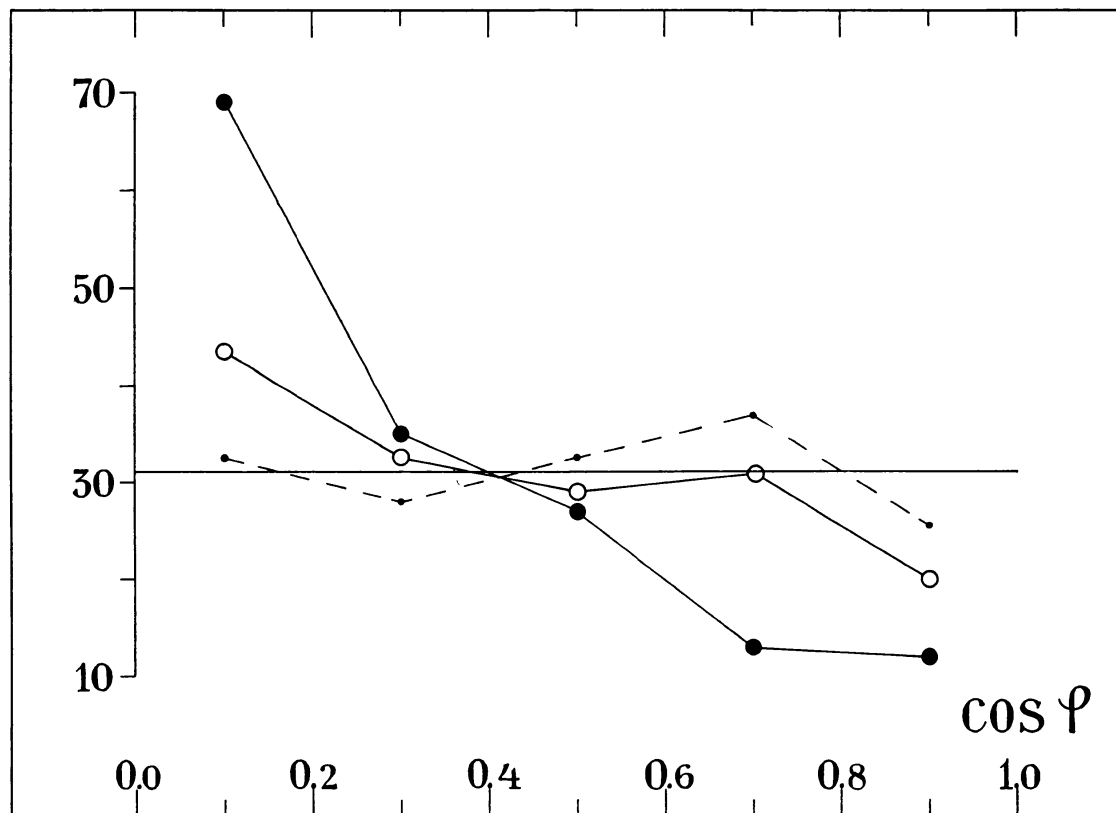


Fig. 16. The distribution of  $\cos \varphi$  as obtained for spiral nebulae in Reiz's catalogue. The broken curve represents the corrected distribution.

is almost *six* times as large as the number (12) in the class  $\cos \varphi = 0.8-1.0$ . The excess is much larger than that obtained from Reinmuth's catalogue. The straight horizontal line corresponds, as before, to a random distribution.

The apparent diameters are now corrected for the systematic measuring errors. As regards the diameter ratios, the correction factors are obtained if the values given in the fifth column of Table 10 are multiplied by the ratio of Reiz to mean observer, as obtained from Fig. 6. The corrected major diameters are obtained if the catalogue diameters are divided by the values given in the fifth column of Table 6. Although Reiz differs from the mean observer as regards the diameter ratios, the major diameters are apparently measured in the same way. A comparison between the major diameters of the artificial nebulae as measured by Reiz and by the mean observer fails to reveal any differences of a systematic nature. Consequently, the systematic differences in the diameter ratios depend exclusively on the minor diameters.

If all nebulae with corrected major diameters smaller than 3'.0 are rejected, there remain 86 objects. The distribution of  $\cos \varphi$ , as corresponding to the corrected diameter ratios, is given by the open circles in Fig. 16. The class frequencies have been reduced to a total number of 156. It appears that the large excess of

nebulae with an edgewise orientation has almost disappeared. A number of 42 objects in the group  $\cos \varphi = 0.0-0.4$  corresponds to a number of 28 in the group  $\cos \varphi = 0.6-1.0$ .

In the next step, the major diameters are corrected for the variations in the surface brightness. It is, as before, assumed that the relative surface brightness can be represented by the expression  $\sqrt{a/b}$ . Hence, each major diameter is divided by the quantity  $(a/b)^{1/6}$ . If all nebulae with resulting diameter values smaller than 3.0 are excluded, there remains a number of 67 objects for the final solution.

The distribution of  $\cos \varphi$  for these 67 nebulae is represented by the broken curve in Fig. 16. *A random distribution has been obtained.* There is, in the group  $\cos \varphi = 0.0-0.4$ , 26 objects whereas a number of 27 is found in the group  $\cos \varphi = 0.6-1.0$ . Thus, the agreement with an accidental distribution is, in spite of the smaller material, as good as that obtained for the nebulae selected from Reinmuth's catalogue.

**17.** *The orientation of nebulae as obtained from the Shapley-Ames catalogue.* The spiral nebulae contained in the SHAPLEY-AMES catalogue<sup>1</sup> will now be investigated as regards their orientation with respect to the celestial plane. The catalogue gives apparent magnitudes for all extragalactic objects down to about the thirteenth magnitude, and represents the best magnitude list available for a larger number of nebulae. However, the catalogue does not give apparent diameters for all of the objects. Furthermore, the published diameters have been collected from various different sources. It has consequently been decided, that the catalogue will be used only for the selection of the material, and that the apparent dimensions will be taken from Reinmuth's catalogue.

Since Reinmuth's catalogue refers only to the northern sky, the objects in the Shapley-Ames catalogue with declinations smaller than  $-20^\circ$  cannot be included in the investigation. Furthermore, the faintest objects have to be excluded on account of classification difficulties. Since these objects are also, as a rule, rather small, their diameters and diameter ratios are not so well determined. It has seemed appropriate to include only those nebulae which have magnitudes brighter than, or equal to 12<sup>m</sup>3.

If all nebulae which have been definitely classified as elliptical or irregular systems are disregarded, there are in the Harvard catalogue ( $\delta > -20^\circ$ ) 258 objects with magnitudes brighter than, or equal to the above limiting value. All these objects are, with one exception (NGC 5584), to be found also in Reinmuth's catalogue. The types of two of the nebulae (NGC 2268 and 5018) have not been given by Shapley and Ames. Since Reinmuth has referred them to the Wolf type *g*, they are presumably elliptical objects<sup>2</sup> and will be excluded. Furthermore the

<sup>1</sup> Harvard Ann 88, No 2, 1932. It may be remarked here that the catalogue given in Harvard Ann 88, No 4, 1934, cannot be used for investigations of this kind since it is not complete down to a certain limiting magnitude, or limiting diameter.

<sup>2</sup> In Harvard Ann 88, No 4, 1934, the object NGC 5018 has been classified as an elliptical nebula.

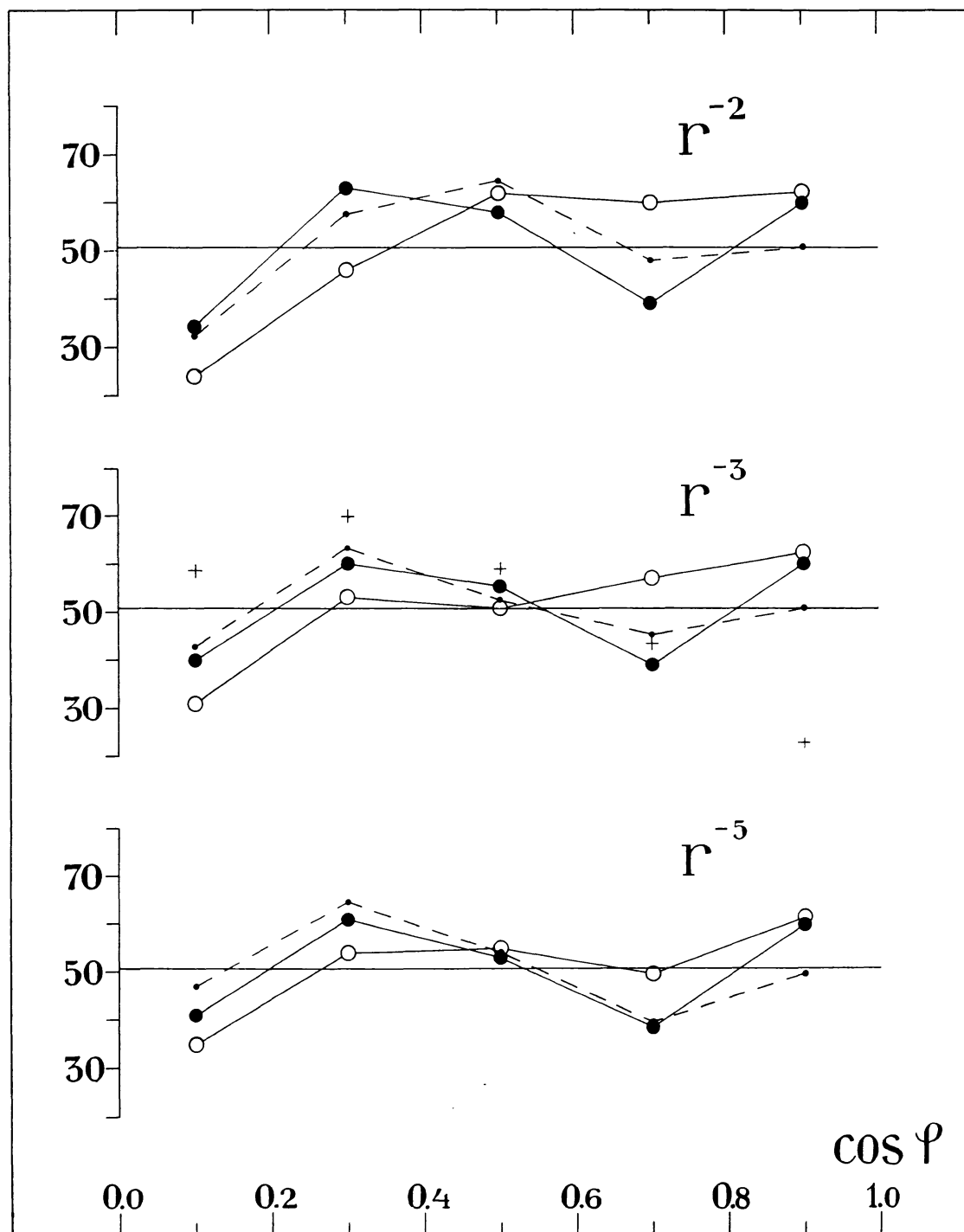


Fig. 17. The distributions of  $\cos \varphi$  as obtained for spiral nebulae in the Shapley-Ames catalogue. The broken lines represent the corrected distributions.



very large systems NGC 224 and 598 will be excluded. The following investigation will be based on the remaining 254 nebulae, which have all been classified as spirals in the Harvard catalogue. It may be remarked that the apparent dimensions of five objects have been taken from the latter catalogue, the Heidelberg catalogue being incomplete in these cases.

The diameter ratios  $\beta/a$  are now computed for the above 254 spirals. The values of  $\cos \varphi$ , as corresponding to  $\beta/a$ , are determined by using the same procedure as above. Three different computations are made, corresponding to the light distributions  $k r^{-2}$ ,  $k r^{-3}$ , and  $k r^{-5}$ .

The distributions of the 254 values of  $\cos \varphi$  are given by the full circles in Fig. 17. The straight horizontal lines represent, as before, random distributions of the inclination angles. It seems, as if the derived distributions agree, on an average, rather well with accidental distributions. A similar result has been obtained in previous investigations, and it has been interpreted as a proof of a random orientation of the nebulae. However, the systematic errors in the diameter ratios, as well as the selection effects in the material, have not yet been taken into consideration. The true interpretation of the result is that *the systematic errors and the selection effects will, as regards the disturbances introduced in the distribution of  $\cos \varphi$ , approximately neutralize each other.*

The systematic corrections are now applied to the apparent diameter ratios. It has been described above how the observed value  $\beta/a$ , as corresponding to Reinmuth's diameters, is transformed into the true ratio  $b/a$ . Three sets of  $b/a$ -values are computed, corresponding to the above three luminosity functions. The values of  $\cos \varphi$  are then derived from the corrected diameter ratios. It may be remarked that the number of nebulae included is still 254.

The open circles in Fig. 17 give the distributions of the new values of  $\cos \varphi$ . It appears that the distributions give a deficit of nebulae with an edgewise orientation to the celestial plane. Thus, the correction of the diameter ratios gives the same result that has been obtained above: the relative number of elongated nebulae is reduced. The reduction is most pronounced in the case corresponding to the light distribution  $k r^{-2}$ , the corrections to the diameter ratios being largest in this case.

We will now try to correct the distributions for the selection effects inherent in the material. It has been mentioned above, that the absolute magnitude of a spiral nebula depends on the inclination of the object to the celestial plane. The occulting matter to be found within the stellar systems causes the largest absorption of light when the object has an edgewise orientation. If there were no absorption, the relative value of the average surface brightness would be equal to  $a/b$ . On account of the absorption, this expression is changed into  $(a/b)^n$ , the exponent  $n$  being smaller than unity. It has been found above, in the investigations of the nebulae selected from Reinmuth's and Reiz's catalogues, that the average value of  $n$  ought to be approximately equal to  $1/2$ . In any case, random distributions of the inclinations are obtained if this value is adopted. It may be remarked, that a value

TABLE 22.

*Numbers of spiral nebulae, with magnitudes brighter than or equal to 12<sup>m</sup>.3, which are included in the solutions I, II, and III. (Shapley-Ames's catalogue,  $\delta > -20^\circ$ .)*

Assumed light distribution	I (no corrections)	II (diameters corr. for measuring errors)	III (magnitudes corr. for absorption and syst. errors)
$k r^{-2}$	254	254	184
$k r^{-3}$	254	254	185
$k r^{-5}$	254	254	189

of  $n$  equal to  $1/2$  corresponds to a maximum difference in magnitude of 0<sup>m</sup>.87, *i. e.* this value represents the loss in absolute magnitude when the inclination changes from  $0^\circ$  to  $90^\circ$ . It is, as before, assumed that the minimum value of  $b/a$  ( $=$  the ratio of the absolute minor and major axes) is, on an average, equal to 0.20.

We may first try to adopt the above value of  $n$ , *i. e.* the total absolute brightness of a spiral nebula is assumed to be proportional to the quantity  $\sqrt{b/a}$ . The corresponding loss in magnitude is computed for each value of  $b/a$ . The apparent magnitudes are then corrected by these amounts, *i. e.* the magnitudes are reduced to  $90^\circ$  inclination (edgewise orientation). The corrections are given by the formula

$$\Delta m = 2.5 \log(5 b/a)^{1/2} \quad (7)$$

All nebulae with corrected magnitudes fainter than 12<sup>m</sup>.3 are rejected. The values of  $\cos \varphi$ , as derived above from the ratios  $b/a$ , remain of course unchanged.

The crosses given in Fig. 17 show the resulting distribution of  $\cos \varphi$ , as corresponding to the light function  $k r^{-3}$ . The deficit of nebulae with an edgewise orientation has now been changed into an excess. In fact, the deviation of the distribution from a random one has become slightly larger than before. The natural conclusion is that the magnitudes of the nebulae have been overcorrected. In order to obtain an accidental distribution the above maximum correction of 0<sup>m</sup>.87 apparently has to be considerably reduced.

Up till now, the possibility of the existence of systematic errors in the *apparent* magnitudes, as given in the Harvard catalogue, has not been taken into consideration. It seems rather probable that the above maximum loss in absolute magnitude of about 0<sup>m</sup>.87 is to a certain degree neutralized by systematic errors in the apparent magnitudes. Comparisons between the Harvard magnitudes and photometrically determined magnitudes<sup>1</sup> give the result that the former values are systematically too faint, the average difference being of the order of size 0<sup>m</sup>.7. The systematic difference apparently depends on the fact that the outmost parts

<sup>1</sup> Cf. the investigations by R. O. REDMAN and E. G. SHIRLEY of elliptical nebulae (MN 96, p. 588, 1936, and MN 98, p. 613, 1938). See also a paper by the writer (Lund Medd, Ser II, No 114, 1945) where two spiral nebulae have been photometrically investigated.

of a nebula, which may represent a considerable part of the total brightness, are recorded only by the photometer. It has been shown previously in this paper (Cf. Table 5) that the apparent surface of a nebula, as measured visually through the eyepiece, is related to the inclination of the object. When the inclination changes from  $0^\circ$  to  $90^\circ$ , the ratio of the measured surface to the »true» surface increases. The increase may, in fact, amount to 100 per cent, or more.<sup>1</sup> It seems highly reasonable to assume that this increase in the surface will produce a corresponding effect in the apparent magnitude, *i. e.* the estimated magnitude grows too bright as the inclination of the nebula becomes larger.

The corrections to be applied to the apparent magnitudes of the spiral nebulae are now given by the formula

$$\Delta m = 2.5 \log(5 b/a)^{1/2} - 2.5 \log(5 b/a)^l = 2.5 \log(5 b/a)^{1/2-l} \quad (8)$$

In this expression the first term refers to the variations in the absolute magnitude, whereas the second term is supposed to represent the systematic error in the estimated apparent magnitude. We may assume that the exponent  $l$  has a value between the limits 0 and  $1/2$ , corresponding to maximum corrections equal to  $0^m.00$  and  $0^m.87$ , respectively. In want of any detailed knowledge of the errors in the Harvard magnitudes, we may try to put  $l$  equal to  $1/4$ . This value corresponds to a maximum correction of  $0^m.44$ , which, considering the size of the systematic errors in the apparent dimensions, does not seem to be an unreasonable amount. A final determination of the exponent  $l$  will, of course, be possible first when we have access to a large number of photometrically determined magnitudes.

The magnitudes of the spiral nebulae are now corrected by the amounts given by the above formula, the exponent  $l$  being equal to  $1/4$ . All nebulae with corrected magnitudes fainter than  $12^m.3$  are rejected. The remaining numbers of objects are given in the fourth column of Table 22.

The resulting distributions of  $\cos \varphi$  are given by the broken curves in Fig. 17. The different class frequencies have been reduced to a total number of 254. There appears to be a small deficit of nebulae with an edgewise orientation if the light distribution is assumed to be equal to  $k r^{-2}$ . For a luminosity function equal to  $k r^{-5}$  this deficit seems to be changed into an excess. For a light function  $k r^{-3}$ , which gives the best representation of the average distribution of light in the outer parts of the spirals, *a random distribution is obtained of the inclination angles*. There is, in the group  $\cos \varphi = 0.0-0.4$ , 77 objects, whereas a number of 70 is found in the group  $\cos \varphi = 0.6-1.0$ . Considering the accidental errors in the class frequencies, we may conclude that the agreement with an accidental distribution is very satisfactory.

It appears from the above discussion that certain difficulties are encountered,

---

<sup>1</sup> According to Table 5, the measuring errors produce an increase in the apparent surface of 26 per cent when the light distribution is equal to  $k r^{-3}$ . If we also consider the increase in surface brightness for nebulae with an edgewise orientation (rel. surface brightness =  $\sqrt{a/b}$ ) we will get an additional increase in the apparent surface of 71 per cent.

when the apparent magnitude is used as a distance indicator for the selection of a material of nebulae representative of a given volume of space. Both the absolute and the apparent magnitudes contain systematic effects related to the inclination angle. It has been assumed that the absolute brightness of a spiral is proportional to  $(b/a)^{1/2}$ , and that the estimated apparent brightness is inversely proportional to  $(b/a)^{1/4}$ . The correctness of the first assumption has been confirmed by the investigations of the orientation of nebulae selected from Reinmuth's and Reiz's diameter catalogues. The second assumption seems to be justified by the result obtained above. Since the probability of a random distribution of the inclinations of the nebulae is *a priori* extremely large, we may, perhaps, consider the magnitude correction given by formula (8) not as an assumption but as a *result* of this investigation.

## CHAPTER IV.

**On the existence of a metagalactic preferential plane.**

**18. Introduction.** In this chapter an investigation will be made of the orientation in space of the principal planes of the spiral nebulae. It is a very interesting question whether the nebular discs are orientated at random in space, or they have an orientation of a more or less systematic nature. In the latter case we may expect to find a certain degree of parallelism between the individual nebular planes. The fundamental plane defined by this parallelism will here be called the *preferential plane*.

In the previous chapter an investigation has been made of the inclinations of the spiral nebulae to the celestial plane. According to the results obtained there the distribution of the inclination angles seems to be of an accidental nature. A random orientation with respect to the celestial plane does not, however, exclude the possibility of the existence of a more or less pronounced preferential plane, as defined above. A certain tendency to parallelism between the nebular discs may not be revealed in an investigation of the inclination angles, supposing that the investigation is based on a large area of the sky.

The problem of determining a possible preferential plane is in many respects identical with the problem of determining the space velocity distribution for stars in our own galactic system by means of the observed peculiar motions. The latter motions are in this case to be replaced by the apparent distances of the stars in the different spiral nebulae from the centres of their respective systems. Starting from these projected distances we are able to derive the distribution in space of the corresponding absolute distances. This distribution will have the same form as the giant galaxy corresponding to all the nebulae included in the investigation, *i. e.* the giant system that would be obtained if all the nebulae were, without any change of their orientation in space, brought together so that their centres coincide. If the derived distribution has a spherical shape, the nebular discs are orientated at random in space. A preferential plane may be said to exist only if the distribution has the form of a rotation ellipsoid, the polar axis being the shortest axis.

The problem of the orientation in space of the spiral nebulae has been discussed in several previous papers. We may mention the investigations by H. KNOX-SHAW,<sup>1</sup>

---

<sup>1</sup> MN 69, p. 72, 1908.

B. MEYERMANN,<sup>1</sup> C. C. L. GREGORY,<sup>2</sup> K. LUNDMARK,<sup>3</sup> and C. G. DANVER.<sup>4</sup> However, it seems justified to state that no conclusive results as regards a possible parallelism between the nebular discs have as yet been obtained. Most of the previous investigations have been based on materials of nebulae containing more or less serious selection effects referring to the orientation of the objects. It may be remarked here that the search for a possible preferential plane has also been carried on along other lines. Thus, an investigation has been made by the writer<sup>5</sup> concerning the orientation in space of the orbital planes of double nebulae. On the other hand, K. LUNDMARK<sup>5</sup> has tried to derive a preferential distribution plane (metagalactic equator) by examining the apparent distributions of the objects included in all available nebular catalogues.

**19. The mathematical theory.** It has been mentioned above that the method used for the determination of the space velocity distribution for stars in our system by means of the observed tangential motions may be applied also to the present problem. The mathematical theory developed for this purpose will be shortly recapitulated here. For further details we refer to the investigations by C. V. L. CHARLIER.<sup>6</sup>

In order to simplify the numerical computations, the sky will first be divided into 48 squares,  $A_1$ — $A_2$ ,  $B_1$ — $B_{10}$ ,  $C_1$ — $C_{12}$ ,  $D_1$ — $D_{12}$ ,  $E_1$ — $E_{10}$ , and  $F_1$ — $F_2$ . In this case, the squares refer to the equatorial system. The  $A$ -squares are situated above a declination of  $+66^\circ.4$ , the  $B$ -squares between  $+30^\circ.0$  and  $+66^\circ.4$ , the  $C$ -squares between  $0^\circ.0$  and  $+30^\circ.0$ , and the  $D$ -squares between  $-30^\circ.0$  and  $0^\circ.0$ . The  $E$ - and  $F$ -squares, representing the southern sky, will not be of any use in this case. In each declination interval the squares are evenly distributed in right ascension, the first square beginning at  $\alpha = 0^h.0$  and the last square ending at  $\alpha = 24^h.0$ . The different areas represent portions of the sky that are of the same size.

For each square a system of rectangular coordinates  $(x, y, z)$  is defined. The  $z$ -axis points towards the centre of the square, whereas the  $x$ -axis and the  $y$ -axis are situated in the celestial plane, directed towards increasing right ascension and declination, respectively.

The next step is the computation, in each square, of the statistical moments of the second order of  $x$  and  $y$ . Generally, each square contains several nebulae. For each of the objects the moments  $\nu_{20}$ ,  $\nu_{02}$ , and  $\nu_{11}$  have to be determined. In a given nebula, every star is represented by a pair of  $x$ - and  $y$ -values. The average values  $\bar{x}$  and  $\bar{y}$  give the position of the centre of the nebula with respect to the centre of the square. Now, the statistical moments are defined by means of the differences  $(x - \bar{x})$  and  $(y - \bar{y})$ :

<sup>1</sup> AN 219, p. 131, 1923.

<sup>2</sup> MN 84, p. 456, 1924.

<sup>3</sup> Upsala Medd 30, 1927.

<sup>4</sup> Lund Ann 10, 1942.

<sup>5</sup> Lund Ann 6, p. 86, 1937.

<sup>6</sup> See *e.g.* The motion and the distribution of the stars, Berkeley, California, 1926.



$$\begin{aligned}
\nu_{20} &= \overline{(x-\bar{x})^2} \\
\nu_{02} &= \overline{(y-\bar{y})^2} \\
\nu_{11} &= \overline{(x-\bar{x})(y-\bar{y})}
\end{aligned} \tag{9}$$

The first moment,  $\nu_{20}$ , gives the square of the dispersion along the  $x$ -axis of the stars in the system, whereas the second moment,  $\nu_{02}$ , gives the square of the dispersion along the  $y$ -axis. The third moment,  $\nu_{11}$ , is a measure of the correlation between the different  $x$ - and  $y$ -values. The arithmetical means of the statistical moments obtained for the different nebulae in each square, *i. e.*  $\overline{\nu_{20}}$ ,  $\overline{\nu_{02}}$ , and  $\overline{\nu_{11}}$ , represent the basic values upon which our investigation will be founded.

In reality, the statistical moments cannot, of course, be computed exactly in the manner indicated above. The determination of the moments will be more closely discussed in the next section.

We will now introduce a system of rectangular coordinates  $X$ ,  $Y$ , and  $Z$ . The  $X$ -axis is directed towards the vernal equinox, whereas the  $Z$ -axis points to the North Pole. The  $Y$ -axis has a right ascension of  $90^\circ$ .

The mean  $\overline{(X^i Y^j Z^k)}$ , which represents a statistical moment in the  $XYZ$ -system, is denoted by  $N_{ijk}$ . The following relations are to be found between the moments  $N_{ijk}$  and the moments  $\nu_{ij}$  defined above:

$$\begin{aligned}
\nu_{20} &= \gamma_{11}^2 \cdot N_{200} + \gamma_{21}^2 \cdot N_{020} + \gamma_{31}^2 \cdot N_{002} + 2\gamma_{21}\gamma_{31} \cdot N_{011} + 2\gamma_{31}\gamma_{11} \cdot N_{101} + 2\gamma_{11}\gamma_{21} \cdot N_{110} \\
\nu_{02} &= \gamma_{12}^2 \cdot N_{200} + \gamma_{22}^2 \cdot N_{020} + \gamma_{32}^2 \cdot N_{002} + 2\gamma_{22}\gamma_{32} \cdot N_{011} + 2\gamma_{32}\gamma_{12} \cdot N_{101} + 2\gamma_{12}\gamma_{22} \cdot N_{110} \\
\nu_{11} &= \gamma_{11}\gamma_{12} \cdot N_{200} + \gamma_{21}\gamma_{22} \cdot N_{020} + \gamma_{31}\gamma_{32} \cdot N_{002} + (\gamma_{31}\gamma_{22} + \gamma_{21}\gamma_{32}) \cdot N_{011} + (\gamma_{31}\gamma_{12} + \\
&\quad + \gamma_{11}\gamma_{32}) \cdot N_{101} + (\gamma_{11}\gamma_{22} + \gamma_{21}\gamma_{12}) \cdot N_{110}.
\end{aligned} \tag{10}$$

The quantities  $\gamma_{ij}$  are the direction cosines for the different equatorial squares, and they have been tabulated by Charlier for the centres of the squares. In this investigation we will use these mean values, although the nebulae are not always symmetrically distributed within the squares. The small errors introduced by this approximation will be of no importance in this case.

The moments  $N_{ijk}$  are now derived from the above equations by means of a least squares solution. There are six unknown quantities to be determined, whereas the number of equations is equal to three times the number of equatorial squares included. Each equation is given a weight equal to the number of nebulae in the corresponding area. The final values of the moments  $N_{ijk}$  obtained in this way represent the total spatial distribution corresponding to all the nebulae included in the investigation.

In the next step, the coordinate system  $XYZ$  is turned in such a way that the correlation moments  $N_{011}$ ,  $N_{101}$ ,  $N_{110}$  disappear. The dispersions  $\sigma_1$ ,  $\sigma_2$ , and  $\sigma_3$  along the new axes are, in accordance with well-known transformations, obtained by solving the following equation of the third degree:



$$\begin{vmatrix} (N_{200}-t) & N_{110} & N_{101} \\ N_{110} & (N_{020}-t) & N_{011} \\ N_{101} & N_{011} & (N_{002}-t) \end{vmatrix} = 0 \quad (11)$$

The squares of the dispersions are equal to the roots of this equation. The directions of the new axes are also easily determined.

The three dispersions derived above indicate the extensions, along the three axes, of the giant galaxy that is composed of all the single nebulae included in the investigation. If two of the dispersions have identical values, and the third dispersion is smaller than these two, a preferential plane evidently exists, *i. e.* the principal planes of the different nebulae are, more or less, parallel to each other in space.

**20.** *The determination of the statistical moments  $\nu_{ij}$ .* The moments  $\nu_{ij}$  which have been defined in equation (9), represent the apparent distribution of stars within each single nebula. Since it is, of course, not possible to determine these quantities in a theoretically correct way, we have to make use of certain approximations. The approximations are based on the assumption that the different spiral nebulae are constructed in a similar way.

Let us first determine the extensions of a nebula along the  $x$ - and  $y$ -axes defined above. These extensions may be denoted by  $\Delta x$  and  $\Delta y$ , respectively. If the position angle<sup>1</sup> of the major axis of the nebula is denoted by  $\psi$ , we arrive at the following relations:

$$\begin{aligned} (\Delta x/a)^2 &= \sin^2 \psi (1 - (b/a)^2) + (b/a)^2 \\ (\Delta y/a)^2 &= \cos^2 \psi (1 - (b/a)^2) + (b/a)^2 \end{aligned} \quad (12 a)$$

The relations have been derived in the same way as the equation (5 b) given in the previous chapter. The quantities  $a$  and  $b$  mean, as before, the apparent major and minor diameters of the nebula.

The dispersions in  $x$  and  $y$ , or the square roots of the moments  $\nu_{20}$  and  $\nu_{02}$ , may now be assumed to be proportional to the extensions  $\Delta x$  and  $\Delta y$ . If all the nebulae are assumed to be built up according to the same model, which is of course only approximately true, the factor of proportionality will be the same for all the objects. Since we are not interested in the absolute size of the dispersions, the factor may be put equal to unity. Let us, furthermore, put the apparent major diameter of each nebula equal to unity. This means that *all the objects included in the investigation are given the same weight, i. e.* that they are placed at about the same unit distance in space. The following simple expressions are now obtained for the moments  $\nu_{20}$  and  $\nu_{02}$ :

$$\begin{aligned} \nu_{20} &= \sigma_x^2 = \sin^2 \psi + (b/a)^2 \cos^2 \psi \\ \nu_{02} &= \sigma_y^2 = \cos^2 \psi + (b/a)^2 \sin^2 \psi \end{aligned} \quad (12 b)$$

<sup>1</sup> It is assumed that the position angle is, as usual, reckoned from the north through the east.

Thus, the statistical moments depend only on the diameter ratio and the position angle. The maximum value of the right members of the equations is equal to unity, whereas the minimum value is equal to the minimum of the square of the diameter ratio.

As regards the correlation moment  $\nu_{11}$  we will make use of the following well-known formula valid for a normal distribution of  $x$  and  $y$ :

$$\operatorname{tg} 2\psi = \frac{2\nu_{11}}{\sigma_y^2 - \sigma_x^2} \quad (13 \text{ a})$$

By starting from this expression we arrive at the following final relation:

$$\nu_{11} = \sin \psi \cos \psi - (b/a)^2 \sin \psi \cos \psi \quad (13 \text{ b})$$

The numerical minimum value of the right member is equal to zero, whereas the maximum value is  $1/2$  (for  $b/a = 0$ ).

It would be of a certain interest to determine the average values of the statistical moments defined in equations (12 b) and (13 b) corresponding to the case that the nebular discs are orientated at random in space, *i. e.* to the case that there is no preferential plane. The following average relations may be used as a starting-point:

$$\begin{aligned} \overline{\nu_{20}} &= \overline{\sin^2 \psi} + \overline{(b/a)^2} \cdot \overline{\cos^2 \psi} \\ \overline{\nu_{02}} &= \overline{\cos^2 \psi} + \overline{(b/a)^2} \cdot \overline{\sin^2 \psi} \\ \overline{\nu_{11}} &= \overline{\sin \psi \cos \psi} - \overline{(b/a)^2} \cdot \overline{\sin \psi \cos \psi} \end{aligned} \quad (14)$$

If the orientation is of an accidental character, the diameter ratio  $b/a$  is independent of the position angle  $\psi$ , and, consequently, the mean of *e. g.* the product  $(b/a)^2 \cdot \cos^2 \psi$  may be put equal to the product of the means of the two factors.

If the position angle is accidentally distributed, the following relations are valid:

$$\begin{aligned} \overline{\sin^2 \psi} = \overline{\cos^2 \psi} &= \frac{\int_0^\pi \cos^2 \psi \, d\psi}{\int_0^\pi d\psi} = 1/2 \\ \overline{\sin \psi \cos \psi} &= \frac{\int_0^\pi \sin \psi \cos \psi \, d\psi}{\int_0^\pi d\psi} = 0. \end{aligned} \quad (15 \text{ a})$$

The mean value of  $(b/a)^2$  may, according to equation (5 b), be expressed in the following way:

$$\overline{(b/a)^2} = (1 - q^2) \overline{\cos^2 \varphi} + q^2, \quad (15 \text{ b})$$

where  $q$  means the average ratio of the absolute minor and major axes of the nebulae, and  $\varphi$  is the inclination to the celestial plane. In the case of a random

orientation, the relative distribution function of the inclination angle is equal to  $\sin \varphi$ , as has been shown in the previous chapter. Thus

$$\overline{\cos^2 \varphi} = \int_0^{\pi/2} \cos^2 \varphi \sin \varphi d\varphi = 1/3 \quad (15 c)$$

By putting the absolute ratio  $q$  equal to the previously derived value of 0.20, we find that the average value of  $(b/a)^2$  will be equal to 0.36.

By introducing the mean values derived above into equations (14) we arrive at the following results:

$$\begin{aligned} \overline{\nu_{20}} = \overline{\nu_{02}} &= 0.68 \\ \overline{\nu_{11}} &= 0. \end{aligned} \quad (16)$$

If the orientation of the nebular planes in space is of a purely accidental nature, we have to expect that the average values of the moments  $\nu_{ij}$  approach, within the limits of the accidental errors, the numerical values given here.

The mean values derived above are based on the true ratios,  $b/a$ , of the apparent diameters of the nebulae. Besides, it has been supposed that the material investigated does not contain any selection effects referring to the orientation of the objects. It has been shown in the previous chapter that the systematic errors in the diameter ratios may, together with the selection effects, cause great disturbances when we are dealing with the inclinations of the nebulae to the celestial plane. Fortunately, these disturbances are considerably reduced in the present case, since the moments  $\nu_{ij}$  mainly depend on the position angle  $\psi$ . It seems safe to assume that the selection effects referring to this angle are, in most cases, inconsiderable. The problem will be further discussed in connection with the numerical solutions given below.

**21. The results as obtained from Reinmuth's catalogue.** The investigation of the orientation in space of the nebulae will first be based on the material collected by Reinmuth in his above-mentioned catalogue of the Herschel nebulae. All *spiral nebulae* with major diameters larger than, or equal to 3.0 will be selected for this purpose. The material to be used here is, in fact, identical with the material used in the previous chapter for the investigation of the inclinations of the objects to the celestial plane. We refer to section 15, where a detailed description of the material is given. For the same reasons as before, elliptical and irregular nebulae will not be included in the investigation.

There are, in Reinmuth's catalogue, 270 spirals with major diameters larger than the above limiting value. The position angles of the major axes have been given for all the elongated nebulae, except one. The material at hand thus comprises 269 objects.

Two complete numerical solutions will be made below. The first solution is based on the apparent diameters as given in the catalogue. The second solution is based on the corrected diameters, *i. e.* the diameters corrected for the systematic measuring errors.

TABLE 23.

*Statistical moments of the second order obtained for spiral nebulae in the different squares. (Reinmuth's catalogue.)*

Square	Number	$\overline{v_{20}}$	$\overline{v_{02}}$	$\overline{v_{11}}$
A 1	8 (5)	0.52 (0.49)	0.69 (0.82)	-0.21 (-0.14)
A 2	5 (2)	0.48 (0.37)	0.63 (0.79)	+0.10 (+0.06)
B 1	3 (2)	0.51 (0.36)	0.61 (0.88)	+0.09 (+0.28)
B 2	3 (0)	0.80	0.35	+0.10
B 4	7 (5)	0.54 (0.56)	0.71 (0.82)	-0.07 (-0.08)
B 5	33 (19)	0.61 (0.64)	0.61 (0.72)	+0.11 (+0.17)
B 6	34 (20)	0.65 (0.75)	0.62 (0.68)	-0.06 ( 0.00)
B 7	9 (2)	0.44 (0.27)	0.65 (0.88)	+0.05 (-0.10)
B 9	1 (1)	1.00 (1.00)	1.00 (1.00)	0.00 ( 0.06)
B 10	3 (2)	0.40 (0.14)	0.76 (0.94)	-0.13 (-0.20)
C 1	10 (5)	0.80 (0.76)	0.53 (0.78)	+0.06 (+0.12)
C 2	1 (1)	1.00 (1.00)	1.00 (1.00)	0.00 ( 0.00)
C 5	4 (1)	0.73 (0.30)	0.45 (0.93)	-0.15 (+0.19)
C 6	27 (16)	0.59 (0.73)	0.63 (0.63)	-0.02 (-0.04)
C 7	70 (30)	0.60 (0.64)	0.62 (0.74)	0.00 (-0.03)
C 8	12 (6)	0.58 (0.60)	0.63 (0.78)	+0.08 (+0.03)
C 9	2 (1)	0.86 (1.00)	0.73 (1.00)	+0.18 ( 0.00)
C 12	3 (0)	0.48	0.69	-0.04
D 1	4 (1)	0.74 (0.55)	0.64 (0.96)	+0.12 (-0.12)
D 2	2 (2)	0.97 (0.98)	0.57 (0.59)	-0.08 (-0.08)
D 3	2 (0)	0.53	0.53	+0.30
D 5	1 (0)	0.54	0.67	+0.37
D 6	5 (2)	0.56 (0.83)	0.80 (0.95)	+0.18 (+0.10)
D 7	15 (9)	0.63 (0.74)	0.66 (0.65)	-0.04 (-0.03)
D 8	2 (1)	0.51 (0.96)	0.59 (0.22)	+0.08 (+0.14)
D 9	1 (1)	0.80 (0.82)	0.41 (0.45)	+0.34 (+0.31)
D 12	2 (1)	0.31 (0.41)	0.80 (0.71)	-0.07 (-0.39)
means		.609 (.661)	.628 (.730)	+0.012 (+0.010)

The distribution in the different equatorial squares of the 269 spirals included in the *first solution* appears from the figures given in the left half of the second column of Table 23. The largest numbers are found in the squares *B*5, *B*6, *C*6, and *C*7, which correspond to areas in, and around the Coma-Virgo region. Several squares are situated in small galactic latitudes and contain no nebulae.

The statistical moments  $v_{20}$ ,  $v_{02}$ , and  $v_{11}$  are now computed for each nebula by means of the relations (12 b) and (13 b). In these equations the ratio  $b/a$  is replaced by  $\beta/\alpha$ , which means, as before, the ratio of the uncorrected diameter values. The average values of the moments, as obtained for each square, are given in the left halves of the third, fourth, and fifth columns of Table 23. It appears that  $\overline{v_{20}}$  and  $\overline{v_{02}}$  range from about 0.3 to 1.0, whereas  $\overline{v_{11}}$  ranges from -0.21 to +0.37.

The mean values of the 269 moments are given at the bottom of the table. We find that the means of  $v_{20}$  and  $v_{02}$  are somewhat smaller than the values derived above for a random orientation. The difference is partly to be explained as a result

of the excess of nebulae with an edgewise orientation (Cf. section 15), and partly as a result of the systematic errors in the ratios  $\beta/\alpha$ .

The moments  $N_{ijk}$ , referring to the equatorial system of coordinates, are now determined by means of relations (10). There are 81 equations available for the determination of the six unknown quantities. Each equation is given a weight equal to the corresponding number of nebulae. The least squares solution gives the following results (with mean errors):

$$\begin{array}{ll} N_{200} = + 0.572 \pm 0.012 & N_{011} = + 0.011 \pm 0.006 \\ N_{020} = + 0.617 \pm 0.006 & N_{101} = + 0.002 \pm 0.008 \\ N_{002} = + 0.634 \pm 0.007 & N_{110} = - 0.037 \pm 0.007 \end{array}$$

The correlation moments are, except the last one, numerically very small.

The coordinate system will now be turned in such a way that the correlation moments entirely disappear. The dispersions along the new axes are obtained by solving equation (11). The following final values (with mean errors) are obtained:

$$\begin{array}{l} \sigma_1 = 0.799 \pm 0.004 \\ \sigma_2 = 0.799 \pm 0.005 \\ \sigma_3 = 0.740 \pm 0.007 \end{array} \quad (17 a)$$

We find that the third dispersion is somewhat smaller than the other two dispersions, which are of the same size. The third axis, corresponding to the smallest dispersion, has the coordinates

$$\begin{array}{l} \alpha = 29^\circ \\ \delta = -5^\circ \end{array} \quad (17 b)$$

The dispersion values obtained here seem to indicate a certain preferential plane, the normal of which has the coordinates given above. The result will be further discussed at the end of this chapter (section 23).

The *second solution* is based on the corrected apparent diameters. It has been described in the previous chapter (section 15), how the major diameters  $\alpha$  and the ratios  $\beta/\alpha$  are corrected for the systematic measuring errors. The corrections are in this case based on the luminosity function  $k r^{-3}$ . The corrected diameters are, as before, denoted by  $a$  and  $b$ . All nebulae with corrected major diameters smaller than 3.0 are excluded from the material. The remaining number of objects amounts to 135.

The distribution of the 135 nebulae in the different equatorial squares is indicated by the figures within brackets in the second column of Table 23. The statistical moments  $\nu_{ij}$ , as computed from equations (12 b) and (13 b), are given (within brackets) in the third, fourth, and fifth columns. In this case, the mean values of  $\nu_{20}$  and  $\nu_{02}$ , as given at the bottom of the table, agree rather well with the values derived above for a random orientation.

The least squares solution of the 69 equations, weighted in the way described above, gives the following results:

$$\begin{aligned}
N_{200} &= +0.594 \pm 0.025 & N_{011} &= +0.006 \pm 0.012 \\
N_{020} &= +0.687 \pm 0.011 & N_{101} &= -0.001 \pm 0.016 \\
N_{002} &= +0.747 \pm 0.014 & N_{110} &= -0.066 \pm 0.013
\end{aligned}$$

As before, the correlation moments  $N_{011}$  and  $N_{101}$  have very small numerical values.

The turning of the coordinate system results in the following dispersions:

$$\begin{aligned}
\sigma_1 &= 0.864 \pm 0.008 \\
\sigma_2 &= 0.849 \pm 0.009 \\
\sigma_3 &= 0.748 \pm 0.015
\end{aligned} \tag{18 a}$$

The same result is obtained as above: two of the dispersions, being of about the same size, are somewhat larger than the third dispersion. The axis of the smallest dispersion has the coordinates

$$\begin{aligned}
\alpha &= 28^\circ \\
\delta &= -1^\circ
\end{aligned} \tag{18 b}$$

The results agree very well with those obtained in the first solution. We arrive at the conclusion that the disturbances caused by the systematic errors in the apparent diameters and by the selection effects in the material are comparatively small in the present case.

**22.** *The results as obtained from the Shapley-Ames catalogue.* The magnitude catalogue given by Shapley and Ames will now be used for the selection of the material of spiral nebulae. The investigation will be based on all spirals with magnitudes brighter than, or equal to  $12^m.3$ . The material is the same as that used in the previous chapter (section 17) for the investigation of the inclinations of the nebulae to the celestial plane. The total number of objects ( $\delta > -20^\circ$ ) is 254. The apparent diameters, and the position angles, have as before to be taken from Reinmuth's catalogue. However, the position angles are not given for five of the objects, and the final number is thus reduced to 249.

Two solutions will be made, the first based on the catalogue diameters and the second on the corrected diameters.

The *first solution* is based on the uncorrected apparent diameters. The moments  $r_{ij}$ , derived in the manner described above, are given in the left halves of columns 3, 4, and 5 of Table 24. It appears that the means of the quantities  $r_{20}$  and  $r_{02}$ , as given at the bottom of the table, are slightly larger than would be expected.

The least squares solution of the 78 equations gives the following results:

$$\begin{aligned}
N_{200} &= +0.660 \pm 0.015 & N_{011} &= -0.001 \pm 0.007 \\
N_{020} &= +0.664 \pm 0.007 & N_{101} &= +0.007 \pm 0.010 \\
N_{002} &= +0.730 \pm 0.009 & N_{110} &= -0.043 \pm 0.008
\end{aligned}$$

The turning of the coordinate system results in the following dispersions:

$$\begin{aligned}
\sigma_1 &= 0.854 \pm 0.005 \\
\sigma_2 &= 0.838 \pm 0.007 \\
\sigma_3 &= 0.788 \pm 0.007
\end{aligned} \tag{19 a}$$

TABLE 24.

*Statistical moments of the second order obtained for spiral nebulae in the different squares. (Shapley-Ames's cat.,  $\delta > -20^\circ$ .)*

Square	Number	$\overline{r_{20}}$	$\overline{r_{02}}$	$\overline{r_{11}}$
A 1	10 (8)	0.70 (0.68)	0.77 (0.78)	-0.11 (-0.10)
A 2	2 (2)	0.47 (0.49)	0.58 (0.60)	-0.36 (-0.35)
B 1	3 (2)	0.48 (0.50)	0.90 (0.94)	+0.22 (+0.18)
2	1 (1)	0.94 (0.95)	0.10 (0.14)	+0.16 (+0.15)
4	9 (6)	0.60 (0.54)	0.79 (0.73)	-0.06 (-0.05)
5	32 (25)	0.65 (0.62)	0.75 (0.74)	+0.06 (+0.06)
6	32 (23)	0.68 (0.70)	0.70 (0.66)	0.00 ( 0.00)
7	8 (4)	0.41 (0.37)	0.83 (0.74)	+0.03 (-0.09)
9	1 (1)	1.00 (1.00)	1.00 (1.00)	0.00 ( 0.00)
B 10	2 (2)	0.55 (0.57)	0.69 (0.73)	-0.08 (-0.08)
C 1	5 (5)	0.89 (0.90)	0.76 (0.78)	+0.02 (+0.02)
2	2 (0)	1.00	1.00	0.00
5	2 (2)	0.38 (0.43)	0.90 (0.92)	-0.01 (-0.01)
6	29 (20)	0.62 (0.62)	0.74 (0.72)	-0.01 (-0.01)
7	59 (42)	0.71 (0.71)	0.64 (0.63)	0.00 (+0.01)
8	5 (5)	0.36 (0.38)	0.86 (0.87)	+0.06 (+0.06)
11	1 (1)	0.98 (0.98)	0.15 (0.20)	+0.08 (+0.07)
C 12	3 (2)	0.34 (0.27)	0.76 (0.86)	-0.05 (+0.15)
D 1	2 (2)	0.37 (0.41)	0.88 (0.89)	-0.04 (-0.05)
2	9 (8)	0.72 (0.74)	0.78 (0.80)	0.00 (+0.02)
3	1 (1)	1.00 (1.00)	1.00 (1.00)	0.00 ( 0.00)
6	5 (5)	0.56 (0.60)	0.95 (0.96)	+0.07 (+0.06)
7	21 (15)	0.72 (0.78)	0.70 (0.64)	0.00 (+0.04)
9	1 (0)	0.80	0.41	+0.34
10	1 (0)	1.00	1.00	0.00
D 12	3 (1)	0.67 (0.41)	0.81 (0.71)	-0.04 (-0.39)
means		.661 (.659)	.726 (.711)	+.004 (+.007)

The third dispersion is, as before, somewhat smaller than the other two dispersions. The corresponding axis has the coordinates

$$\begin{aligned} \alpha &= 45^\circ \\ \delta &= -2^\circ \end{aligned} \tag{19 b}$$

The result agrees rather well with those obtained in the previous section.

The *second solution* is based on the corrected diameter values. The diameter ratios are corrected in the way described above. Corrections are also applied to the apparent magnitudes in the way described in the previous chapter (section 17). All nebulae with corrected magnitudes fainter than 12<sup>m</sup>.3 are excluded. The remaining number of objects is 183.

The values computed of the moments  $r_{ij}$  are given within brackets in Table 24. The means, which are given at the bottom of the table, agree rather well with the values corresponding to a random orientation.



TABLE 25.  
*Summary of results.*

Solution	N	$\sigma_1$	$\sigma_2$	$\sigma_3$	$\sigma_3/\sigma_1$	$\alpha$	$\delta$
Reinm. I	269	$0.799 \pm .004$	$0.799 \pm .005$	$0.740 \pm .007$	0.93	$29^\circ$	$-5^\circ$
Reinm. II	135	$0.864 \pm .008$	$0.849 \pm .009$	$0.748 \pm .015$	0.87	28	-1
Sh.-A. I	249	$0.854 \pm .005$	$0.838 \pm .007$	$0.788 \pm .007$	0.92	45	-2
Sh.-A. II	183	$0.850 \pm .006$	$0.844 \pm .008$	$0.762 \pm .010$	0.90	38	0
mean		$0.842 \pm .004$	$0.833 \pm .005$	$0.760 \pm .006$	0.90	$35^\circ$	$-2^\circ$

The least squares solution of the 69 equations gives the following results:

$$\begin{aligned} N_{200} &= +0.625 \pm 0.019 & N_{011} &= +0.001 \pm 0.009 \\ N_{020} &= +0.667 \pm 0.009 & N_{101} &= -0.001 \pm 0.012 \\ N_{002} &= +0.723 \pm 0.011 & N_{110} &= -0.067 \pm 0.010 \end{aligned}$$

The turning of the coordinate system results in the following dispersions:

$$\begin{aligned} \sigma_1 &= 0.850 \pm 0.006 \\ \sigma_2 &= 0.844 \pm 0.008 \\ \sigma_3 &= 0.762 \pm 0.010 \end{aligned} \tag{20 a}$$

The dispersions have very nearly the same values as those derived above. The coordinates of the axis corresponding to the smallest dispersion are

$$\begin{aligned} \alpha &= 38^\circ \\ \delta &= 0^\circ \end{aligned} \tag{20 b}$$

These values also agree with those previously derived.

**23. Summary of results.** In Table 25 a summary is given of the results obtained in the above four solutions. The successive columns give the number of nebulae included in the solution, the values of the three final dispersions (with mean errors), the ratio of the smallest and the largest dispersion, and the coordinates of the axis corresponding to the smallest dispersion. The arithmetical means of the different quantities are given at the bottom of the table.

As regards the numbers given in the second column it ought to be remarked that these partly refer to the same nebulae. Thus, about 60 per cent of the objects included in the solutions *Sh.-A. I* and *Sh.-A. II* are also included in the solutions *Reinm. I* and *Reinm. II*, respectively. The total number of different nebulae included in the four solutions amounts to 362.

A comparison between the dispersion values obtained in the different solutions shows that the disturbances caused by the systematic errors in the diameters of the nebulae, as well as by the selection effects in the material, are comparatively

small. Whereas the dispersions vary somewhat from one solution to another, the ratio  $\sigma_3/\sigma_1$  is very much the same in the different cases. The four solutions also give nearly the same values as regards the coordinates of the axis corresponding to the smallest dispersion.

The spatial distribution corresponding to all the included spiral nebulae has, according to the above investigations, the form of a slightly oblate spheroid. A comparison between the mean dispersions, as given at the bottom of Table 25, gives the results

$$\begin{aligned}\sigma_1 - \sigma_2 &= 0.009 \pm 0.006 \\ \sigma_1 - \sigma_3 &= 0.082 \pm 0.007\end{aligned}$$

Considering the size of the mean errors the first difference is apparently not significant, whereas the second difference, being more than ten times the mean error, is presumably of a real nature.

The results obtained so far seem to indicate the existence of a certain meta-galactic preferential plane, the normal of which has the coordinates  $\alpha = 35^\circ$  ( $215^\circ$ ) and  $\delta = -2^\circ$  ( $+2^\circ$ ). The corresponding galactic coordinates are  $l = 137^\circ$  ( $317^\circ$ ),  $b = -55^\circ$  ( $+55^\circ$ ). However the tendency to parallelism between the nebular discs is apparently very small,<sup>1</sup> the ratio between the smallest and largest dispersions, as derived above, being as large as 0.90. It seems necessary to postpone a final discussion regarding the existence of a possible preferential plane until further observational material, especially referring to the diameters and position angles of small and faint nebulae, has been accumulated.

---

<sup>1</sup> This is demonstrated by the fact that the same dispersion ratio as the one derived above is obtained, if 14 per cent of the nebulae are parallel to the preferential plane, and if the remaining 86 per cent are orientated entirely at random.

## Appendix.

The 11 tables contained in the Appendix give the results of the visual diameter determinations. The major and the minor diameters of the photographic images of the artificial nebulae have, by means of scale and eyepiece, been measured by five different persons, as is described in section 5. All the artificial nebulae have distributions of light of the form  $k r^{-n}$ , the exponent  $n$  ranging from 0.5 to 7.0.

*Column 1* in the different tables gives the observer. The numbers refer to K. Lundmark (I), A. Reiz (II), S. Cederblad (III), H. Kristenson (IV), and the writer (V).

*Columns 2—6* give the measured major and minor diameters, in millimeters. The denotations *A—E* in the column heads refer to different values of  $\cos \varphi$  (Cf. Fig. 1), namely 1.0 (*A*), 0.8 (*B*), 0.6 (*C*), 0.4 (*D*), and 0.2 (*E*). The value of  $\cos \varphi$  is approximately equal to the true (photometric) ratio of the minor and the major axis (Cf. Table 4).

The two last rows of each table give the means of the measured diameters (corresponding to the »mean observer») and the resulting ratios of the minor and major diameters, with mean errors.

*Series 1.  $I = k r^{-0.5}$ .*

*(exposure time 20s; focal ratio f/50)*

Observer	<i>A</i>	<i>B</i>	<i>C</i>	<i>D</i>	<i>E</i>
I	5.6 × 5.4 6.0 5.8	6.6 × 3.7 6.8 3.0	7.5 × 2.9 8.0 2.7	8.5 × 2.2 7.8 1.8	11.4 × 1.2 10.2 1.2
II	2.9 × 3.2 3.0 3.3	4.0 × 2.2 3.4 2.3	4.7 × 1.6 4.8 1.8	5.7 × 1.0 6.3 1.2	6.6 × 0.6 7.4 0.6
III	3.2 × 3.0 2.8 2.8	3.6 × 2.5 4.5 2.5	4.6 × 1.6 5.5 1.7	6.3 × 1.0 6.8 1.3	7.8 × 0.4 9.0 0.7
IV	4.0 × 4.1 3.7 3.8	4.2 × 3.4 4.1 2.5	5.0 × 2.3 4.4 2.2	6.3 × 1.3 5.6 1.6	8.0 × 0.6 10.0 0.8
V	3.8 × 3.6 3.6 3.6	4.2 × 2.7 4.5 2.8	5.5 × 2.2 5.5 2.2	6.2 × 1.3 7.0 1.4	9.5 × 0.7 10.0 0.7
means	3.86 × 3.86	4.59 × 2.76	5.55 × 2.12	6.65 × 1.41	8.99 × 0.75
diameter ratio	1.000 ±.025	0.601 ±.030	0.382 ±.024	0.212 ±.015	0.083 ±.007

Series 2.  $I = k r^{-1.0}$ .

(exposure time 240s; focal ratio f/22)

Observer	A	B	C	D	E
I	5.8 ×5.5 6.2 5.9	6.8 ×5.5 6.3 4.8	7.0 ×3.9 8.6 3.4	9.0 ×2.5 9.0 2.3	10.0 ×1.2 14.8 1.4
II	4.5 ×5.0 3.9 4.2	4.5 ×4.0 4.5 3.8	5.0 ×2.8 6.0 2.4	6.5 ×1.9 6.8 1.7	9.0 ×0.8 7.6 0.8
III	3.2 ×3.3 3.5 3.5	3.3 ×2.6 4.7 2.6	4.0 ×1.9 5.1 2.4	5.1 ×1.2 6.6 1.6	7.5 ×0.5 7.7 0.7
IV	4.0 ×4.0 4.0 3.6	4.0 ×3.5 5.0 3.8	5.0 ×3.0 6.0 2.8	5.5 ×1.5 6.0 2.0	7.0 ×0.5 11.0 0.8
V	4.0 ×3.7 3.9 3.7	4.5 ×2.7 4.2 2.9	4.5 ×2.2 4.8 2.0	7.5 ×1.5 5.2 1.6	9.5 ×0.5 8.8 0.7
means	4.30×4.24	4.78×3.62	5.60×2.68	6.72×1.78	9.29×0.79
diameter ratio	0.986 ±.029	0.757 ±.046	0.479 ±.011	0.265 ±.010	0.085 ±.008

Series 3.  $I = k r^{-1.5}$ .

(exposure time 30s; focal ratio f/32)

Observer	A	B	C	D	E
I	8.0 ×7.7 7.5 7.2	8.2 ×5.0 8.2 5.0	8.2 ×3.6 8.5 4.2	13.1 ×2.3 11.3 2.7	13.5 ×1.2 12.6 1.0
II	5.5 ×5.2 5.4 5.2	5.3 ×4.0 6.0 3.8	5.0 ×2.2 6.0 2.5	7.5 ×1.7 7.0 1.8	8.0 ×0.8 9.7 0.9
III	5.7 ×5.6 5.8 5.6	6.0 ×4.3 5.5 3.7	6.8 ×3.6 6.4 3.0	7.7 ×2.1 8.0 2.2	8.5 ×0.7 8.7 0.9
IV	5.4 ×5.5 5.0 5.2	5.5 ×4.2 5.3 4.2	6.2 ×3.2 5.5 3.0	6.0 ×1.8 6.0 2.0	7.5 ×0.7 7.5 0.9
V	5.8 ×5.6 6.0 5.7	6.0 ×4.5 5.7 3.8	5.9 ×3.0 6.3 3.1	7.5 ×2.1 7.8 2.1	9.0 ×0.9 8.8 0.9
means	6.01×5.85	6.17×4.25	6.48×3.14	8.19×2.08	9.38×0.89
diameter ratio	0.973 ±.012	0.689 ±.022	0.485 ±.017	0.254 ±.019	0.095 ±.004

*Series 4.  $I = k r^{-2.0}$ .*

*(exposure time 45s; focal ratio f/22)*

Observer	<i>A</i>	<i>B</i>	<i>C</i>	<i>D</i>	<i>E</i>
I	11.5 × 11.8 10.5 10.0	13.0 × 8.2 13.3 7.2	13.5 × 6.3 13.5 6.6	13.8 × 3.4 14.6 3.8	14.2 × 1.6 16.0 2.0
II	8.2 × 8.5 8.0 8.0	9.0 × 7.0 7.7 6.2	9.5 × 5.6 8.6 4.6	10.2 × 2.6 9.5 2.5	12.1 × 1.3 10.9 1.1
III	7.7 × 7.8 7.3 7.4	7.7 × 6.2 7.4 5.9	8.2 × 5.0 8.3 5.0	9.1 × 2.5 8.5 2.9	10.4 × 1.3 9.8 1.2
IV	7.2 × 7.7 7.0 7.5	7.8 × 6.2 7.5 6.0	8.5 × 5.0 8.2 4.5	8.5 × 2.7 8.5 2.8	9.7 × 1.3 11.2 1.1
V	8.3 × 7.8 8.7 8.0	8.6 × 6.5 9.0 5.8	9.6 × 4.9 9.0 4.3	9.6 × 2.8 9.2 2.9	12.0 × 1.5 11.5 1.3
means	8.44 × 8.45	9.10 × 6.52	9.69 × 5.18	10.15 × 2.89	11.78 × 1.37
diameter ratio	1.001 ±.020	0.716 ±.043	0.535 ±.026	0.285 ±.015	0.116 ±.003

*Series 5.  $I = k r^{-2.0}$ .*

*(exposure time 120s; focal ratio f/22)*

Observer	<i>A</i>	<i>B</i>	<i>C</i>	<i>D</i>	<i>E</i>
I	7.0 × 7.0 8.0 8.0	7.5 × 6.8 7.8 6.3	8.0 × 4.8 11.4 4.5	9.5 × 2.8 11.0 3.4	11.8 × 2.1 12.5 2.0
II	6.0 × 6.2 7.0 7.4	7.7 × 3.8 7.5 5.0	8.8 × 2.4 9.0 2.9	9.5 × 1.9 9.0 1.7	10.0 × 0.8 11.0 0.7
III	7.4 × 7.0 7.7 7.8	6.5 × 5.6 7.2 5.7	6.5 × 3.8 7.3 3.6	7.9 × 2.7 8.4 2.2	8.1 × 0.9 9.1 0.8
IV	5.5 × 6.0 4.5 5.0	6.4 × 5.0 6.5 4.5	6.5 × 4.0 8.0 3.5	7.5 × 2.3 10.0 1.8	7.5 × 1.2 11.0 1.0
V	7.3 × 7.5 7.4 8.0	7.1 × 5.2 7.5 6.8	8.2 × 4.1 7.8 4.5	8.4 × 2.6 10.0 2.5	10.8 × 1.2 11.0 1.0
means	6.78 × 6.99	7.17 × 5.47	8.15 × 3.81	9.12 × 2.39	10.28 × 1.17
diameter ratio	1.031 ±.021	0.763 ±.048	0.467 ±.041	0.262 ±.021	0.114 ±.015

Series 6.  $I = k r^{-2.5}$ .

(exposure time 150s; focal ratio  $f/22$ )

Observer	<i>A</i>	<i>B</i>	<i>C</i>	<i>D</i>	<i>E</i>
I	$9.3 \times 9.6$ 8.3 8.7	$9.8 \times 7.2$ 9.3 7.5	$9.1 \times 5.8$ 9.0 4.8	$9.6 \times 3.5$ 9.6 3.7	$10.4 \times 1.8$ 10.0 1.6
II	$9.8 \times 10.5$ 9.8 9.9	$9.5 \times 8.5$ 9.2 6.9	$9.8 \times 5.2$ 9.4 5.2	$10.5 \times 3.0$ 9.8 3.3	$10.6 \times 1.2$ 10.6 1.0
III	$8.9 \times 8.7$ 9.2 9.2	$9.6 \times 6.7$ 9.5 7.9	$9.0 \times 4.6$ 9.6 4.4	$10.2 \times 3.3$ 9.8 3.2	$9.9 \times 1.4$ 11.3 1.4
IV	$9.0 \times 9.5$ 8.0 7.7	$9.5 \times 7.0$ 8.5 5.5	$9.0 \times 5.5$ 9.0 3.5	$9.5 \times 2.8$ 9.5 2.2	$10.5 \times 1.0$ 10.5 1.0
V	$9.5 \times 9.5$ 9.2 9.5	$9.5 \times 7.8$ 9.7 7.2	$10.1 \times 5.5$ 9.7 5.5	$10.3 \times 3.5$ 10.1 3.4	$10.2 \times 1.6$ 10.5 1.5
means	$9.10 \times 9.28$	$9.41 \times 7.22$	$9.37 \times 5.00$	$9.89 \times 3.19$	$10.45 \times 1.35$
diameter ratio	$1.020$ $\pm .009$	$0.767$ $\pm .017$	$0.534$ $\pm .019$	$0.323$ $\pm .016$	$0.129$ $\pm .014$

Series 7.  $I = k r^{-3.0}$ .

(exposure time 180s; focal ratio  $f/22$ )

Observer	<i>A</i>	<i>B</i>	<i>C</i>	<i>D</i>	<i>E</i>
I	$8.7 \times 8.4$ 8.3 8.2	$9.2 \times 6.9$ 8.6 6.3	$8.8 \times 4.7$ 8.8 5.2	$8.4 \times 3.0$ 8.6 2.7	$9.2 \times 1.6$ 9.8 1.5
II	$7.8 \times 8.4$ 8.0 9.0	$7.5 \times 6.5$ 8.0 6.4	$7.9 \times 4.6$ 8.7 4.7	$8.5 \times 2.4$ 9.5 2.5	$9.8 \times 1.1$ 10.0 1.4
III	$8.8 \times 8.4$ 7.9 7.8	$8.5 \times 6.9$ 7.9 6.7	$8.7 \times 5.1$ 8.6 4.9	$8.8 \times 2.7$ 9.0 2.9	$9.8 \times 1.3$ 9.1 1.2
IV	$8.0 \times 8.0$ 7.5 7.5	$8.5 \times 6.5$ 7.5 6.0	$9.0 \times 4.0$ 8.0 4.0	$9.0 \times 2.3$ 8.5 2.2	$9.5 \times 1.2$ 8.5 1.0
V	$8.5 \times 8.5$ 8.0 8.0	$8.5 \times 6.8$ 8.0 6.5	$8.8 \times 4.8$ 8.5 4.6	$9.0 \times 3.0$ 9.0 2.8	$9.0 \times 1.5$ 8.7 1.4
means	$8.15 \times 8.22$	$8.22 \times 6.55$	$8.58 \times 4.66$	$8.83 \times 2.65$	$9.34 \times 1.32$
diameter ratio	$1.009$ $\pm .020$	$0.797$ $\pm .016$	$0.543$ $\pm .016$	$0.300$ $\pm .016$	$0.141$ $\pm .010$

Series 8.  $I = k r^{-4.0}$ .  
(exposure time 120s; focal ratio f/22)

Observer	<i>A</i>	<i>B</i>	<i>C</i>	<i>D</i>	<i>E</i>
I	8.3 × 8.0 8.0 7.7	8.3 × 6.5 7.8 6.0	8.4 × 5.0 8.5 4.4	8.5 × 3.4 8.6 2.9	8.2 × 1.6 8.3 1.5
II	7.3 × 7.6 7.1 7.4	7.5 × 5.9 7.3 6.0	7.6 × 4.2 7.5 4.1	7.8 × 2.8 7.6 2.6	8.3 × 1.1 8.3 1.0
III	7.2 × 7.1 7.1 7.0	7.4 × 5.6 7.2 5.7	7.4 × 4.3 7.2 4.1	7.5 × 2.9 7.9 2.6	8.2 × 1.4 8.0 1.2
IV	6.6 × 7.0 7.0 7.0	6.6 × 5.4 7.0 5.5	7.0 × 3.9 7.0 4.2	7.5 × 2.8 7.5 2.5	8.5 × 1.2 8.5 1.2
V	7.3 × 7.3 7.3 7.0	7.2 × 5.6 7.2 5.6	7.2 × 4.1 7.3 4.2	7.4 × 2.8 7.3 2.6	7.8 × 1.3 7.7 1.3
means	7.32 × 7.31	7.35 × 5.78	7.51 × 4.25	7.76 × 2.79	8.18 × 1.28
diameter ratio	0.999 ±.016	0.786 ±.007	0.566 ±.006	0.360 ±.004	0.156 ±.010

Series 9.  $I = k r^{-5.0}$ .  
(exposure time 180s; focal ratio f/22)

Observer	<i>A</i>	<i>B</i>	<i>C</i>	<i>D</i>	<i>E</i>
I	10.0 × 10.2 10.0 10.0	10.3 × 8.1 9.6 8.3	10.7 × 6.2 10.7 5.6	11.1 × 3.6 10.8 3.8	10.6 × 1.7 11.5 1.7
II	9.5 × 9.5 9.5 9.8	9.8 × 7.6 9.6 7.5	9.9 × 6.0 9.6 5.8	10.1 × 3.5 10.5 4.0	10.3 × 1.4 10.5 1.4
III	9.7 × 9.2 9.3 9.3	9.7 × 7.5 9.2 7.2	9.9 × 5.6 9.6 5.5	9.6 × 3.5 10.0 3.7	9.9 × 1.5 9.7 1.6
IV	9.6 × 9.6 9.5 9.8	9.6 × 7.6 9.5 7.2	9.8 × 5.8 9.6 5.5	9.8 × 3.5 9.6 3.7	10.4 × 1.6 10.2 1.6
V	9.6 × 9.5 9.7 9.5	9.5 × 7.6 9.8 7.5	9.8 × 5.8 9.8 5.5	9.8 × 3.6 10.0 3.8	10.1 × 1.6 10.3 1.6
means	9.64 × 9.64	9.66 × 7.61	9.94 × 5.73	10.13 × 3.67	10.35 × 1.57
diameter ratio	1.000 ±.009	0.788 ±.008	0.576 ±.008	0.362 ±.006	0.152 ±.004



*Series 10.  $I = k r^{-6.0}$ .*

*(exposure time 180s; focal ratio  $f/22$ )*

Observer	<i>A</i>	<i>B</i>	<i>C</i>	<i>D</i>	<i>E</i>
I	13.5 × 13.2 12.6 12.4	14.2 × 10.4 12.6 9.8	14.5 × 7.8 14.7 7.1	14.5 × 5.6 14.7 5.0	14.5 × 2.6 14.7 2.4
II	12.0 × 12.0 11.4 11.2	12.0 × 9.5 11.2 9.0	11.8 × 7.7 11.5 6.4	12.8 × 4.9 11.9 4.5	13.5 × 2.5 12.2 2.0
III	13.0 × 12.7 12.0 12.0	12.8 × 10.4 12.5 9.3	13.0 × 7.5 12.2 6.8	13.4 × 4.7 12.7 4.5	14.2 × 2.5 13.5 2.1
IV	12.5 × 12.2 12.1 12.2	12.5 × 10.5 11.9 9.2	12.5 × 7.5 12.0 6.8	13.2 × 4.5 12.2 4.6	14.0 × 2.3 13.2 2.2
V	12.5 × 12.6 12.1 12.0	12.7 × 10.0 12.3 9.5	12.7 × 7.5 12.5 7.1	13.1 × 4.6 12.7 4.5	13.7 × 2.3 13.7 2.2
means	12.37 × 12.25	12.47 × 9.76	12.74 × 7.22	13.12 × 4.74	13.72 × 2.31
diameter ratio	0.990 ±.003	0.783 ±.008	0.567 ±.014	0.361 ±.005	0.168 ±.002

*Series 11.  $I = k r^{-7.0}$ .*

*(exposure time 180s; focal ratio  $f/22$ )*

Observer	<i>A</i>	<i>B</i>	<i>C</i>	<i>D</i>	<i>E</i>
I	13.2 × 13.4 13.0 12.8	13.2 × 10.7 13.2 9.8	13.5 × 7.6 13.3 7.5	13.5 × 4.8 14.0 4.6	13.8 × 2.5 14.0 2.3
II	12.8 × 12.8 12.5 12.4	12.6 × 10.0 12.5 9.6	12.9 × 7.3 12.4 6.9	12.8 × 4.6 12.5 4.5	13.4 × 2.2 13.2 2.2
III	12.8 × 13.0 12.7 12.6	12.9 × 10.2 12.8 10.0	13.0 × 7.9 12.7 7.4	13.1 × 5.0 12.7 4.8	15.0 × 2.5 14.0 2.3
IV	13.1 × 13.3 13.0 13.4	13.0 × 10.6 13.0 10.2	13.0 × 8.0 13.1 7.5	13.5 × 5.0 13.3 5.0	14.2 × 2.6 13.7 2.4
V	13.1 × 13.0 12.9 12.8	13.0 × 10.5 13.0 10.2	13.0 × 7.8 13.0 7.7	13.2 × 5.1 13.3 5.1	14.5 × 2.5 14.0 2.5
means	12.91 × 12.95	12.92 × 10.18	12.99 × 7.56	13.19 × 4.85	13.98 × 2.40
diameter ratio	1.003 ±.005	0.788 ±.004	0.582 ±.009	0.368 ±.008	0.172 ±.003

## Table of Contents.

	Page
Summary .....	3
Chapter I. Investigation of the systematic errors in the apparent diameters of nebulae.	
1. Introduction .....	5
2. The experimental arrangements .....	6
3. Description of the sectors .....	9
4. The plate material .....	14
5. Visual measurement of the photographic images of the artificial nebulae	15
6. Measurement of the artificial nebulae in the photometer .....	18
7. The results .....	20
Chapter II. Investigation of the diameters given in Reinmuth's catalogue.	
8. Reinmuth's catalogue of nebulae .....	30
9. Relation between Reinmuth and the Mean Observer .....	30
10. Reinmuth's diameter ratios for elliptical nebulae .....	32
11. Reinmuth's diameter ratios for spiral nebulae .....	34
Chapter III. On the inclinations of the spiral nebulae to the celestial plane.	
12. Introduction .....	40
13. The inclination and the apparent diameter ratio .....	42
14. The distribution of the inclination angles .....	43
15. The orientation of nebulae as obtained from Reinmuth's catalogue ....	48
16. The orientation of nebulae as obtained from Reiz's catalogue .....	55
17. The orientation of nebulae as obtained from the Shapley-Ames catalogue	58
Chapter IV. On the existence of a metagalactic preferential plane.	
18. Introduction .....	64
19. The mathematical theory .....	65
20. The determination of the statistical moments $\nu_{ij}$ .....	67
21. The results as obtained from Reinmuth's catalogue .....	69
22. The results as obtained from the Shapley-Ames catalogue .....	72
23. Summary of results .....	74
Appendix .....	76

Tryckt den 15 jan. 1946.